The Pennsylvania State University

The Graduate School

College of Engineering

EVALUATING THE CORROSION PROTECTION OF POST-TENSIONING

GROUTS: STANDARDIZATION OF AN ACCELERATED CORROSION TEST

A Thesis in

Civil Engineering

by

Alexandre R. Pacheco

Submitted in Partial Fulfillment
of the Requirements
for the Degree of

Doctor of Philosophy

December 2003

The thesis of Alexandre R. Pacheco was reviewed and approved* by the following:

Andrea J. Schokker
Assistant Professor and Henderson Professor of Civil Engineering
Thesis Adviser
Chair of Committee

Howard W. Pickering
Distinguished Professor of Metallurgy

Jeffrey A. Laman
Associate Professor of Civil Engineering

Daniel G. Linzell
Assistant Professor of Civil Engineering

Andrew Scanlon
Professor of Civil Engineering
Head of the Department of Civil and Environmental Engineering

*Signatures are on file in the Graduate School.

ABSTRACT

Post-tensioning grouts, typically a mixture of cement and water (sand, mineral chemical admixtures can also be used), are not only designed to transfer stresses between cables and precast concrete, but also to protect prestressing strands against corrosive phenomena. A recent concern regarding post-tensioned structures is the possibility that corrosive agents may reach grouted steel tendons and start a sequence of events culminating in catastrophic collapse. This possible scenario motivated the creation of the Accelerated Corrosion Test (ACT) intended to measure the degree of corrosion protection for grouts used in post-tensioning applications. This test is currently recommended by the Post-Tensioning Institute (PTI). Although already in use, the ACT is not fully developed and researchers have been pointing out the need for further studies to evaluate the influence of the IR drop effect on ACTs (a loss in the applied potential due to the resistivity of corrosion cells) because this phenomenon is likely to skew results for grouts of significant different resistivity. Five different categories of grout (plain, prepackaged, with corrosion inhibitors, with silica fume, and with fly ash) were tested in an electrochemical setup capable of compensating for IR drop effects. Procedures are recommended for adoption in an improved version of the ACT standard.

TABLE OF CONTENTS

LIST OF FIGURES

LIST OF TABLES

ACKNOLEDGEMENTS

Alexandre R. Pacheco

University Park, Pennsylvania

December 2003

1 INTRODUCTION

1.1 GENERALITIES

Concrete has continued to gain in popularity worldwide over the years. The main reason for this is perhaps related to the fact that concrete is, basically, a compound of simple, easy to find, and inexpensive materials: a binder (portland cement), fine and coarse aggregates, and water. When properly combined, forming concrete, these materials are capable of undergoing a variety of severe conditions for long periods and in many different applications. With such attractive advantages, in the past, concrete was applied everywhere, with little concern to durability. In fact, it could be inferred that concrete was applied as though it would never deteriorate, being considered virtually eternal. Experience, however, contradicted appearances. In the last decades, concrete has been found to also suffer its share of burden imposed by time.

Resistant to several adverse conditions, concrete have been particularly susceptible to certain combinations of environmental agents, compromising eventually its integrity. The main cause for this particularity is related to the fact that concrete is incapable of sustaining the same magnitude of stresses in tension that it does when in compression (brittle behavior). Therefore, a new element had to be introduced in order to reinforce the concrete capability to sustain tension stresses: steel. Steel is, up to this date, the best material elected to fulfill this assignment.

Due to its higher strength and ductility as a structural material, steel has played an important role in its partnership along the years with concrete, forming what is known as "structural concrete". That is true not only because of its reinforcing role, but also because of the extended structural performance it can provide when applied as strands in prestressed concrete elements.

However, despite its vital contribution, the presence of steel in concrete has added another important factor that needs to be considered when structural durability is a focus: the material susceptibility to electrochemical corrosion. Indeed, when it comes to structural concrete, the condition that concerns more structural engineers, contractors, authorities, and researchers by far is the corrosion of the reinforcing and prestressing steel. The reason for that is three-fold: serviceability, safety, and the cost involved in structural repair and rehabilitation. In addition, even structural aesthetics is affected by the corrosive phenomena.

Numerous publications provide impressive numbers for expenditures on the corrosion problem related to structural concrete construction. Considerable resources have continuously been spent in order to rehabilitate structures attacked by corrosion. For a certain structure, the more time taken to initiate repairs, the higher the cost to repair it. Moreover, with the rate of structural deterioration increasing over time, safety becomes a major factor.

Most researchers working on corrosion of steel in cementitious media have agreed that the mechanism of corrosion of steel is due to mainly one aspect: the failure of the passive film that forms around the steel. This passive film is usually negatively affected by infiltration of chlorides in the concrete or because of concrete carbonation

(combination of the concrete $Ca(OH)_2$ with diffused CO_2). In both cases, the high concrete pH (more than 12.5) drops, reducing or eliminating the action of the thin protective passive film existent on the steel and leading to corrosion.

In most of the cases, only the structure serviceability (and aesthetics) is compromised when corrosion takes place. Cracking, spalling, and staining of the concrete due to the corrosion products, which can reach 4 to 10 times its original volume, generating internal tensile stresses in the concrete, are easily noticed when corrosion is at an advanced level of activity. In addition, at this point, it may be possible that structural deflections would increase due to the consequent reduction of reinforced cross section and additional cracking caused by the corrosion products. Such indications demand immediate action and are signs that rehabilitation costs are already steeply escalating. Therefore, instead of waiting for such signs to happen, it is recommended to proceed with monitoring inspections and any necessary repairs along the structure's life span.

One of the ways to protect the reinforcement inside a structure is to work with concrete of high quality, and to limit the crack width during the design phase, hindering the access of aggressive agents to the steel. High Performance Concrete (HPC) can be engineered to allow a minimum of porous volume or to have increased capability of corrosion protection of the reinforcement, and prestressing typically reduces cracking occurrences. However, regular monitoring of concrete structures can never be left aside.

The inherent difficulty to detect early signs of corrosion of the reinforcement may be increased several fold when prestressed concrete or, more specifically, post-tensioned elements are present in the structure. Post-tensioning strands are commonly located inside metallic or plastic ducts and among dense cages of non-prestressed reinforcement.

As a result, assessment of their condition is very difficult to make. Nevertheless, it is when safety is considered that post-tensioned structures show reasons for concern. Their serviceability may be completely unaffected with no signs of corrosion degradation, and even so a point localized corrosion (pitting corrosion) may occur, leading to a subtle break of a wire or more that could lead to, at the extreme, a structural catastrophic collapse. Therefore, not just serviceability is compromised when the structure is post-tensioned, but safety itself may be at significant higher risk when compared to other reinforced concrete structures.

Due to the geometric characteristics of the steel strands used in prestressed concrete, and due to their stressed condition in the structure, corrosion may be facilitated more than in regular reinforcing bars (corrosion under stress). The contact between the steel wires allows an intense and concentrated type of corrosion known as crevice corrosion, which may also develop due to pitting corrosion. Moreover, being constituted of several wires, one strand presents a larger superficial area exposed to aggressive agents like chlorides that are highly aggressive to steel and are particularly common in coastal regions or where deicing salts are used.

The oldest post-tensioned concrete structures in the US are approximately 50 years old and there are already a few examples that show corrosion activity on embedded tendons (including fairly young structures). Therefore, it can be expected that, as these structures become older, more problems related to tendon corrosion may be noticed.

When the structural concept is based upon grouted post-tensioning, another element has to be considered during the design phase: the cement grout in which the tendons are embedded. In that case, the cement grout also has to have specific properties in order to

protect the post-tensioning tendons. The grout is the last line of defense against penetration of aggressive agents and, more specifically, against corrosion attack of the prestressing tendons.

In spite of the constant study and improvement of grout technology, there is still a gap concerning the corrosion protection degree of grouts used in post-tensioning applications. The main reason for this is the need for more data from tests intended to evaluate grouts' corrosion resistance.

At this time, the only test method recommended for evaluation of the corrosion protection of grouts is given by the Post-Tensioning Institute (PTI) "Guide Specification for Grouting of Post-Tensioned Structures" (2003) and is known as the ACT test. Although this test was idealized in the last decade, there is still a lack of information regarding its efficiency. Most concerning is the high dispersion of data commonly observed in the test, usually amounting to a 30% coefficient of variance, but with more than 100% reported in some investigations. Moreover, little data is available to assess limitations that the ACT test may have. Additionally, other important issues need to be studied, such as the effects of curing age for grout testing, and the behavior of newer prepackaged grouts and their resistivity on the test. Another aspect is the possibility of applying different electrochemical techniques that would lead to faster analyses, since the current test often needs a month or more to give a result. Popular electrochemical techniques such as the corrosion polarization (half-cell test), the linear polarization resistance (LPR), and the Tafel scan could be considered in the test procedures to perhaps reduce data scattering and increase efficiency of the method. Furthermore, a

standardization of the method with considerations for specific conditions that affect results is an important gap still to be fulfilled.

1.2 BACKGROUND

Quality control or means to evaluate construction materials play a fundamental role in engineering, being not only closely related to the required structural serviceability but also to repair expenditures and structural lifespan. The cause-effect relationships that involve these aspects can be also extended to current techniques and practices related to construction materials and their applications. As a result, it is not surprising that every structural material has a practice or test method providing limits and general rules of application. When it comes to post-tensioned structures, however, it is interesting that the material used to embed the steel prestressing strands, namely the portland cement grout, has been subjected to more intense studies only in the last decade. This is easy to understand, since the post-tensioning system of construction is relatively young and corrosion problems related to grouts have only recently begun to be noticed. Originally, the only concern had been the development of grouts with appropriate placement characteristics in order to avoid filling flaws inside the encasing ducts.

Indeed, most of the works targeting grout performance have primarily focused on problems related to poor fluidity and bleeding resistance. Schupack (1971) had different grout mixes produced and tested under adverse conditions, as in high vertical rises and in ducts with sharp curvatures. The grouts that produced the best results in terms of void

and bleed prevention were those using water-reducing, anti-bleeding, and expansive

admixtures. Schupack (1974) again addressed grout problems related to bleeding and

then developed a pressurized bleed resistance test (procedure given today in PTI 2003) to

appropriately qualify grouts regarding their bleed resistance. Corrosion of post-

tensioning cables due to low-quality grout was not yet a major concern. Two decades

later, however, the same author mainly addressed tendon corrosion occurrences, but

correlating them to construction practices (Schupack 1994). In that work, the author

comments that an inspected 35-year-old bridge had an estimated loss of 2 to 3 wires in

the tendons due to corrosion caused by chloride contamination of the post-tensioning

grout. Dickson et al. (1993), also in field inspections, found moderate corrosion in a

post-tensioned bridge after 34 years of its construction.

Lankard et al. (1993), in an experimental investigation, had seven different types of

grout tested for bleed resistance using the Schupack pressure bleed test. While their

control grout, a plain mixture of cement type II and water at a water-cementitious ratio of

0.44, had 38% of bleed, a plain grout with 5% of polysaccharide gum had only 1% of

bleed. The most valuable contribution of the article, however, was the creation of a

method to test the corrosion protection capability of grouts: the ACT or accelerated

corrosion test (procedures in PTI 2003). Specifically, the authors conceived a specimen

that combined both grout and steel cable in a suitable manner that emulated a section of a

post-tensioning tendon system, and used a well-known technique in electrochemistry, the

potentiostatic polarization method (ASTM G 5 1999), to evaluate their grouts for

corrosion protection. Also emulating a field situation, the authors used saltwater as

electrolyte for the corrosion reactions. They reported that, based on preliminary

investigations, 5% of sodium chloride by mass should be used for the electrolyte in order to simplify the test by avoiding tensioning the strands during the experiment. Upon testing their control and microsilica grouts, times to allow corrosion of 100 and 465 hours, respectively, were found. The authors briefly mentioned that the microsilica grout took more time to develop the same level of corrosion damage than the plain control grout. No details regarding possible shortcomings with the test, recommended number of specimens, or data scattering were addressed. A very similar experimental setup to the ACT was used by Hussain and Rasheeduzzafar (1994) to test concretes with improved corrosion characteristics due to cement replacements of 30% class F fly ash in their mixes. The times to corrosion, however, were found with polarization corrosion tests (half-cell measurements), instead of monitoring current levels. No comments regarding experimental difficulties were given, with the work focusing only on the fly ash's excellent performance.

The ACT data scattering was a major concern in the work by Hamilton (1995) and by Hamilton et al. (2000). Crack-controlled specimens were used to try to minimize this problem, having as a justification the fact that both grouts on stay cables and in post-tensioning ducts are prone to cracking (Hamilton 1998). They modified the original ACT specimen design to isolate one crack and control its width to a maximum value of 0.13 mm (0.005 in.). However, the variability of the results remained high, with coefficients of variation ranging from 14 to 69% (mostly from 20 to 40%). Outside of the variability due to the crack formation, the authors explain data discrepancies based on possible resistivity differences between the tested grouts. The discrepancies found would be associated with the voltage drop effect, a common source of error in electrochemical

measurements that consists of a loss on the applied voltage due to the resistivity of the system being measured (usually in the electrolyte phase). Besides the significant variability, another problem observed by the authors was the result obtained for a grout with calcium nitrite, a widely used corrosion-inhibiting admixture in the field that, in fact, reduced the corrosion performance of the grout mixtures tested. In addition to the regular result given by an ACT (the time-to-corrosion, t_{corr}, or the time in hours necessary for grouts to cease their corrosion protection under the test conditions), the authors investigated the trends of two other measurements: the open-circuit potential (E_{oc}) and the current density (i_{corr}) prior to the onset of corrosion. Weak or no signs of correlation were found between these variables and the ACT results. Another aspect of the ACT that could be confirmed is that even cracked specimens can take several days to corrode. For instance, a control grout took 272 hours (11 days) to allow corrosion.

Although fluidity and bleed resistance of grouts was the focus of the experimental study conducted by Schokker (1995) and by Schokker et al. (2002), the ACT had an important role in the development of high performance grouts for post-tensioning applications in those works. Five different grouts were tested for corrosion protection, with results ranging from 300 hours (13 days) to 1,000 hours (42 days). The authors incorporated in their version of the ACT method several modifications proposed earlier by Koester (1995). In addition to redesigning the specimen dimensions, Koester proposed the reduction of the electrical potential applied on ACT specimens from 600 mV above the potential given by a saturated calomel electrode, i.e., +600 mV$_{SCE}$, to +200 mV$_{SCE}$, significantly reducing data scatter. However, a few grouts tested still showed high variability in the data and the time required to obtain an ACT result became more

pronounced, as can be noticed from the number of hours aforementioned. Furthermore, these authors highlighted the necessity to compensate ACT experiments for the voltage drop effect, which may otherwise distort test results from grouts with pronounced resistivities, mainly when compared with more electrically conductive subjects. The authors also testing strand from two different sources found consistent variation in results when materials were not kept constant.

The modeling of diffusion has been considered in several studies on cementitious materials because the ingress of chlorides and the attack of the steel reinforcement structures can be directly related to service life estimations (induction period or initiation stage). Several approaches to determine structural service life based on the diffusion of chlorides are being considered by researchers. Examples of studies that applied experimental approaches to determine the chloride diffusion in concrete are the works by Hornain et al. (1995) and Li (2001). The experimental approach was defended by the latter by claiming that analytical approaches need to consider too restrictive boundary conditions that are difficult to be met in reality (e.g. homogeneous materials and semi-infinite planes). Andrade et al. (2003), reviewing analytical solutions, also make similar comments, saying that service life predictions have to consider numerous parameters and phenomena, and many are difficult to quantify. Peng et al. (2002) used a neural network analysis approach to model chloride diffusion in concrete, adapting to conditions that would be difficult to consider with other mathematical models (unsteady states of chloride profiles).

Probabilistic models, such as the one used by Kirkpatrick et al. (2002), are also adopted by researchers to predict service life of structures related to chloride-induced

corrosion. Several analytical models try to determine the remaining service life of structures, i.e., after the onset of corrosion, which characterizes the propagation stage in structural service life. Ahmad (2003) reviewed models for prediction of the remaining service life of concrete structures and suggests an experimental approach for the determination of cracking and concrete spalling.

Studies regarding admixtures in cementitious materials are extensive. For instance, silica fume grouts had superior placement characteristics when compared to plain grouts in a work by Diederichs and Schutt (1989), mainly when the cement replaced by silica fume was 5%, suggesting an optimum content. Rasheedzzafar et al. (1990) found that the cement alone influences corrosion behavior when testing type I cement, which performed significantly better in corrosion tests when compared with type V due probably to the higher C_3A content of the first type. Loretz and French (1995) found that the optimum silica fume content in concretes would tend to be a replacement of less than 9% and Diamond (1997) surprisingly confirms that, contrary to what is observed in concretes, undispersed silica fume in grouts tend to produce alkali-silica reactions that can lead to distress and cracking of the grout matrix. The optimum cement replacement in concretes is found by Idriss et al. (2001) as 8%, during LPR measurements in corrosion tests. Corrosion inhibitors are discussed by Berke (1991), who highlights the importance of calcium nitrite for corrosion protection in concrete. Gu et al. (1997) run linear polarization resistance (LPR) and electrochemical impedance spectroscopy (EIS) tests and found increased corrosion protection when inhibitors based on sodium nitrite and dinitrobenzoic acid were used in concrete samples.

Baweja (1996), using potentiodynamic procedures, found that blended cement concretes have improved corrosion characteristics when compared with plain cement concretes. Montemor et al. (2000), using the EIS technique, found that a 30% cement replacement by type C fly ash significantly increased corrosion test performances in concretes with high water-cementitious ration (0.57).

Rha (2001) showed with EIS measurements that mineral admixtures such as blast furnace slag and microsilica tend to modify the microstructure of mortars near the steel reinforcement surface, reducing porosity and pore size distribution at these sites. Montemor et al. (2003) reviewed electrochemical techniques for onsite applications, recommending repeatedly half-cell tests as a first approach and then LPR measurements. They comment that EIS results are difficult to interpret and need to have their equivalent circuits reevaluated for every change in conditions. In addition, transient techniques such as the galvanostatic pulse may suffer deviations of results when non-activation behavior is expected. Andrade et al. (1990), Zivica (2001), and Millard et al. (2001) used LPR tests in reinforced concrete samples to find corrosion rates and, in the last two works, related them with levels of damage or with environmental conditions.

Baweja (1999) compared results from LPR, polarization corrosion, resistivity measurements, gravimetric mass loss, and EIS tests, obtaining satisfactory agreement between them. An important result regarding the ohmic drop effect in electrochemical tests in concrete samples was found by Berke et al. (1990), estimating that up to 27% overestimation of LPR readings can occur because of those effects and Escalante (1990) claims that the current interruption technique can eliminate 95% of the error related to them. Another important result for this work was given by Al-Tayyib and Khan (1988),

affirming that LPR measurements do not significantly affect concrete samples exposed to 5% NaCl solutions and Tafel scans can be done afterwards. They also reported anodic Tafel constants varying from 400 to 500 mV/decade, while cathodic constants would be in range from 250 to 350 mV/decade. Another interesting result is given in the work by El Maaddawy and Soudki (2003) when checking the applicability of Faraday's law in tests with concrete samples. They found that a satisfactory prediction of mass losses given by the formula would be limited by a 7.27% of loss and that the volume of corrosion products involving the reinforcement would hinder good predictions after that.

Regarding the monitoring of concrete structures in the field, Schiessl and Raupach (1992) give an example of corrosion sensors for bridges, while Liu et al. (2002) use time domain reflectometry (TDR) to detect the location of corrosion damages in steel rebars and cables. The corrosion sensors are usually installed into critical locations of the structure, structurally speaking, or where corrosive attacks would be more likely to occur, such as in joints, or parts subjected to wetting cycles.

Characterization tests of grouts and concretes are usually related to porosity and permeability aspects. Breysse (1997), measuring porosity by simple drying from saturated samples and by mercury intrusion porosity (MIP), stated that porosity is highly dependent on the method used after finding differences as high as 80% during the measurements. Al-Amoudi et al. (1993) found that porosity and permeability would reach values that are more appropriate when blast furnace slag is added to concretes. Moreover, they found good correlations between those properties and corrosion rates, stating that permeability and porosity could be used to predict long-term corrosion performances of plain and blended cement concretes.

1.3 OBJECTIVES

In this work, further refinements of the ACT method are developed, which were possible by incorporating voltage drop correction in the analysis of several different types of grouts. By testing compensated and uncompensated systems for the voltage drop effect, the magnitude and implications of previous results containing this kind of error could be determined. Furthermore, alternative electrochemical techniques are evaluated and considered in an attempt to develop a more effective test method.

1.3.1 General Goal

The main goal of this work is to appropriately characterize corrosion systems typically used in ACTs, contributing with a new standard method to fill an important gap in the current state-of-the-art of post-tensioning structures.

1.3.2 Specific Goals

- To measure the effect of voltage drops in ACTs;

- To measure the influence of grout age and type on voltage drops;

- To investigate possible problems in current ACT cell design;

- To propose a new, more complete, and efficient ACT method.

2 BASIC THEORY

This chapter presents the theoretical background behind the aspects addressed during the research. It starts with an explanation on corrosion and pertinent analytical approaches. Then experimental aspects such as the ohmic or voltage drop effect and electrochemical techniques are presented and, at the end, the Accelerated Corrosion Test is addressed.

2.1 CORROSION: AN ELECTROCHEMICAL PROCESS

Corrosion is a destructive process on metals. Upon corroding, metals return to a natural state that requires less energy and is more stable. However, this return to a more stable state, characterized by chemical hydroxide compounds, is not useful for engineering purposes. In fact, when metals undergo corrosive phenomena, economic, safety, and aesthetic factors can be severely affected. Because of these implications, corrosion has been an important subject in electrochemistry that, together with other relevant subjects such as the development and design of batteries, fuel cells, and electroplating processes, has been extensively studied. All these subjects, including the understanding of corrosion, are based on electrochemical phenomena and can be studied under the same theoretical approaches and analyzed with similar tools.

Being an electrochemical process, corrosion is characterized by an electrical flux of charge (electrons and ions) through solid and liquid phases in a closed circuit.

Specifically, it is possible to draw a parallel between the situation encountered in a pure electrical circuit and in a metal undergoing corrosion. Consider the illustration in Figure 2.1.

$$Fe = Fe^{++} + 2e^-$$

H_2O; NaCl

Fe Fe^{++}
$2e^-$ Cl^-

e^- +   -   I
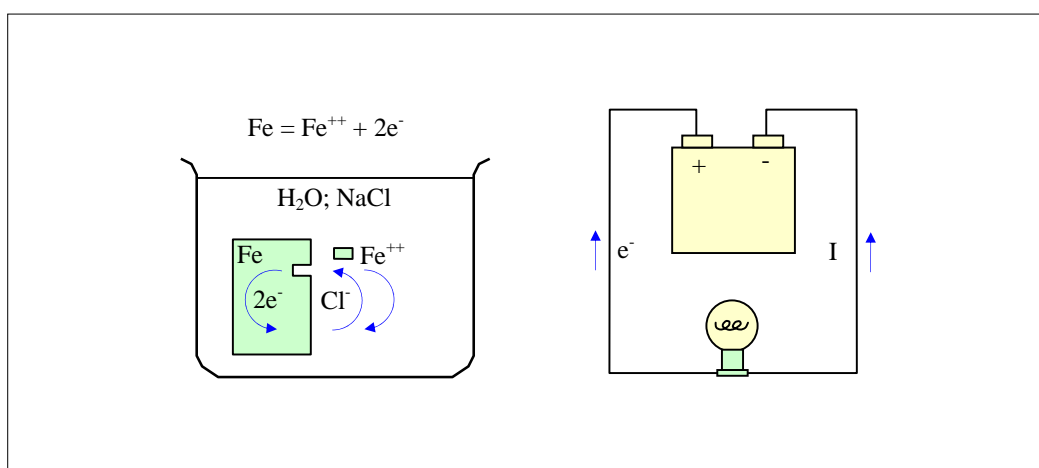
Figure 2.1 - Electrochemical and electronic circuit

On the left, a piece of steel (predominantly iron, Fe) is oxidizing, i.e., the steel loses positively charged ions (Fe^{++} cations) at anodic sites to the electrolyte. The corresponding electrons to the original Fe atom flow through the metallic phase towards cathodic sites, where reduction reactions occur (not shown). The circuit is completed in the aqueous phase, where negatively charged ions (Cl^- anions, for instance) flow from cathodic sites towards anodic ones and positively charged ions flow from anodic sites towards cathodic sites. Typically, at the cathodic sites, Fe cations combine with water molecules to form hydrated corrosion products (reddish products that usually result from

steel corrosion). This sequence of events proceeds continuously until the entire piece of

steel is dissolved.

2.1.1 Electromotive Force Potentials (EMF Series)

It should be noticed that, under the conditions illustrated previously,

instrumentation of the continuous process of corrosion is virtually impossible, since there

is no means to know where cathodic and anodic sites would occur and, additionally, they

are occurring on the same body. Therefore, another electrode is added to the system, as

illustrated in Figure 2.2. This element, being inert because of its significantly low

electronegative potential (C, Au, Pt), creates a condition for cathodic sites to form on its

surface (the cathode), keeping anodic sites on the oxidizing metal (the anode).
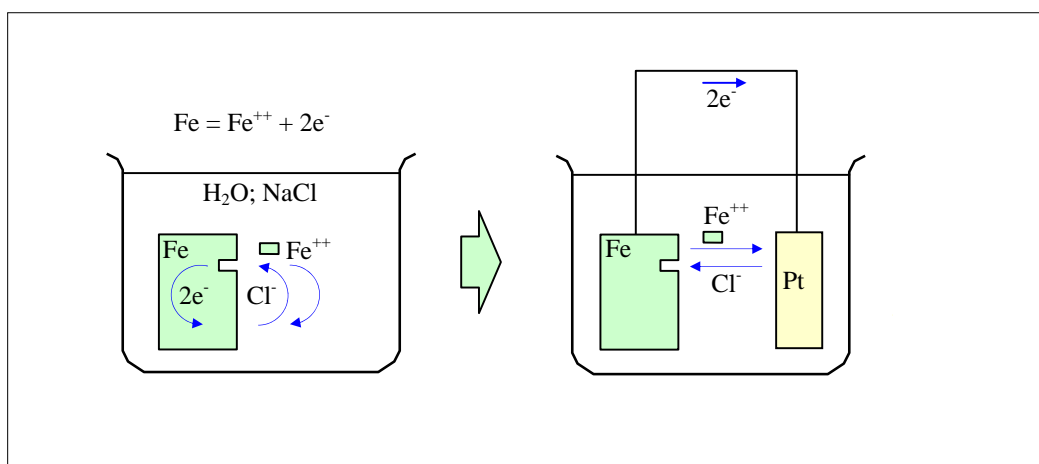
Figure 2.2 – Isolation of cathodic and anodic sites

Any element chosen from Table 2.1 that is above Iron should work as an inert element (or counter electrode) in the cell because, thermodynamically, this element would be more stable than the corroding metal. Iron would act as a cathode when coupled with Zinc, for instance, which is more electronegative. Usually platinum is chosen as a counter electrode in experiments because it is also an excellent catalyst for reactions to occur.

Table 2.1 - EMF Series

	Element
Noble (+)	Gold
	Platinum
	Copper
	Hydrogen
	Iron
	Chromium
	Zinc
	Aluminum
	Sodium
	Potassium

2.1.2 Instrumentation

The separation into electrodes (the cathode and the anode) allows for instrumentation of the system using gauges to measure potential differences and currents. It should be noticed that, since measured potential differences between the electrodes would be a net result of anodic and cathodic reaction potentials, an auxiliary element,

with an independent chemical reaction, has to be introduced in the cell in order to provide

a baseline value for the measurements. In laboratory experiments, the SCE scale is

typically used. This is illustrated in Figure 2.3.
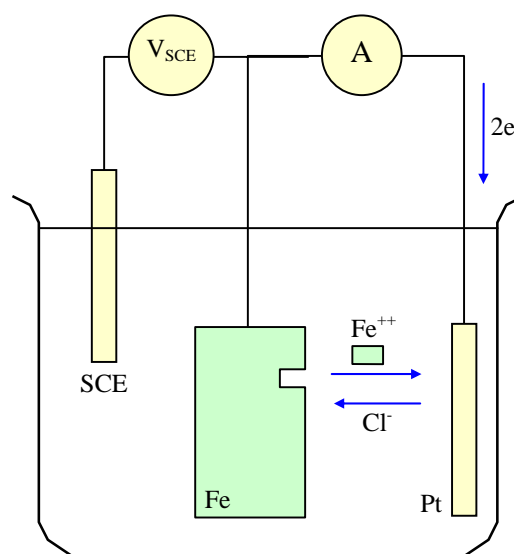
Figure 2.3 - Cell instrumentation

The SCE scale is given by the Saturated Calomel Electrode, which produces a

baseline potential of 241 mV above the equilibrium potential for hydrogen evolution.

Incidentally, this reaction would characterize another type of auxiliary electrode, the

Standard Hydrogen Electrode (SHE). Half-cell measurements made in the field usually

use a Copper-Copper Sulfate Electrode (CSE), which gives other values of potential for

the same reactions. The transformation between all these scales (and any other) is

straightforward and can be made as indicated in Figure 2.4.
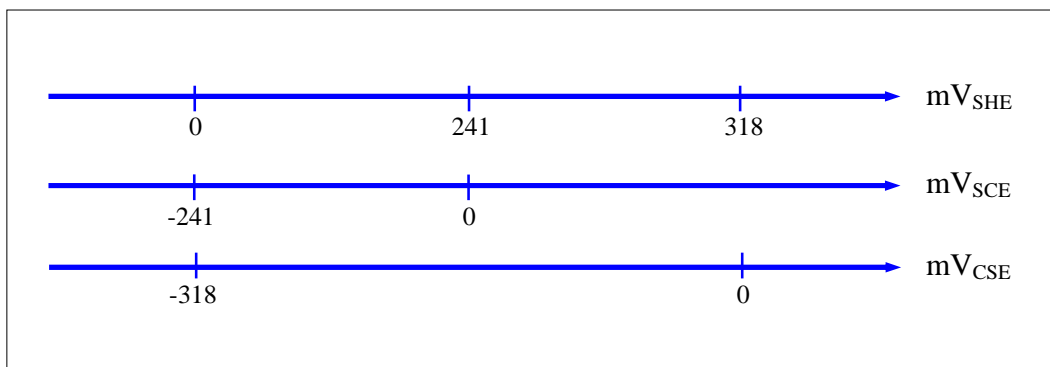
Figure 2.4 - Three scales given by different reference electrodes

In the figure, it can be seen that the saturated calomel electrode is 241 mV above the potential given by the hydrogen electrode and the copper-copper sulfate electrode is 318 mV above that potential. Thus, for instance, a potential of -447 mV$_{SHE}$ is equivalent to -688 mV$_{SCE}$ and to -765 mV$_{CSE}$.

2.2 THE BUTLER-VOLMER EQUATION

In the previous section, two electrochemical systems were illustrated and each one of them would parallel a purely electronic system (also illustrated). In an electronic system, the relationship between potential difference (E) and electric current (I) is given by the well-known Ohm's law (E = I R), where R is the system's electrical resistance. On the other hand, the existence of a liquid phase in the corroding systems creates a more complex situation, where metal-electrolyte interfaces and ionic mass transport play

important roles. Thus, in this case, and particularly at the interfaces, the relationship between potential and current is not linear, but exponential. This behavior is represented by one of the most fundamental equations in electrochemistry, namely the Butler-Volmer equation (see, for instance, Jones 1996 or Stansbury & Buchanan 2000):

$$i = i_0 \left(e^{2.3\frac{\eta}{\beta_a}} - e^{-2.3\frac{\eta}{\beta_c}} \right)$$

Equation 2.1

In Equation 2.1, the overpotential η (which is given by $\eta = E - E_o$, where E is the applied potential and E_o is the reaction's equilibrium potential) is exponentially related to the current density, i (which is given by $i = I/A$, where I is the current and A is the exposed area to the electrolyte). The exchange current density, i_o, can be found in the literature (see, for instance, Jones 1996) and represents the current flow (per unit of area) between products and reactants when the reaction is at equilibrium. The constants β_a and β_c are called Tafel constants, which were named after the German physical chemist Julius Tafel.

The Butler-Volmer equation is the analytical representation of the anodic and cathodic responses of an element in electrochemical equilibrium (both reactions occur at the same time and rate). Figure 2.5 shows a plot of each term of the equation, as well as their summation. It is important to notice that, at a certain distance from the origin, one of the terms becomes insignificant in relation to the other one, and straight lines result when a semi-log scale is used. In this case, it is a common practice to plot the potentials in the linear ordinate axis, while the current densities are plotted in the logarithmic abscissa axis. The slopes of each branch give the values of the Tafel constants for the

reaction. Another important aspect is that, in the linear plot, the behavior of the combined result (sum) is approximately a straight line when small values of potential are considered.
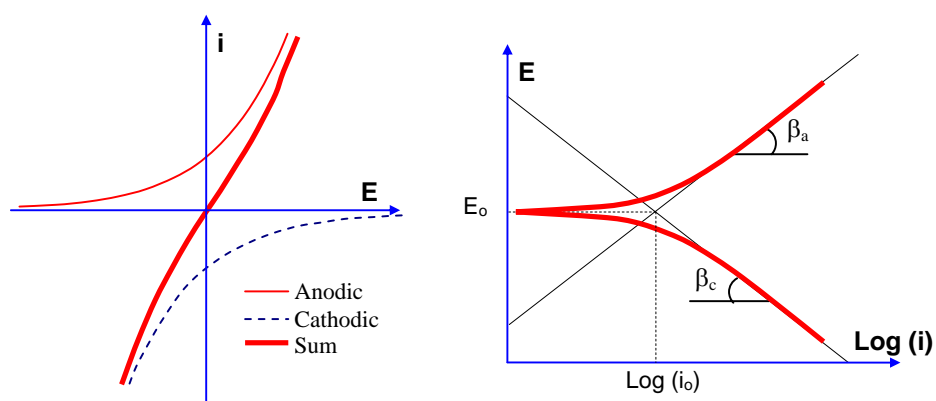
Figure 2.5 - Typical linear and semi-log plots of the Butler-Volmer equation

2.3 THE MIXED POTENTIAL THEORY

In order to analytically represent corrosion systems, a Butler-Volmer equation has to be written not only for the corroding (oxidizing) species, but also for every participating reducing reaction in the cell. The plots are then superimposed to obtain a final mixed result, which have to be described now by a Butler-Volmer equation with i_o and E_o renamed as i_{corr} and E_{corr}, respectively, since they are a result of this superposition and represent the entire cell. An example of anodic and cathodic reaction superimposition, producing a mixed plot, is given in Figure 2.6. The corrosion potential and corrosion current density can be found graphically from the mixed curve.
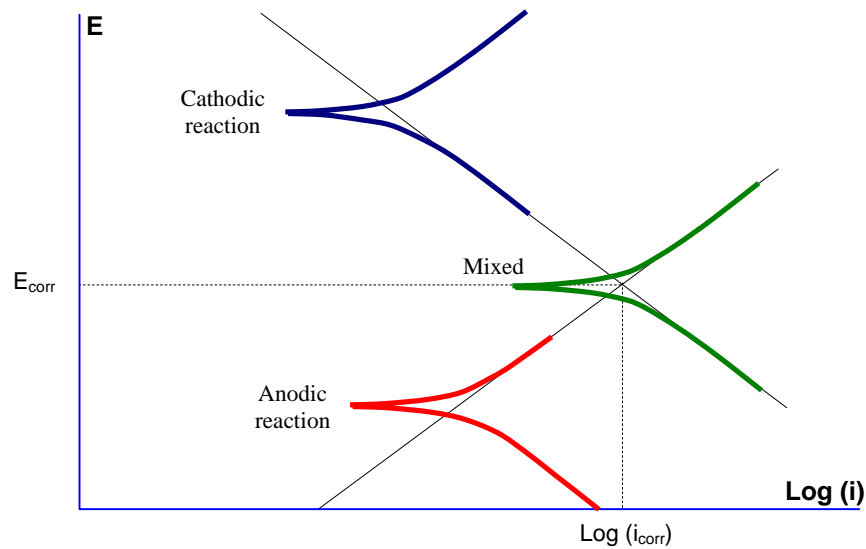
Figure 2.6 - The mixed-potential theory

An experimental result for a cell containing a segment of the prestressing strand used in this work in an electrolyte solution containing 1% by mass of CaO is given in Figure 2.7. As can be seen, differently from the theoretical curve, far from E_{corr}, passive response (i becomes independent of E) and transpassive behavior are present. A passive response can be expected in such a system because of the high pH (>12.5) of the electrolyte.
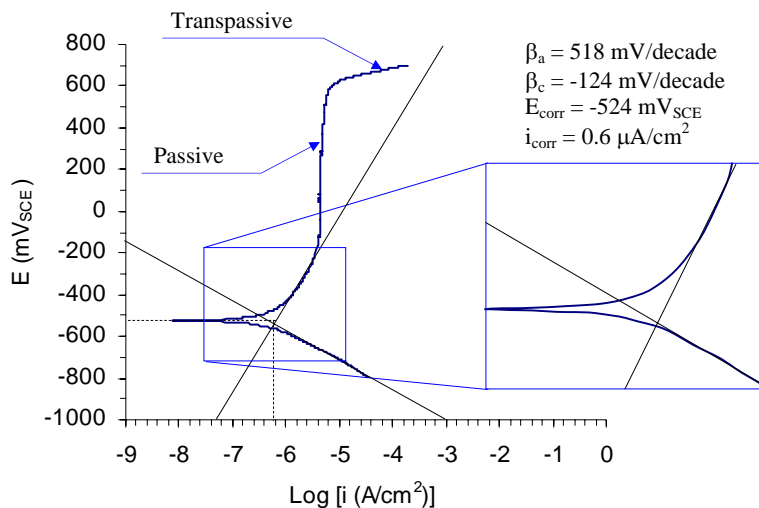
Figure 2.7 - Potentiodynamic behavior of steel in a 1% by mass CaO solution

From the potentiodynamic plot presented, additional considerations can be made. The first one is that, again differently from theoretical curves, the Tafel slopes do not meet at the E_{corr}-i_{corr} point and adjustments have to be made. The second is related to the units that Tafel constants are given (mV per decade). It can be noticed that their units should be something such as mV/Log (A/cm^2), since their calculation follows from $\Delta E/\Delta i$. However, that would be an awkward combination of units and it is usually preferred to report Tafel constants in variations of potentials in sets of ten units (or decade) of the Log scale. Typically, for simplicity, even the "decade" is frequently omitted and only the "mV" is kept as Tafel constant unit. Incidentally, authors mention (see, for instance Jones 1996) the need for a development of at least "one decade" of the Tafel slopes in order to be satisfactorily determined. In the example given above (and

commonly in grouted samples such as the ones tested in this work), the anodic Tafel

slope does not meet this criterion.

2.4 THE NERNST EQUATION AND pH EFFECTS

In one of the previous sections, the dissolution of steel was represented by the

following anodic half-cell reaction:

$$Fe \rightarrow Fe^{++} + 2e^{-}$$ **Equation 2.2**

This type of equation can be written in general form and in the cathodic direction as:

$$aA + mH^{+} + ne^{-} \rightarrow bB + dH_2O$$ **Equation 2.3**
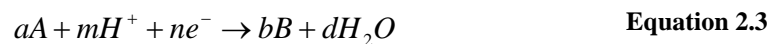
The equation that accounts for concentrations and activity of the elements involved

in such reactions is given by the Nernst equation (see Stansbury & Buchanan 2000):

$$E = E_0 + 2.303 \frac{RT}{nF} Log \frac{(A)^a (H^+)^m}{(B)^b (H_2O)^d}$$ **Equation 2.4**

where the parentheses indicate the activity of gases in atmospheres or a corrected value of

concentration in gram equivalents per liter for solutions. R is the universal gas constant,

T is the temperature in Kelvin, and F is the Faraday constant. E is the corrected value of

potential and E_o is the equilibrium potential of the reaction. When the appropriate values

of the constants are used and the hydrogen evolution equation ($2H^+ + 2e^- = H_2$ or, when

the solution is neutral or alkaline: $2H_2O + 2e^- = H_2 + 2OH^-$) is considered, the following

version of Equation 2.4 can be found, where E is given in mV_{SHE}:

$$E = -59\,pH$$
<div align="right">**Equation 2.5**</div>

The same calculations can be made for the oxygen reduction reaction ($O_2 + 4H^+ +$

$4e^- = 2H_2O$ or, when the solution is neutral or alkaline, $O_2 + 2H_2O + 4e^- = 4OH^-$), which

gives:

$$E = 1,229 - 59\,pH$$
<div align="right">**Equation 2.6**</div>

Upon plotting these two equations in a pH-potential or Pourbaix diagram, the

graph shown in Figure 2.8 is found, which shows the conditions of stability for water

according to values of potential and pH (detailed calculation can be found, for instance,

in Jones 1996).

Similar constructions can be made for any other element, including corroding

metals as steel. These would show the conditions that the metals would have to have in

order to corrode, be immune to corrosion, or even passivated.
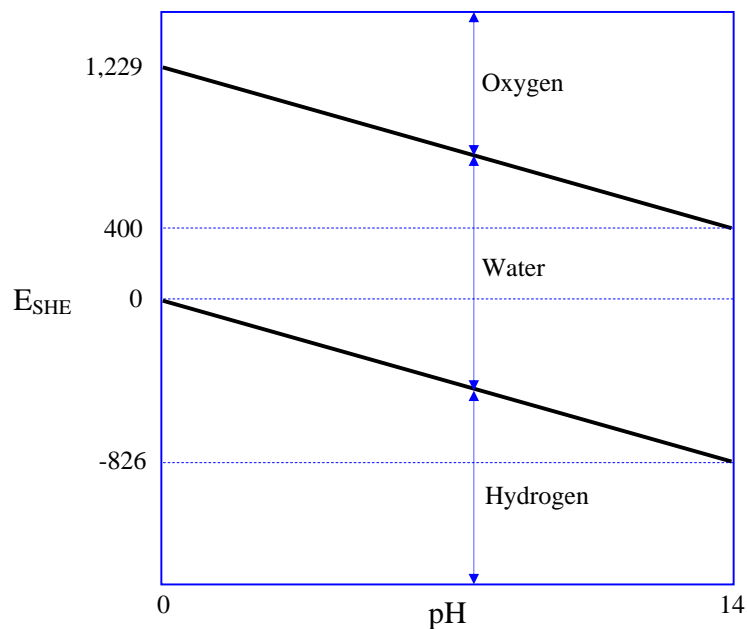
Figure 2.8 - Pourbaix diagram for water

2.5 THE VOLTAGE DROP EFFECT

Any electrochemical system inherently provides a certain degree of electrical resistance, which is variable according to the characteristics of each system. This is true even for pure electronic circuits that do not involve any aqueous phases. Naturally, in these circuits, the amount of resistivity is usually negligible, since metallic phases are excellent electric conductors. In electrochemical circuits, however, the error generated in measurements because the voltage applied is reduced by a certain amount in the electrolyte can be important and has to be minimized or compensated accordingly.

One of the most used methods to compensate for voltage drops is the one known as the Current Interruption Method (Escalante 1990). In this method, the current is interrupted at certain instants, with consequent drop of the potential being applied. Part of this potential has an instantaneous character because it is a result of the IR wasted in the electrolyte, i.e., the voltage drop error. Through extrapolation of the transient part of the potential that is tending to return to an equilibrium value, a very precise approximation of the instantaneous potential drop can be determined. With the amount of voltage drop due to the system resistivity determined, the error is compensated as the experiment is run. This process is illustrated in Figure 2.9.
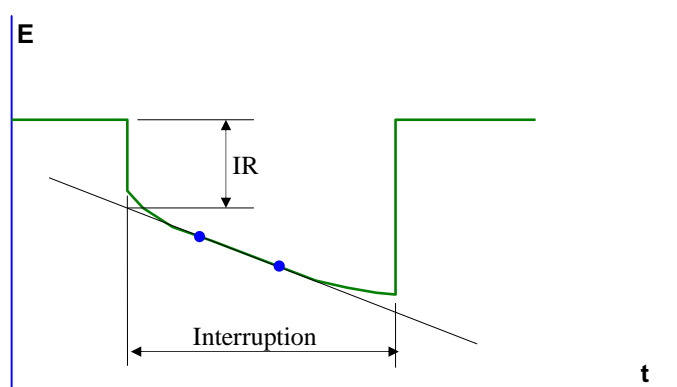
Figure 2.9 - IR compensation by current interruption

Another method used to compensate such errors is the Positive Feedback method (Berke 1990). This method consists of feeding a determined portion of the output

potential back into the potentiostat. That portion redirected depends on the system being tested and is difficult to determine.

2.6 EXPERIMENTAL TECHNIQUES

Several techniques can be used to assess different aspects of materials and conditions of a given electrochemical system. They can be classified according to the nature of their electrical signal as DC (direct current) and AC (alternate current) techniques. DC methods are the ones most used in laboratorial and field applications due to their relative simplicity in use and data interpretation. They involve an application of either current or voltage with respective measurement of voltage or current. On the other hand, while AC techniques measure the same variables, they need to be considered in a time frame. Consequently, the data analysis is typically processed in a frequency domain.

Examples of DC methods are Polarization Corrosion, Potentiostatic Polarization, Linear Polarization Resistance (LPR), and Potentiodynamic Polarization. Examples of AC techniques are Electrochemical Impedance Spectroscopy (EIS) and Electrochemical Noise (for details on these methods, see, for instance, Jones 1996 or Stansbury & Buchanan 2000). DC techniques are the ones used for the methodology behind this work and are therefore detailed next.

2.6.1 The Polarization Corrosion Method

This method, also known as the Half-Cell Potential method, consists on the measurement of the equilibrium potential of corroding cells, E_{corr}. Although a regular voltmeter can be used for this task, one must consider the fact that corrosion potential measurements need time to reach a steady-state condition. The time necessary to obtain a stable measurement depends upon the corroding cell characteristics, and may vary from a few minutes to several hours.
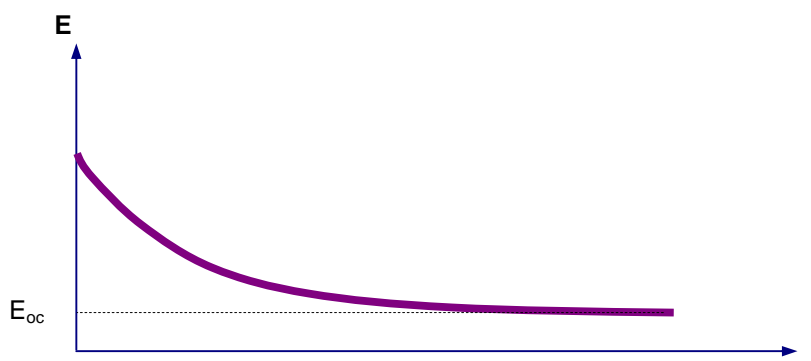
Figure 2.10 - Typical output plot from a polarization corrosion test

This method is widely used to monitor corrosion activity of reinforced concrete structures in the field. The values given in Table 2.2 indicate the probability of corrosion for different magnitudes of half-cell measurements (ASTM C876 1999).

Table 2.2 - Probability of corrosion for different corrosion potentials

E_{corr} (mV$_{CSE}$[*])	E_{corr} (mV$_{SCE}$[**])	Probability
More positive than -200	More positive than –461	Higher than 90% that no corrosion is occurring
Between –200 and -350	Between –461 and –611	Corrosion is uncertain
More negative than -350	More negative than –611	Higher than 90% that corrosion is occurring

* The half-cell reaction is given by a copper-copper sulfate reference electrode.
** The half-cell reaction is given by a (standard) calomel reference electrode.

2.6.2 The Potentiodynamic Polarization Method

During a potentiodynamic polarization test, or polarization scan, a relatively large range of potentials (e.g., ± 250 mV or even ± 600 mV) is applied on the corroding metal and the correspondent current values are measured. The pair of values is typically plotted in a semi-log scale in order to allow the identification of the Tafel slopes (β_a and β_c). The intersection of lines extrapolated from these slopes give the pair of values corresponding to the E_{corr} and i_{corr} of the ongoing electrochemical reaction.
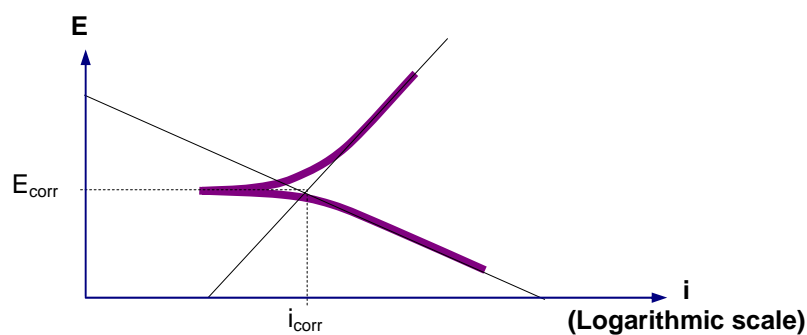
Figure 2.11 - Typical output plot from a potentiodynamic polarization test

This electrochemical method is very popular in corrosion investigations in laboratory because it allows a complete description of the corrosion behavior of a system. Procedures for this method can be found in ASTM G 5 (1999) "Standard Reference Test Method for Making Potentiostatic and Potentiodynamic Anodic Polarization Measurements".

2.6.3 The Linear Polarization Resistance Method (LPR)

The LPR is another technique largely applied to reinforced concrete structures in the field due to simplicity in application and data interpretation. Although the procedure follows the same idea behind the Polarization Scan method, the range of potentials applied to the corroding metal is considerably small (typically $\pm$ 20 mV). This small range of potentials is used because only a short region around the inflection point between the anodic and cathodic responses can be approximated by a linear function.

The information gathered from LPR readings is comprised of the system polarization resistance ($R_p = \Delta E/\Delta i$) calculated at zero current density, and by i_{corr}, which is also considered a measure of the system's corrosion rate (ASTM G102 1999). The corrosion rate, however, should be carefully considered since it relates to the polarization resistance value through Tafel constants (β_a and β_c), which are typically assumed values for a certain system. For instance, LPR equipment used to assess concrete structures typically use β_a and β_c ranging from 112 to 224 mV.
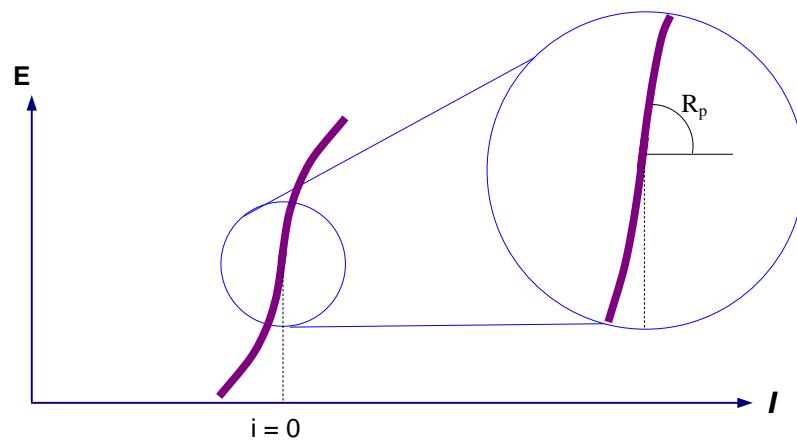
Figure 2.12 - Typical output plot from a LPR test

Procedures for this method can be found in ASTM G59 (1997) "Standard Test Method for Conducting Potentiodynamic Polarization Resistance Measurements", where the relationship between Tafel constants, polarization resistance and corrosion rate is given by:

$$i_{corr} = \frac{\beta_a \beta_c}{2.303(\beta_a + \beta_c)} \frac{1}{R_p}$$

Equation 2.7

2.6.4 The Potentiostatic Polarization Method

The potentiostatic test is characterized by the application of steps of potential on the corroding metal in order to acquire correspondent current values. Although, similar

plots to the ones resulted from a polarization scan can be obtained (ASTM G5 1999), it is

the result gathered when only one potential step is used that is of particular interest for

this research. A one-step potentiostatic procedure is the basis for the Accelerated

Corrosion Test (ACT), which is used to assess grouts regarding their degree of corrosion

protection. The ACT is detailed next.

2.7 CORROSION SERVICE LIFE PREDICTION

The service life of a structure can be divided between an Initiation Period, which

starts with the construction of the structure and ends at the depassivation of the

reinforcement, and a Corrosion Period, which starts with the reinforcement depassivation

and ends with a critical structural condition. This is illustrated in Figure 2.13.
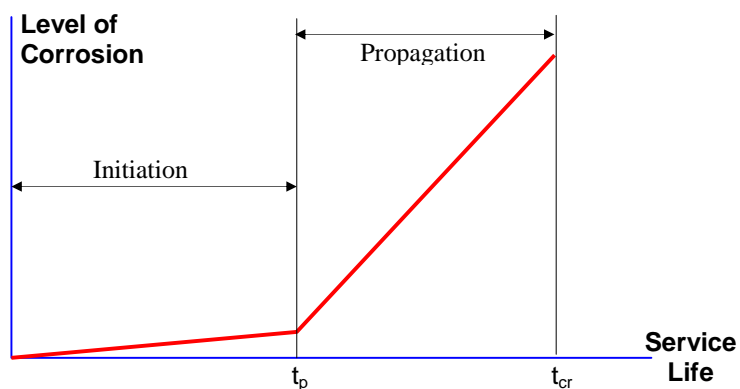
Figure 2.13 - Service life stages related to structural corrosive processes

The corrosion period can be divided in depassivation, propagation, and critical stages. Depassivation is the loss of the passive layer by the reinforcement, and takes an initiation period t_p to be completed, due to carbonation or action of aggressive agents. During the propagation period, the structure is severely affected by corrosion in a steady state rate, which culminates with the critical stage, characterized by spalling and intense cracking and staining of the structure. The structural service life is therefore given by the critical time, which is the sum of the initiation plus the propagation periods. The initiation period is usually assessed from diffusivity and permeability properties, while the propagation period would be related to the internal distress caused by the increasing volume of corrosion products.

2.8 ADDITIONAL CONSIDERATIONS

2.8.1 Faraday's Law and the Corrosion Rate

The relationship between current and mass loss is given by Faraday's law:

$$m = \frac{Ita}{nF}$$

Equation 2.8

where F is Faraday's constant (96,497 C), n is the number of electrons per moles of metal oxidized, a is the atomic weight, and t the time elapsed of corrosion. Dividing both sides by the area (A) of the metal being dissolved, by the time (t) of the dissolution, by the

metal density (d), and considering that a/n is the equivalent weight (W) of the metal, the

equation above can be rewritten for corrosion rate (r) in units of length per a certain time

as:

$$r = \frac{W}{dF} i_{corr}$$

<div align="right">**Equation 2.9**</div>

where i_{corr} is the current density measured in the corrosion process. Therefore, corrosion

current density is directly proportional to corrosion rates and, because of this, many

authors simplify and refer to corrosion current densities merely as corrosion rates.

When steel is considered, Equation 2.9 can be rewritten as:

$$r = 11,594 i_{corr}$$

<div align="right">**Equation 2.10**</div>

where r is given in mm/year for corrosion current densities in A/cm^2.

2.8.2 Faraday's Law and the Gravimetric mass loss

A common experimental procedure used to determine corrosion rates of samples

is to weigh the amount of mass loss by the metal during its oxidation. The initial and

final masses are determined and, by subtraction, the mass loss is found. With the mass

lost during the corrosion process (m), Equation 2.8 can be used again to obtain:

$$i_{corr} = \frac{F}{W} \frac{m}{At}$$

<div align="right">**Equation 2.11**</div>

The difficult part of applying this method is the necessity of precise measurements of mass loss to minimize errors, which is a complicated task to be accomplished because the removal of the corroded material from specimens is likely to accidentally removing non-corroded material as well as leaving behind undetected corrosion products.

2.8.3 The Accelerated Corrosion Test (ACT)

The ACT test is being currently recommended by the Post-Tensioning Institute for assessment of the corrosion resistance of post-tensioning portland cement grouts (PTI 2003). The ACT subjects specimens composed of segments of grouted post-tensioning strands to a constant potential of +200 mV_{SCE}, while current values are monitored. The specimens should be immersed in a saltwater solution of 5% NaCl by mass.

The test is finished when all specimens being tested fail due to intense corrosion development that is detected from an abrupt increase in the monitored electric current. This is illustrated in Figure 2.14. The averaged time required for each of the specimens to fail, t_{corr}, is then computed for characterization of the tested grout.
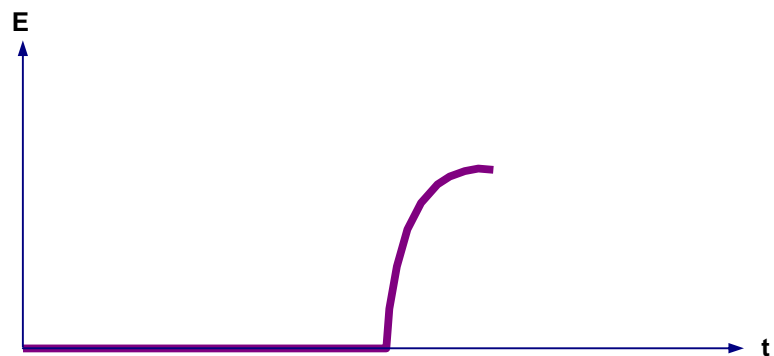
Figure 2.14 - Typical output plot from ACT tests

Currently, PTI specifies that a given grout will satisfy an ACT test if its t_{corr} is greater than or equal to the t_{corr} obtained for a plain grout (only cement and water) at a water-cementitious ratio of 0.45. In addition, it is recommended by some state Departments of Transportation that t_{corr} values reach at least 1,000 hours (or 42 days of test duration) for final acceptance of grouts for post-tensioning applications based on the commentary discussion in the PTI specification (PTI 2003).

3 EXPERIMENTAL PROGRAM

This chapter presents the elements that composed the experimental investigation. It starts with a definition of the groups to be tested based on the study variables and the test methods utilized, and give details such as number of specimens and the testing sequence. Then, the equipment used for the manufacture of the specimens as well as the setups used in the tests are specified.

3.1 EXPERIMENTAL PROGRAM PLAN

3.1.1 Grout Groups

Five different grout groups were selected for the experimental program: prepackaged, with fly ash, with silica fume, with corrosion inhibitor, and with no admixtures (plain). The main idea when defining these groups was to obtain a variety of performance levels during the tests. Grouts that were available from the market (prepackaged grouts) were expected to give the best performances during the experimental program due to low water-cementitious ratios used, producing values at the higher end of a spectrum of values for the parameters to be measured. Grouts with fly ash in their mixture were also expected to perform well due to the increased resistivity typically conferred by fly ashes (Schokker 1999). Their performance, however, was known to be sensitive to curing periods, since fly ashes tend to hydrate at lower rates

when compared with cement. Silica fume grouts were expected to perform satisfactorily

if the amount of cement replaced by the admixture were appropriate. Grouts with

corrosion inhibitors in their mixture had to be selected for the experiments, since too little

is known about their performance in ACTs. The main difficulty is related to their

dosages, since the amounts given by manufacturers are amounts recommended for

concrete, instead of grout. Finally, in order to obtain baseline results that could be

compared with the other groups, which contained mineral and chemical admixtures, a

plain grout group was also considered for the experimental program.

3.1.2 Variables

One of the variables of the study was the curing age of fly ash grouts. The curing

age of this group was varied in order to make possible the determination of the minimum

period that a fly ash grout should be moist cured to develop a satisfactory performance in

an ACT experiment.

The replacement amount of silica fume in grouts was also varied, defining another

variable of the study. This variable tried to define the replacement amount that produces

the best result for silica fume grouts.

The most important variable, however, due to its significance to the testing and

approval of post-tensioning grouts, was the compensation for IR drop effects in ACTs.

The spectrum of grout performances and resistivities that was achieved throughout the

experimental program, with different groups and grout conditions, was intended to

determine significant discrepancy in magnitudes generated when compensation is not

available in electrochemical systems used to conduct ACT tests. Moreover, the

determination of these discrepancies was aimed at the assessment of the ACT practices

currently in use that are recommended by the Post-Tensioning Institute and, for instance,

the Florida DOT.

Crossing specific values of the three variables (curing period, amount of silica fume

replacement, and IR drop compensation) and the five groups (plain, with fly ash, with

silica fume, with corrosion inhibitor, and prepackaged), Table 3.1 was obtained.

Naturally, the amount of silica fume is only considered in the silica fume group.

Table 3.1 - Combination of variables for the experimental program

Grout Group	Curing Period (days)	IR Drop Compensation
Plain grout	7, 14, 21, 28, 56	Yes and No (7, 28, 56)
Fly ash grout (30% of Type F)	7, 28, 56	Yes and No
Silica fume grout (3, 5, and 7%)	7,28, 56	Yes and No (28)
3 corrosion inhibitor grouts	28	Yes and No
5 prepackaged grouts	28	Yes

The plain grout, which was the control group, was tested for five different curing

periods (7, 14, 21, 28, and 56 days), in order to detail its gain in performance at early

ages. All these ages were tested with IR drop compensation. In addition, three ages (7,

28, and 56 days) were tested without compensation to determine the overall effect of IR drop from various curing times. The same approach was considered for the fly ash grout group, but with no detailing of the gain in performance at early ages (14 and 21 days). For this group, a 30% replacement of the cement mass by fly ash was specified. This large amount was considered to make the effects of the admixture more significant. Type F fly ash is the type commonly used in the region and was the one available in the laboratory for the experiment program.

Three percentages of microsilica were chosen (3, 5, and 7%), considering that a low percentage should have been the optimum amount. The percentages chosen were tested at three different ages (7, 28, and 56 days) with compensation for voltage drops, while only the age of 28 days was considered with no compensation.

Three corrosion inhibitors were selected for the tests according to a criterion of active ingredients in their formula, which were different from each other. One corrosion inhibitor was based on calcium nitrite, a largely used inhibitor in structural concrete because of its renowned performance, but that had limited results in previous investigations with grout (Hamilton 1995, Koester 1995, Schokker 1999). Another corrosion inhibitor was based on organic chemicals, while the other one is a combination of organic and inorganic products. The three corrosion inhibitors were tested with and without voltage drop compensation only at 28 days of curing, since performance curves with time were considered in other groups.

Five prepackaged grouts were selected for the experimental program because of their important participation in the market and their availability. These grouts were considered only with IR drop compensation since the effects of various admixtures on IR

compensation were established with the other tests in Table 3.1. The testing times could have been considerably long otherwise.

3.1.3 Tests and measurements

The experimental program was based upon a sequence of electrochemical tests that were executed for each grout condition specified previously. Additional observations and measurements were also accomplished to determine specific conditions that would occur on corrosion cells, and to characterize the subjects tested.

3.1.3.1 Electrochemical Tests

Among the numerous electrochemical methods commonly used in electrochemistry and that were available in the systems acquired for the experiments, four methods were chosen due to their simplicity and popularity: the corrosion potential test, the potentiostatic polarization test, the potentiodynamic polarization test, and the potentiodynamic linear polarization resistance (LPR) test.

The choice for the corrosion potential test was justified with the possibility that the open circuit potential, E_{oc}, the parameter obtained in that test, could work as an indicator of grout corrosion performance (Koester 1995).

The potentiostatic polarization test is the basis of the ACT method and therefore had to be considered in the experimental program. Its product, specifically the time-to-corrosion (t_{corr}) is associated with a grout's degree of corrosion protection, which is key information when considering IR drop implications on grout approval. The potentiostatic polarization test is going to be referred to in this work many times as "the potentiostatic test" and, since it was applied to ACT specimens, as "the ACT test" as well, mainly when limitations on grout approval are cited. The reference "ACT test or method" is also used to identify the method currently specified by the Post-Tensioning Institute for testing of grouts regarding their corrosion protection.

The other two types of tests were chosen because of their simplicity and classical role in electrochemistry. Moreover, they can be used to determine the corrosion rate (i_{corr}), which was likely to be associated with grouts' corrosion protection (Hamilton 1995, 2000). The potentiodynamic linear polarization resistance test, which is going to be referred to in this work as "linear polarization resistance test", "polarization resistance test", or merely as "LPR", provides a measurement of resistance to the currents observed in a corrosion cell. Therefore, it is reasonable to infer that grouts producing higher polarization resistances would tend to protect post-tensioning strands for longer periods. The potentiodynamic polarization test, which is going to be addressed in this work as "the Tafel scan" or merely as "the potentiodynamic test", provides measures of several electrochemical parameters.

The settings initially used in each of the electrochemical tests mentioned above are presented in Table 3.2

Table 3.2 - Settings for each electrochemical test

Test	Value
Corrosion Potential:	
Sample period (min)	0.2
Potentiostatic:	
Sample period (min)	30
Initial E (mV$_{SCE}$)	+200
Potentiodynamic:	
Initial E (mV) vs. E$_{oc}$	–250
Final E (mV) vs. E$_{oc}$	+250
Scan rate (mV/s)	5
Sample period (s)	1
Linear Polarization Resistance:	
Initial E (mV) vs. E$_{oc}$	–20
Final E (mV) vs. E$_{oc}$	+20
Scan rate (mV/s)	0.5
Sample period (s)	0.2

It should be noted that the potential used in the potentiostatic test (+200 mV$_{SCE}$) is the same potential specified by PTI. Additionally, the potentials shown for the potentiodynamic tests were tentative and had to be adjusted several times as the work progressed in order to better define Tafel slopes (one-decade long slopes).

3.1.3.2 Additional measurements

Preliminary potentiostatic tests in this work indicated that the failure of the grout protection would tend to occur typically at the top of the specimens' testing regions and would more likely face counter electrodes. The cause of this probable concentration of current gradients at the top part of testing regions was assumed to be the short length of

the counter electrodes adopted in those tests (8.5 cm or 3.3 in.). It was decided then, among the options considered (such as the adoption of more than one counter electrode in the cells, or even curving them around the specimens), to replace the counter electrodes being used with longer ones, which were 17 cm (6.7 in.) long, and to monitor the occurrence of the first spots of corrosion. Figure 3.1 shows the referential system used during this monitoring. Not only were the first signs of corrosion products registered along the testing region of specimens, but also around their periphery.
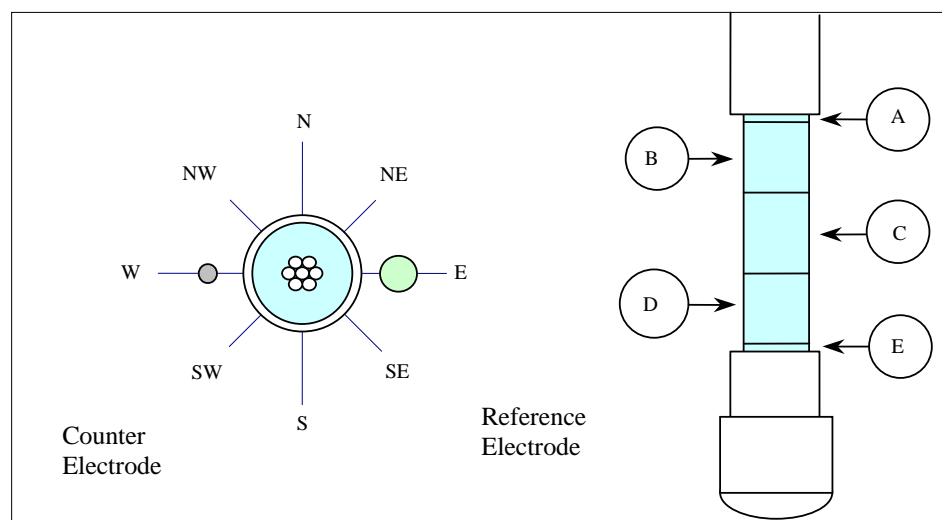
Figure 3.1 - Referential system used to locate first spots of corrosion on ACT specimens

Additionally, in order to characterize the different grouts tested (each grout specimen resulting from a certain condition applied to a certain grout group), determinations of volume of permeable voids, which is considered in this work a measure

of the grout's porosity, were accomplished according to ASTM C642 (1997) "Standard test Method for Density, Absorption, and Voids in Hardened Concrete". The characterization of each grout was important because their qualification with respect to porosity corroborated and explained their performances during the electrochemical tests.

The grouts were also characterized by the amount of electric charge that passed through their thickness during the potentiostatic tests. The values of charge were calculated considering the times-to-corrosion in each cell and the passing current values below 10 mA. Further details about this measurement are given in Chapter 4.

3.1.4 Nomenclature

In order to easily identify the different test conditions executed during the experiments and during the discussion and presentation of the results in this document (Chapters 4 and 5), a codified nomenclature was created. It is composed, at the beginning, by two or three letters, followed by two digits, and a final letter. The two letters at the beginning of the test codes indicate the grout group (PG: plain grout, PP: prepackaged, CI: corrosion inhibitor, FA: fly ash, and SF: silica fume). A third letter only occurs in the corrosion inhibitor group, in order to identify one of the three inhibitors used (A, B, or C). The following two digits indicate the curing period of the grout (07, 14, 21, 28, or 56 days). The ending letter indicates whether the test was accomplished with IR drop compensation (Y), or without (N). Table 3.3 gives all the codes that were used to identify each one of the 37 different conditions that were tested.

Only potentiostatic tests were considered for tests with no compensation for voltage drops. Hence, when results concerning other electrochemical tests are presented in this document (potentiodynamic or LPR tests), many times the last letter of the test code is omitted, meaning that the parameters presented were obtained from tests that were accomplished under compensated conditions, even if their potentiostatic tests were run without compensation.

Table 3.3 – Nomenclature used throughout the work

Grout Group/Description	Test Identification
Prepackaged Grouts (w/c = variable)	
The five grout types should be moist cured for 28 days. ACT should compensate for IR effects.	PP A 28Y; PP B 28Y; PP C 28Y PP D 28Y; PP E 28Y
Plain Grouts (w/c = 0.45)	
Moist cured for 7, 14, 21, 28, and 56. IR drop compensation on and off.	PG 07Y; PG 14Y; PG 21Y PG 28Y; PG 56Y PG 07N; PG 28N; PG 56N
Grouts with Corrosion Inhibitor (w/c = 0.45)	
The grouts with each of the three corrosion inhibitors should be moist cured for 28 days. IR compensation on and off.	CI A 28Y; CI B 28Y; CI C 28Y CI A 28N; CI B 28N; CI C 28N
Silica Fume Grouts (w/c = 0.45)	
Cement replacement of 3, 5, and 7% of silica fume. Moist cured for 7, 28, and 56 days. IR compensation on and off.	SF3 7Y; SF3 28Y; SF3 56Y SF5 7Y; SF5 28Y; SF5 56Y SF7 7Y; SF7 28Y; SF7 56Y SF3 28N; SF 28N; SF7 28N
Type F Fly Ash Grouts (w/c = 0.45)	
Cement replacement of 30% of fly ash. The grouts should be moist cured for 7, 28, and 56 days. IR compensation on and off.	FA 7Y; FA 28Y; FA 56Y FA 7Y; FA 28N; FA 56Y

It should be noticed from the table that all mixtures produced in the lab (non-prepackaged) were mixed with a 0.45 water-cementitious ratio. This ratio is currently specified by PTI to be used in ACT control mixes and, therefore, was adopted for the other mixes as well for comparison purposes.

3.1.5 Materials

The cement used to obtain the four grouts produced in the laboratory was a Type II cement fabricated by Lafarge Co. (cement mill test report is given in Appendix D). This type of cement was chosen because, due to lower amounts of C_3A in its formulation when compared, for instance, with Type I, the curing process tends to generate less heat at a slower rate, which is likely to minimize distress and shrinkage cracking in the grouts.

The batch water used was initially intended to be a deionized one, with conductivities as low as 0.20 $\mu S/cm$. However, a malfunction in the laboratory deionizer was detected only after most of the tests had been executed and, for consistency sake, tap water was then used since no significant conductance difference between the two waters was detected. The effect of this problem on the test results and the differences in ACTs in general due to low and high conductivity waters are currently unknown. More details are given in Chapter 5.

As commented previously, the fly ash used was a Class F fly ash, which is less reactive than Class C ashes due to lower quantities of CaO (less than 10% compared to 10 to 30%). The criterion to favor one instead of the other, however, was only the

availability of the material. The condensed silica fume used was provided by Elkem

Materials, Inc.

The five prepackaged grouts chosen for the experimental program are given in

Table 3.4. The water-cementitious ratios shown are suggested values by the

manufacturers.

Table 3.4 - Code, denomination, and w/c ratio of the prepackaged grouts

Product Code	Product Denomination	w/c
A	Sika Cable Grout	0.23
B	W. R. Grace DCI Five Star Special Grout 400	0.27
C	Master Builders Masterflow 816	0.33
D	Master Builders Masterflow 1205	0.30
E	Sika Cable Grout Repair	0.27

The corrosion inhibitors used, which are based on different active ingredients, are

given in Table 3.5. A difficulty with their use was related to the necessary dosages to use

for the grouts, since they are intended for use in concrete.

The amount used for the inhibitor B was adapted, as a suggestion of the

manufacturer, from 15 L per m^3 of concrete (3 gal per yd^3) to 55 L per m^3 of grout (11.3

gal/yd^3), while the amount for inhibitor C was recommended to remain at the same

amount commonly used in concrete: 5 L/m^3 (1 gal/yd^3).

Table 3.5 - Code, denomination, and amounts used for the corrosion inhibitors

Code	Product Denomination	Amount Used	Active Ingredients	Notes
A	W. R. Grace DCI	121 L per m^3 of grout (24.44 gal/yd^3)	Ca(NO$_2$)$_2$ (Calcium nitrite)	1 L replaces 0.84 L (0.14 gal/lb); Added to water
B	Sika FerroGard901	55 L per m^3 of grout (11.3 gal/yd^3)	Organic and inorganic (Aqueous amino alcohol solution)	1L replaces 1 L (0.12 gal/lb); Added to grout.
C	Master Builders Rheocrete 222+	5 L per m^3 of grout (1 gal/yd^3)	Organic (Aqueous Amines and Esters solution)	Added to water

The recommended amount of inhibitor A in structural concrete is of 30 L per m^3 of concrete (6 gal/yd^3), as a maximum (higher amounts accelerate the setting time of concrete). Hamilton (1999) used 29 L/m^3 in his work, with poor ACT results. Koester (1995), through contacts with the product manufacturer, increased the amount used to 80 L/m^3 with still unsatisfactory ACT results. In this work, based on the amount of chlorides in the corrosion cells and extrapolation of the dosages given by the manufacturer together with the amount used by Koester, the amount of the inhibitor A was increased to 121 L/m^3.

3.1.6 Number of replicates

The number of specimens used in each of the experiments was determined based upon three aspects: power analyses of the experiments (see, for instance, Kraemer & Thiemann 1987 or Cohen 1988), the number of stations available, and a time limit of two years. Considering the power analyses, the number of specimens were based upon a significance level of 5% and a power of 80%, i.e., each test considered probabilities of 5% (alpha) and 20% (beta) of Type I and Type II errors to occur, respectively. A Type I error occurs when a null hypothesis (e.g.: "there is no difference between two grout test results") is wrongly rejected, while a Type II error occurs when this null hypothesis is wrongly accepted. The final numbers, which are shown in Table 3.6, were then defined after consideration of the other two aspects (number of stations available and the time limit of two years).

Table 3.6 - Grout tests and their sample sizes

GROUP	n = 8	n = 4
PLAIN	PG 07Y, PG 14Y, PG 21Y, PG 28Y, PG 56Y PG 07N, PG 28N, PG 56N	–
PREPACKAGED	PP A 28Y, PP B 28Y, PP C 28Y PP D 28Y, PP E 28Y	–
WITH CORROSION INHIBITOR	CI C 28Y CI C 28N	CI A 28Y, CI B 28Y CI A 28N, CI B 28N
WITH SILICA FUME	–	SF3 07Y, SF3 28Y, SF3 28N, SF3 56Y SF5 07Y, SF5 28Y, SF5 28N, SF5 56Y SF7 07Y, SF7 28Y, SF7 28N, SF7 56Y
WITH FLY ASH	–	FA 07Y, FA 28Y, FA 56Y FA 07N, FA 28N, FA 56N

3.1.7 Testing Sequence

The testing sequence illustrated in Figure 3.2 was planned in order to minimize the number of specimens to be cast for each grout condition (8 or 4) and was based on two basic assumptions. The first assumption is that specimens presenting defects that are likely to affect potentiostatic results (such as air bubbles and voids) would amount to a maximum of 2 (occurrence of 20 to 33% of defective specimens), but could still be used in potentiodynamic tests, since these tests take considerably less time to run. The second assumption is that LPR measurements should not impose any significant changes on ACT specimens that would prevent them to be used in potentiostatic tests, since LPR polarization potentials (± 20 mV vs. E_{oc}) are significantly low, when compared with the potential that was applied in the potentiostatic tests ($+200$ mV$_{SCE}$ or, approximately, $+440$ mV vs. E_{oc}).

The first step in the sequence was to take two specimens (either with or without defects) per grout condition for potentiodynamic measurements to obtain the corrosion behavior of the specimens for passive (undamaged) conditions. Grouts that were going to be tested in uncompensated potentiostatic tests contributed two more specimens, doubling the number of results in this step for those grouts. The potentiodynamic curves obtained with this step allowed the determination of corrosion potentials (E_{corr}), corrosion rates (i_{corr}), and Tafel constants (βa, βc, and constant B).
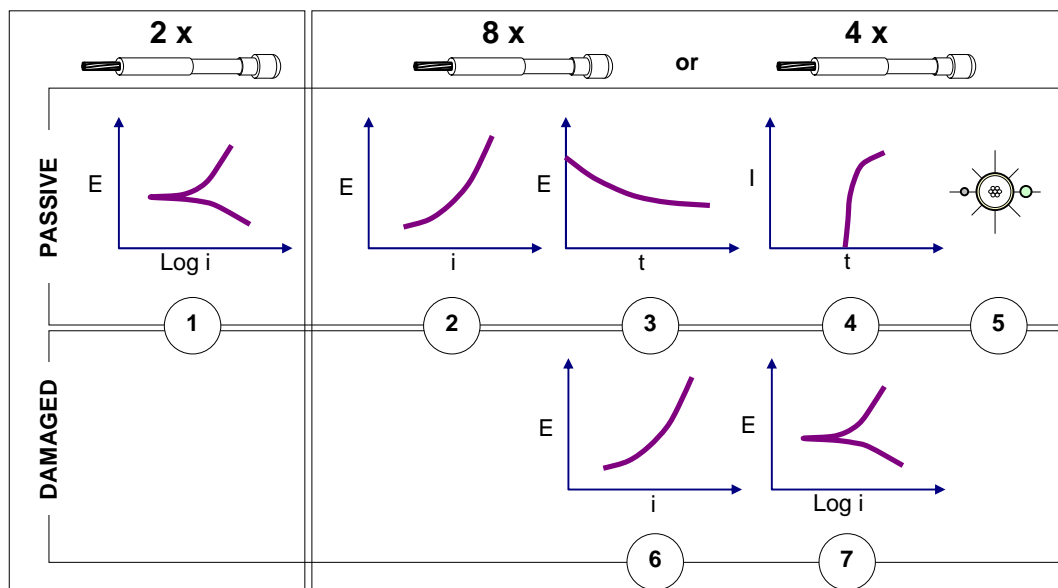
Figure 3.2 - Testing sequence for one grout condition

In the second step, eight remaining specimens (four in the cases specified in Table 3.6), free of defects, were used in LPR measurements. Again, grouts that were going to be tested in uncompensated potentiostatic tests contributed with more specimens, doubling the number of results. The polarization resistances, R_p, for the passive conditions of the specimens were then determined.

As a third step in the sequence, the open circuit potentials, E_{oc}, were determined in polarization corrosion measurements. Eight (four in the cases specified in Table 3.6) results were determined for each grout condition. Once again, this number would double when considering the results for grouts intended for uncompensated ACTs.

The fourth step was the execution of the potentiostatic tests. Upon finishing the corrosion polarization measurements, the measurements would start, providing after a period of 16 ± 2 days, on average, the t_{corr} values for the grouts tested.

The fifth step was the location, for each specimen, of the first spot of corrosion. In order to more easily identify the location of the first spot, the level of damaged imposed on the specimens should not be severe. Therefore, after the specimens experienced current not higher than 20 mA, the cable to the stations would be disconnected. The pictures shown in Figure 3.3 illustrate how difficult the identification of the local where the corrosion products first occurred may be for high levels of corrosion.

Figure 3.3 - Volume of corrosion products for low and high level of currents

After the corrosion of the specimens, the sixth and seventh steps would be accomplished. The specimens would be run again, first in LPR tests, and then in

potentiodynamic scans in order to determine the variables collected during the first two steps for damaged conditions. In addition to this sequence of tests, samples of each grout were collected to determine their volume of permeable voids for grout characterization and potentiodynamic tests with steel samples not encased by grout were executed.

3.2 SPECIMEN MANUFACTURE AND RELATED APPARATUS

The ACT specimen, which is represented in Figure 3.4, is a fundamental part of this study. The main idea behind its conception is to expose a fixed amount of strand incased in grout to an aggressive media, an electrolyte, in which corrosion is facilitated.

The critical part of the specimen is the testing region (*c*, in the figure). Prior to testing, careful visual examination of this region is necessary in order to check for defects such as cracks and voids left by air pockets or bubbles. These kinds of occurrences would weaken the grouts' capability to protect the strand, skewing test results.
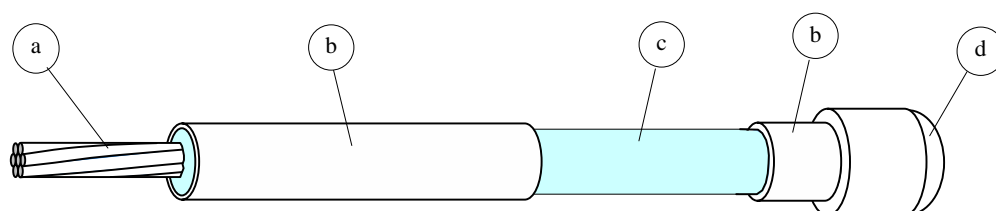
a: Seven-wire post-tensioning steel strand. Length: 360 mm (14 in.). Diameter: 12.7 mm (0.5 in.)

b: Clear plastic Tubing. Longer length: 150 mm (6 in.). Shorter length: 60 mm (2.4 in.)

c: Testing Region (exposed grout). Diameter: 25.4 mm (1 in.). Length: 90 mm (3.5 in.)

d: 25.4 mm (1 in.) plastic cap.

Figure 3.4 – Schematic of the specimens used

The fabrication of the specimens necessary for this study was comprised of four distinctive steps. First, each part of the casing assemblage that would be part of the specimen was prepared. Then, the parts were appropriately assembled together to form the required number of casings. Finally, the casting and curing steps took place. This sequence is represented in Figure 3.5 and is detailed in the next sections.

Figure 3.5 - The manufacture of an ACT specimen: in the middle, casing/specimen parts and products for caulking, gluing, and taping; on the left, an assembled casing; and, on the right, a completed specimen.

3.2.1 Casing/Specimen Parts Preparation

Figure 3.6 specifies and gives the dimensions of the different parts that, when assembled together, and upon casting and curing of a certain grout to be tested, will

compose an ACT specimen. Plastic casings, a segment of prestressing strand and plastic

spacers comprise these different parts and should be prepared as described in the

following sections.

a: Plastic spacer with outer diameter that snuggly fits inside casings

b: Seven-wire prestressing steel strand. Length: 360 mm (14 in.)

c: Long plastic tubing. Internal diameter: 25.4 mm (1 in.). Length: 150 mm (6 in.)

d: Middle plastic tubing with two longitudinal slits (see detail). Internal diameter: 25.4 mm (1 in.). Length: 90 mm (3.5 in.)

e: Short plastic tubing. Internal diameter: 25.4 mm (1 in.). Length: 60 mm (2.4 in.)

f: 25.4 mm (1 in.) plastic end cap

Figure 3.6 - Specimen parts to prepare before casing assemblage and casting steps

3.2.1.1 Casings

Clear rigid PVC tubing measuring 25.4 x 31.75 x 3.175 mm (1 x 1.25 x 1.125 in.)

in internal diameter, external diameter, and thickness, respectively, was used to make the

casing segments. The use of clear, instead of opaque tubing, facilitates visual observation

during the casting procedure. Figure 3.7 shows one of these tubes, measuring originally

183 cm (6 ft), ready to be cut with a bench saw to the required sizes of each casing

segment, i.e., 15, 9, and 6 cm (6, 3.5, and 2.4 in.).

Figure 3.7- Clear tubing positioned in a bench saw for cutting of casing parts

After cutting the casing segments, the parts are separated and the longitudinal

diametrically opposed slits are made on the middle casing segment (shown previously in

Figure 3.6). The slits were made so that only a thin wall (approximately 1 mm or 0.039

in.) would be left, facilitating the task of breaking them to remove the middle casing

segments later on, when exposing the testing regions to the corrosion cell's electrolyte.

The previous method used to expose testing regions (Koester 1995, Schokker 1999),

which used grinding or cutting tools, often resulted in a damaged grout surface and may

have led to significant scatter in results.

The casing parts were then cleaned with pressurized air and stored separately, as shown in Figure 3.8, which also shows some 25.4 mm (1 in.) end caps and plastic spacers. The spacers were cut from large round reinforcing bar spacers available for structural concrete construction. The final outside diameter of these spacers allowed a snug fit inside the casings.

Figure 3.8 - Casing parts ready for the assemblage procedure

3.2.1.2 Prestressing Strand Segments

The steel used for the specimens is a seven-wire prestressing strand that follows ASTM A426 (2002) "Standard Specification for Steel Strand, Uncoated Seven-Wire for

Prestressed Concrete". Details about the strand properties are given in Appendix C of this work.

The strand was received in reels, which were then cut to the required size (360 cm or 14.2 in.) with an abrasive cut-off saw and had their extremities beveled afterwards in a bench grinder, as shown in Figure 3.9. The beveling at both ends was executed for safety reasons, since sharp edges typically result from the cutting process. The beveling also facilitates the attachment of the plastic spacers, during the casting step.

Figure 3.9 – Cutting and beveling of strand segments

Prior to the casting procedure, the strand segments were then cleaned with acetone to remove impurities such as dust, spots of rust, and oil. This is illustrated in Figure 3.10.

Figure 3.10 - Acetone was used to clean the strands prior to the casting step

3.2.2 Casing Assemblage

The assemblage step proceeded after the preparation of the necessary quantities of casing parts. This step was accomplished with the use of auxiliary metal pipes that were necessary for an adequate assemblage of the casings. These metal pipes allowed a proper finishing at the junctions, reduced the possibility of casing defects, such as leakages and misalignments, and minimized the amount of caulking material used. Too much caulking material can induce accumulations inside of the casings, which are likely to reduce the grout cover at those locations. Pictures and details of the two auxiliary supports used in this step are shown in Figure 3.11.
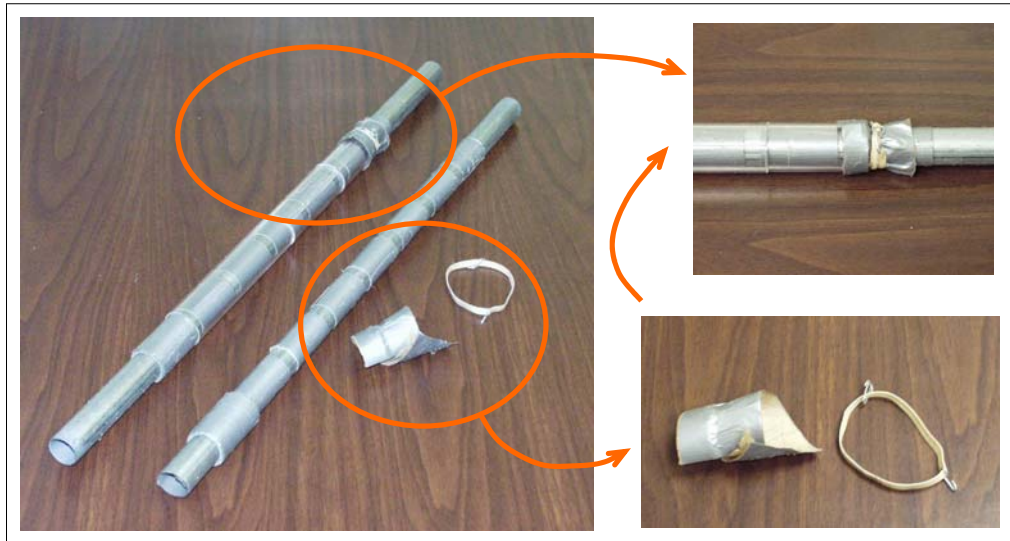
Figure 3.11 – Auxiliary tubing supports used in the assemblage of the ACT casings

After caulking the junctions, the three sections of each casing were held together with duct tape and the end caps were cemented to the extremities that corresponded to their short plastic tubing sections. The specimens were left undisturbed for a minimum of one hour to allow the caulking to vulcanize before submitting the casings to a leakage test. The casings were filled with water, and any leakage was then identified and fixed. A set of assembled casings already caulked, taped, and leakage tested is shown in Figure 3.12.
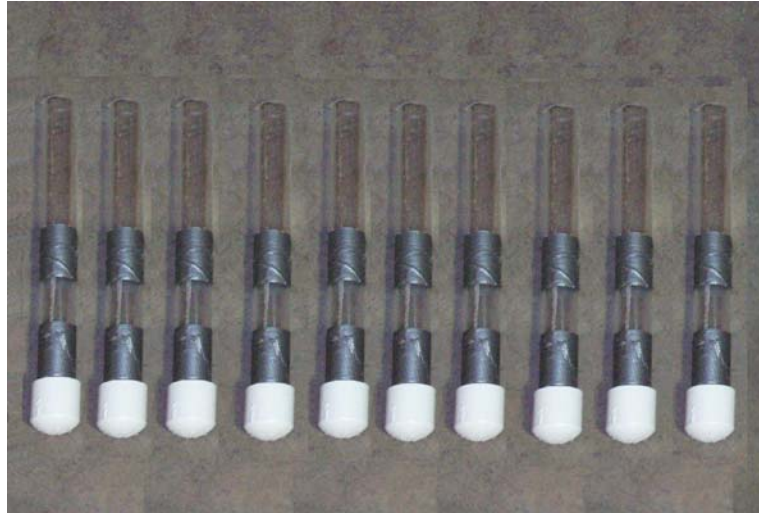
Figure 3.12 - Set of assembled casings

The sets of assembled casings were then placed in a rack to keep them in an upright position. Their respective cleaned prestressing strands, with a spacer attached to their bottom end, were placed inside the casings. The assembled casings ready for grouting are pictured in Figure 3.13.

Figure 3.13 - Set of casings with placed strands ready for the casting procedure

3.2.3 Specimen Casting

With the sets of casings prepared, each casing already with its respective strand segment appropriately cleaned, and with a spacer attached at its bottom end, the preparation of the sets of specimens would continue with the mixing and casting procedures. Firstly, however, quantities of grout mixing materials for each type of grout would be measured. Cement and mineral admixtures (silica fume and fly ash) were weighed (mass determination), while chemical admixtures (corrosion inhibitors) were quantified by volume.

Figure 3.14 - Grout mixing and specimen casting ready to begin

The grout was mixed in a cylindrical container measuring 30 cm (11.8 in.) in diameter and 40 cm (15.7 in.) in height using a high-shear blade with a varying speed mixer (a 0-2,500 rpm drill). Figure 3.14 shows these and other utensils necessary for flow cone tests, which gives a measure of grouts' fluidity.

The same batching order was adopted throughout the mixes. The water was always placed in the mixing container first. Then, the cementitious materials would be slowly added, with low rotation of the varying speed mixer used. The inhibitors A and C were added to the batch water, while B was added to the freshly mixed grouts, according to manufacturers specifications. Each grout mix would take approximately 4 minutes to complete. After completion of mixing, the grouts were tested for fluidity in the flow cone.

The flow cone test was executed according to the ASTM C939 "Standard Test Method for Flow of Grout for Pre Placed Aggregate Concrete" and the results (typically between 12 and 45 seconds in the regular test and between 5 and 10 seconds in the modified) indicated that no superplasticizer was necessary throughout the mixings. The casting of the specimens would then take place, following the sequence of steps illustrated in Figure 3.15. As it is indicated in the figure, the first step was to have each casing prepared for casting. Then, as a second step, one third of each casing volume would be filled with grout and, in order to prevent voids and minimize air bubbles, the strands would be slowly moved and the casings tapped to induce moderate vibration on the casings. This procedure is repeated in the third and fourth steps. The last step, which completes the casting procedure, is the attachment of the second spacer to each strand at the top of the casings.
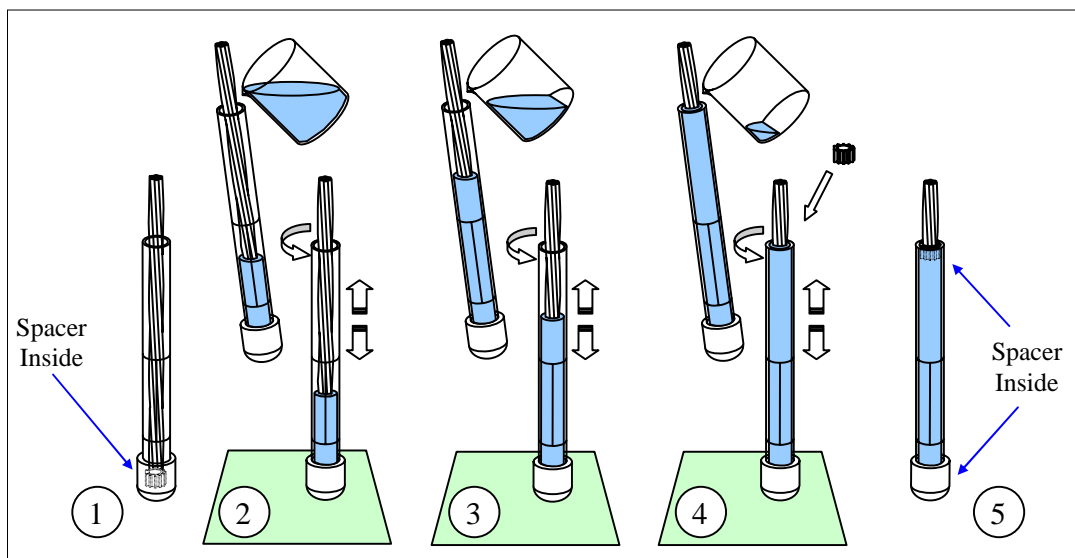
Figure 3.15 - Procedure used to cast the ACT specimens

3.2.4 Specimen Curing

After completion of the casting step, each specimen would receive an identification label and the set of specimens would be taken to the moist room for a specified curing period. A picture of the moist room utilized is shown in Figure 3.16. Inside the chamber, the temperature and relative humidity were kept, respectively, at 23 ± 1.7^o C (75.2^o F) and at a minimum of 95%.

While in the moist room, each specimen's protruding strand was protected against corrosion with a plastic cover. This protection avoided the corrosion of the strands due to the high humidity inside the moist room. If corrosion protection is not used, the strands will severely corrode, and the corrosion layer formed will have to be removed before the instrumentation step in order to allow appropriate cable connection.

Figure 3.16 – Moist room used in the curing process of ACT specimens

3.3 THE ACT SETUP AND RELATED APPARATUS

An ACT setup is composed of a potentiostat, a multiplexer, and corrosion cells. A potentiostat is an electronic instrument that controls the voltage difference between the working and the reference electrodes, maintaining this difference at a specified value. In this research, the potentiostats were set to apply a voltage difference of 200 mV above the potential given by the reference electrodes used. Multiplexers connect corrosion cells to potentiostats, allowing one potentiostat to control several cells at the same time. In this work, an eight-channel multiplexer was used to connect a maximum of eight stations to their respective potentiostat. Corrosion cells occur in each one of the stations that are monitored by the user. Typically, the potentiostats apply voltage differences to corrosion cells and currents are monitored.

The schematic presented in Figure 3.17 illustrates how the electrochemical setups used in this work are arranged together. As can be seen, in addition to the parts mentioned, controller circuitry is installed together with the potentiostat in a microcomputer machine in order to control the entire system automatically.

a: Corrosion cell or station
b: Eight-channel multiplexer
c: Potentiostat and controller boards.
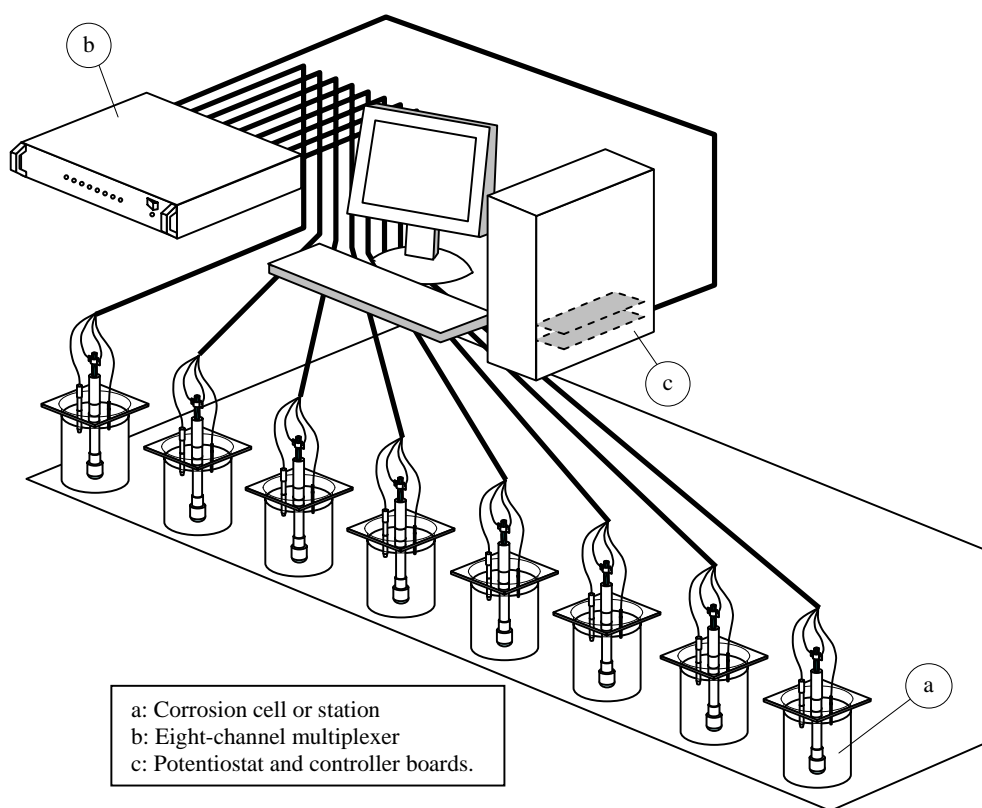
Figure 3.17 - Schematic of the ACT setups used

3.3.1 Electrochemical measurement system

The electrochemical measurement systems used in this work were manufactured by Gamry Instruments. The potentiostat, a PCI4/300, is capable of a current resolution of 1 fA (f = 10^{-15}), a voltage resolution of 2 μV, and a maximum current output of 300 mA. The multiplexer, an ECM8, with eight channels, has a "local" potentiostat in each of its channels, being capable of polarizing the stations when they are not being polarized by the potentiostat. Figure 3.18 presents the three systems used in this work.

Figure 3.18 - Setups A (top left), B (top right), and C (bottom) were used in the tests

At first, only one setup was available for the tests. Five months later, the second setup was acquired, doubling the capacity of ACT tests. The third system was acquired seven months later, tripling the initial capacity of corrosion cells to be used in this research. Nonetheless, a reduction on the number of specimens had to be considered. This is detailed in the next sections.

3.3.2 Corrosion Cell

Figure 3.19 presents schematics of the corrosion cells used in this work. They were assembled in 3 L beakers containing saltwater solution as electrolyte. The electrolyte was obtained by the dissolution of 5% of salt by solution mass in water (for comparison, seawater typically has 3% of salt). The water line would be marked in every station in order to allow the addition of more water at a weekly basis to compensate for evaporation of the electrolyte in each cell.
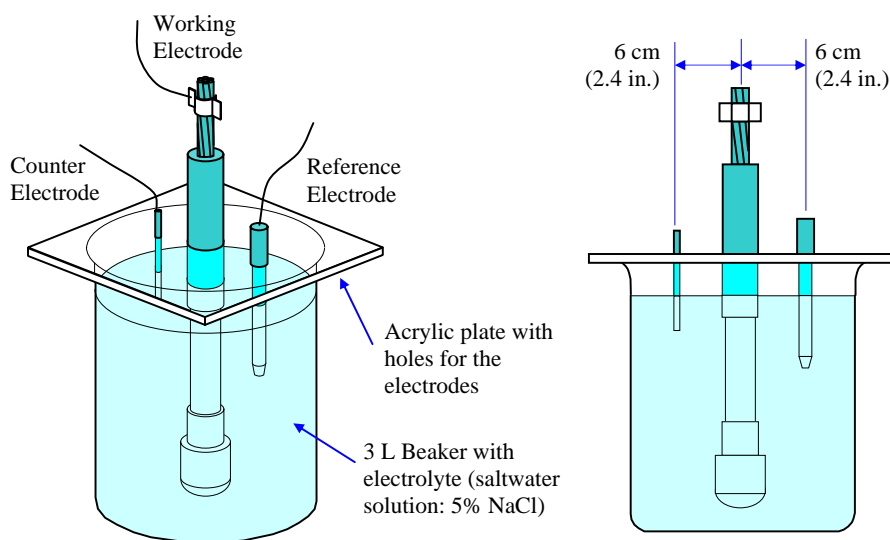
Figure 3.19 - Schematics of the corrosion cells (stations) used

Reference, counter (auxiliary), and working electrodes (ACT specimens) complete the necessary circuitry to measure the variables of interest. In addition, an acrylic plate with holes to support the electrodes completed the stations.

The reference electrode used in each corrosion cell was manufactured by Fisher Scientific. It was a plastic-bodied gel-filled Accumet™ saturated calomel electrode (SCE), which is commonly used in laboratory applications.

The counter electrodes are segments of platinum clad wires from Anomet Products Inc. Each segment, containing a double platinum thickness, 40% of niobium by cross-sectional area for increased mechanical and electrochemical protection of its copper core, measured 16.5 cm (6.5 in.) in length and 3.175 mm (0.125 in.) in diameter. The extremities of the counter electrodes were covered with a layer of silicone, to avoid corrosion of the copper core, and with a layer of epoxy for mechanical protection of the silicone layer. Both reference and counter electrodes are picture in Figure 3.20.

Figure 3.20 - Reference and counter electrodes used

The specimens (working electrodes), at the end of their curing process, had their middle plastic casing removed for exposure of their testing regions. Immediately after the casing removal, each specimen was taken directly to its respective station in order to prevent drying shrinkage of the exposed section of grout, minimizing the occurrence of cracking (sequence of steps are illustrated in Figure 3.21). The use of a lathe or any other method to expose the testing region is likely to take too much time, facilitating the occurrence of cracking. In addition, even precise and careful cutting may damage the grout layer, increasing the tests' standard deviation. With specimens in their stations, the corrosion cells were then complete and the electrochemical measurements started.

1 – Specimen taken from moist room

2 – Removal of the middle plastic casing

3 – The specimen is immediately put in its station to avoid drying shrinkage cracking of the testing region
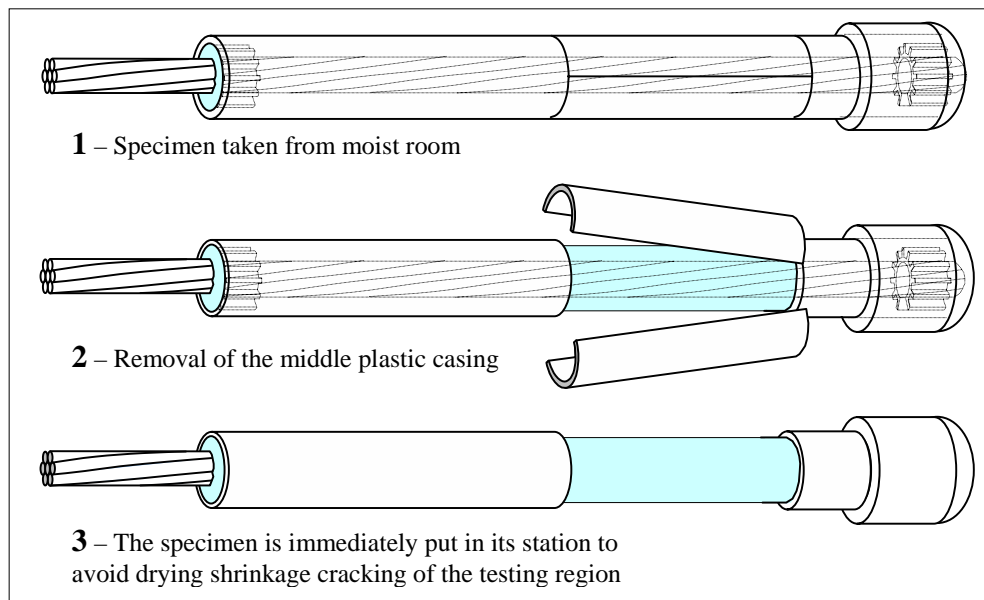
Figure 3.21 - ACT Specimens are working electrodes in the corrosion cells used

4 RESULTS AND ANALYSES

This chapter presents and discusses the results obtained from the experimental program. It begins with a characterization of the grouts studied, analyzing two different aspects related to their density: volume of permeable pores and charge accumulated on potentiostatic polarization tests. Then, these two variables, together with open circuit potential (E_{oc}); corrosion potential (E_{corr}); corrosion current density (i_{corr}); Tafel constants (β_a and β_c); and polarization resistance (R_p), are analyzed with respect to their relationship with the main variable, t_{corr} (time-to-corrosion).

4.1 GROUT CHARACTERIZATION

4.1.1 Volume of Permeable Voids

Three main different phenomena are likely to dictate the ionic mass transport through ACT grout specimens: capillary absorption, diffusivity (mass transport due to concentration gradients), and permeability (mass transport due to pressure gradients). These phenomena depend on physical characteristics of systems such as tortuosity (a measure of pore connectivity), pore size, and porosity (amount of pore voids). These characteristics, once measured, can be used to qualify different grouts. While tortuosity and pore size are difficult properties to determine, porosity can be found through simple steps and, therefore, was the property chosen to characterize the grouts tested in this

work. The procedure for determination of porosity or, more specifically, volume of permeable pores of cementitious materials is given in ASTM C642 (1999) and was used to characterize the different grouts tested in the experimental program according to their porosity. The results for grouts tested at 28 days are presented in Figure 4.1.

Grout	V (%)
PP E 28Y	28 ± 1
PP B 28Y	29
PP C 28Y	31 ± 1
PP D 28Y	33 ± 1
PG 28Y	35 ± 1
CI A 28Y	35 ± 1
SF5 28Y	36
SF7 28Y	38 ± 1
CI B 28Y	38
SF3 28Y	38 ± 1
CI C 28Y	39
FA 28Y	41 ± 1
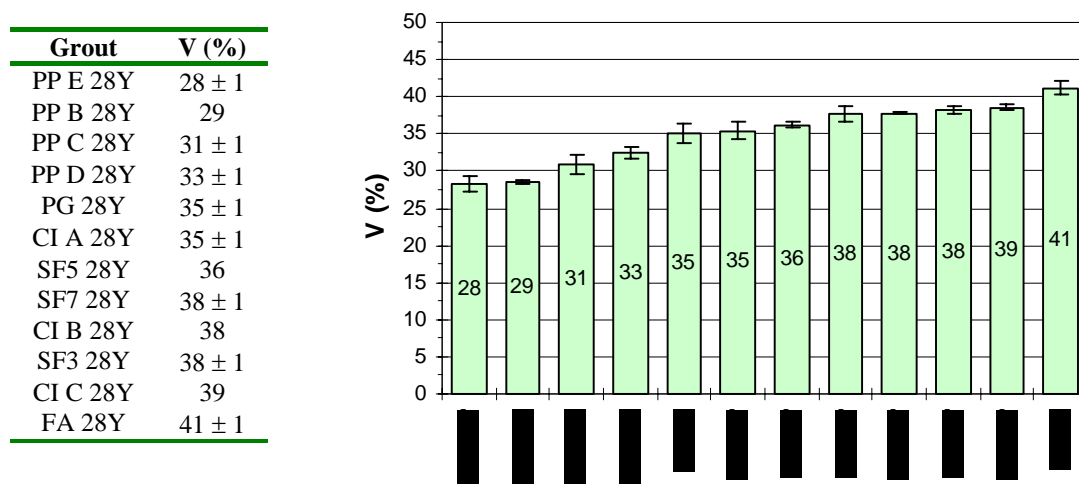
Figure 4.1 - Volume of permeable pores for different grout types at 28 days

As can be seen, the porosities are evenly distributed from a value as low as 28% of permeable voids to an amount as high as 41%. At the lower extreme are the prepackaged grouts, while, at the higher end, are the grouts with pozzolans and corrosion inhibitors B and C in their mixes.

4.1.2 Electric Charge

Figure 4.2 presents ACT results for two specimens: one cast with a grout containing fly ash, which reaches 10 mA almost instantaneously after the onset of corrosion, and for another cast with a prepackaged grout, which reaches the same level of current after a much longer process. While the fly ash specimen generates an electric charge of 11 coulombs, the prepackaged one generates 2,939 coulombs, indicating a significant difference in behavior due to the grout used. Therefore, it seems that measurements of electric charge developed in ACT tests can also be used to characterize the grouts tested.
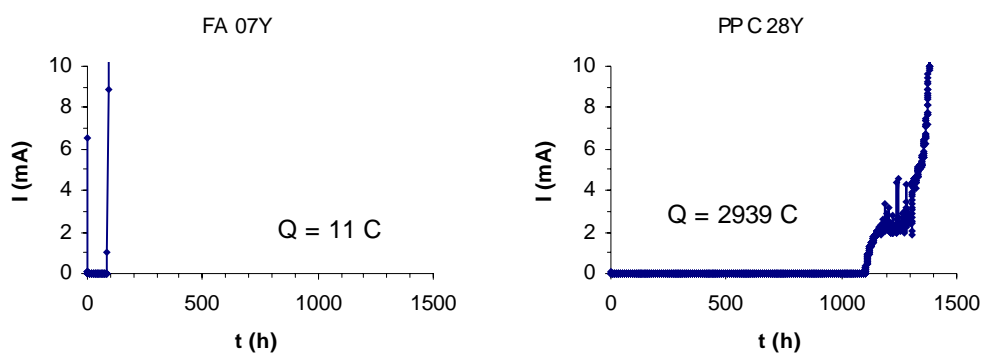
Figure 4.2 – Minimum and maximum electric charge values calculated from ACT results

During an ACT, when the chlorides contained in the solution reach the prestressing strand of one of the specimens being tested, the readings in current for this specimen suffer an abrupt increase. The elapsed time for this event to occur characterizes

the specimen's individual t_{corr}, and the measured current should continue to increase as more chlorides are drawn to the prestressing strand. The surface area of steel protected by grout begins to diminish, exposing more and more steel surface to corrosive processes. If the circuit is maintained, the attacked area continues to grow far beyond the testing region limits, engulfing eventually the whole strand. This process is pictured in Figure 4.3, where increasing current intensities were measured.
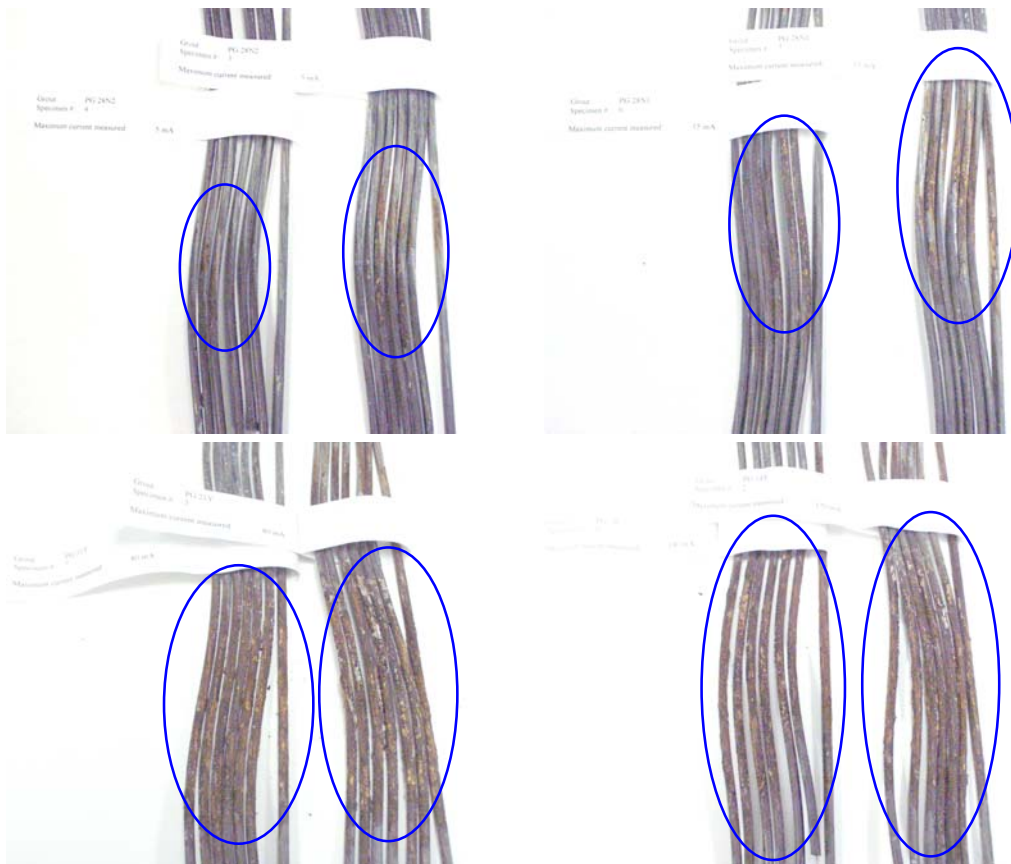
Figure 4.3 - Severity and extension of the corrosive attack on prestressing strands for different levels of maximum current intensity measured (Top left: I_{max} = 5 mA; Top right: I_{max} = 15 mA; Bottom left: I_{max} = 80 mA; Bottom right: I_{max} = 170 mA)

Figure 4.4 presents calculated charge values for the grouts tested in this work that were allowed to reach electric currents higher than 10 mA in their ACT tests. The charge values were then calculated considering $t \geq t_{corr}$ and $I \leq 10$ mA as limits.

Grout	Q (C)
FA 07Y	21 ± 4
SF7 07Y	84 ± 28
SF7 28Y	96 ± 15
SF5 56Y	98 ± 19
SF5 28Y	124 ± 13
SF5 07Y	125 ± 14
SF7 56Y	125 ± 27
SF3 56Y	125 ± 16
FA 28Y	132 ± 18
PG 14Y	136 ± 30
SF3 07Y	137 ± 64
PG 07Y	179 ± 25
CI A 28Y	215 ± 68
CI C 28Y	226 ± 34
CI B 28Y	232 ± 41
SF3 28Y	282 ± 45
PG 56Y	319 ± 94
PG 28Y	355 ± 49
FA 56Y	441 ± 95
PG 21Y	504 ± 104
PP D 28Y	717 ± 100
PP C 28Y	2327 ± 341
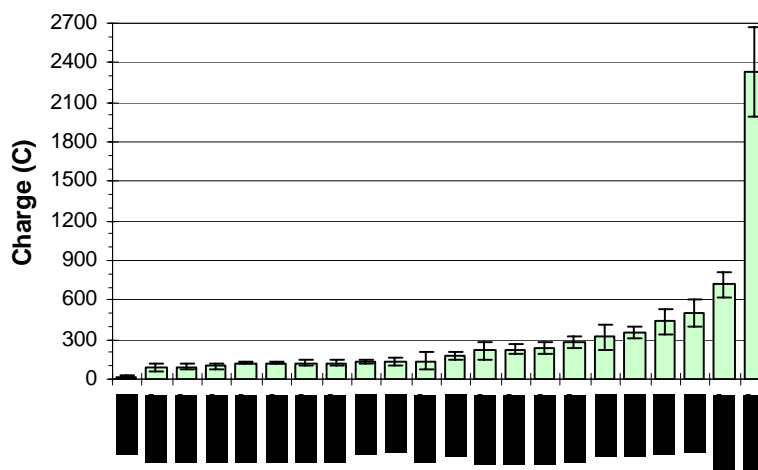
Figure 4.4 - Electric charge values calculated from ACT results

As can be seen, the charge values significantly increase along the grout series, being very sensitive and reaching significant amounts at the end of the series. This behavior is probably not only related to the porosity of the cementitious matrices, but also to the other aforementioned physical properties, namely pore size, tortuosity, and permeability of the grouts. The most important aspect that can be drawn from the

measurements taken, however, is that the grouts with pozzolans are clearly not performing as expected with respect to porosity measurements or electric charge measurements. This result is surprising considering the favorable results often found in concrete with these products. The only exceptions are the 3% silica fume grout at 28 days and the fly ash grout at 56 days. The low silica fume content and the long curing period probably helped each one of these cases, respectively. The favorable results with these two mixes show the potential of pozzolans, but percent replacement and cure time appear to have significant effects. This is discussed in detail in the next sections.

4.2 POTENTIOSTATIC POLARIZATION

4.2.1 ACT Limits for Grout Approval and IR drops

Figure 4.5 shows the amount of time on average, t_{corr}, required for each type of grout tested to allow corrosion of the embedded prestressing strand. Only the results obtained with voltage drop compensation are present in the graph. A vertical line at the top of each column represents the experimental standard error in the measurement (the standard deviation divided by the square root of the number of replicates tested). The grout represented by column PP B 28Y in the graph never corroded after 3,200 hours. Horizontal solid lines represent limits currently found in the PTI grouting specification. Condition 1 represents the true PTI specification recommendation of having a t_{corr} greater than a plain grout with water-cementitious ratio of 0.45. Condition 2 of 1,000 hours is

mentioned in the commentary of the PTI specification and is used in the Florida DOT

specification as well.
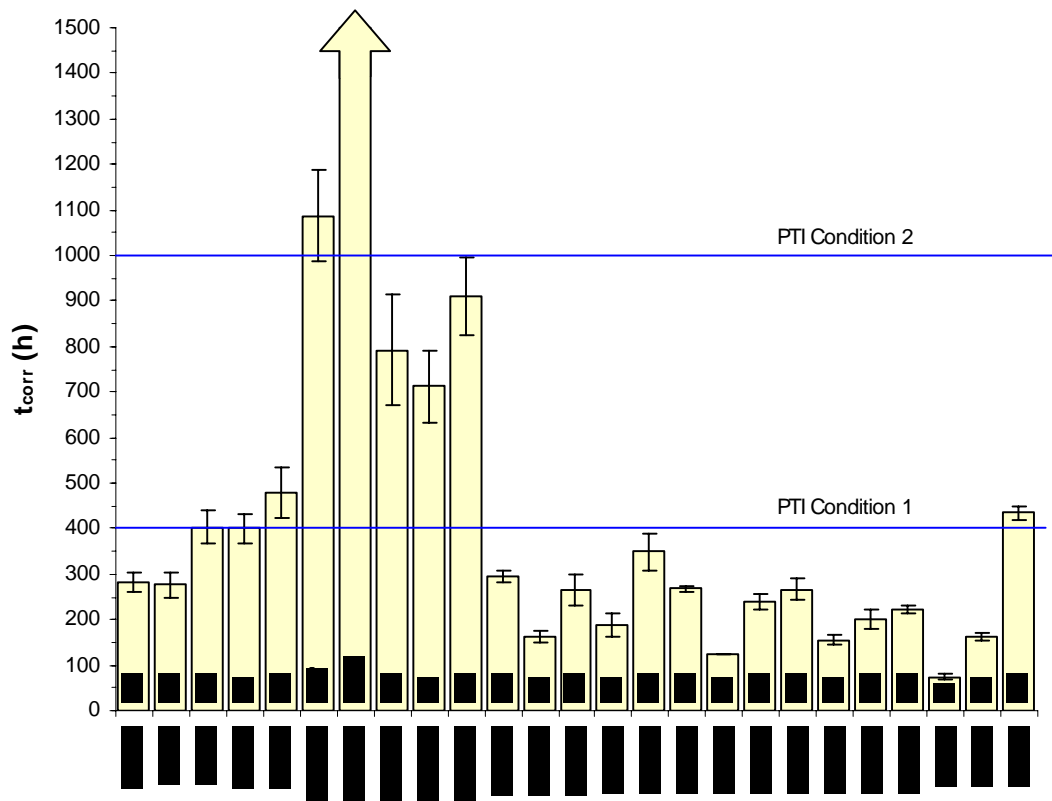
Figure 4.5 – Times-to-corrosion for different types of grout (IR comp on)

As can be seen, the variable t_{corr} is strongly influenced by the type of grout. The

time-to-corrosion can be as low as 74 hours or far surpassing 1,000 hours. All

prepackaged grouts (PP) that were tested easily pass PTI Condition 1, i.e., their t_{corr}

values are higher than the one measured for the control mix (plain grout at 28 days – PG

28Y). However, only two of them pass PTI Condition 2 (PP A 28Y and PP B 28Y), indicating, perhaps, an excessively stringent condition.

With the exception of the prepackaged grouts, all grout types were also tested without compensation for voltage drops, and these results are reported in Table 4.1. The results show that, when the option for compensation of the voltage drop is not engaged, an average discrepancy can reach a value either as low as 11% or as high as 46%. It should be noticed, however, that one of the grouts presented a time-to-corrosion 149% above its respective compensated value.

<div align="center">Table 4.1 – Influence of IR drop on ACTs</div>

Grout Test	t_{corr} found with IR compensation (h)	t_{corr} found with no IR compensation (h)	Difference Range (%)
PG 07	282 ± 23	315 ± 60	$0 – 45$
PG 28	401 ± 33	474 ± 35	$1 – 38$
PG 56	479 ± 55	630 ± 77	$4 – 67$
CI A 28	295 ± 13	617 ± 85	$72 – 149$
CI B 28	163 ± 14	177 ± 11	$0 – 26$
CI C 28	265 ± 34	329 ± 20	$4 – 51$
SF3 28	349 ± 40	329 ± 0	$0 – 6$
SF5 28	240 ± 17	307 ± 0	$20 – 38$
SF7 28	200 ± 20	266 ± 0	$21 – 48$
FA 07	74 ± 7	62 ± 12	$0 – 10$
FA 28	162 ± 9	183 ± 32	$0 – 41$
FA 56	435 ± 15	552 ± 32	$16 – 39$
		Mean (%)	**11 – 46**

The control grout produced a t_{corr} equal to 401 h when tested under IR drop compensation (characterizing Condition 1) and produced a t_{corr} equal to 474 h when no

compensation was used. This difference amounts to 18%, but could have been 38%, considering the deviation as indicated in the table.

In order to illustrate the implication of these results, upon applying a 46% discrepancy to Condition 2 and 38% to Condition 1 in Figure 4.5, the horizontal lines shift to the positions shown in Figure 4.6. Under these altered conditions, all the prepackaged grouts meet the new required minimum value. Moreover, at least seven other grouts, including early age ones (whose properties are knowingly not fully developed yet) meet or are close to meeting Condition 1.
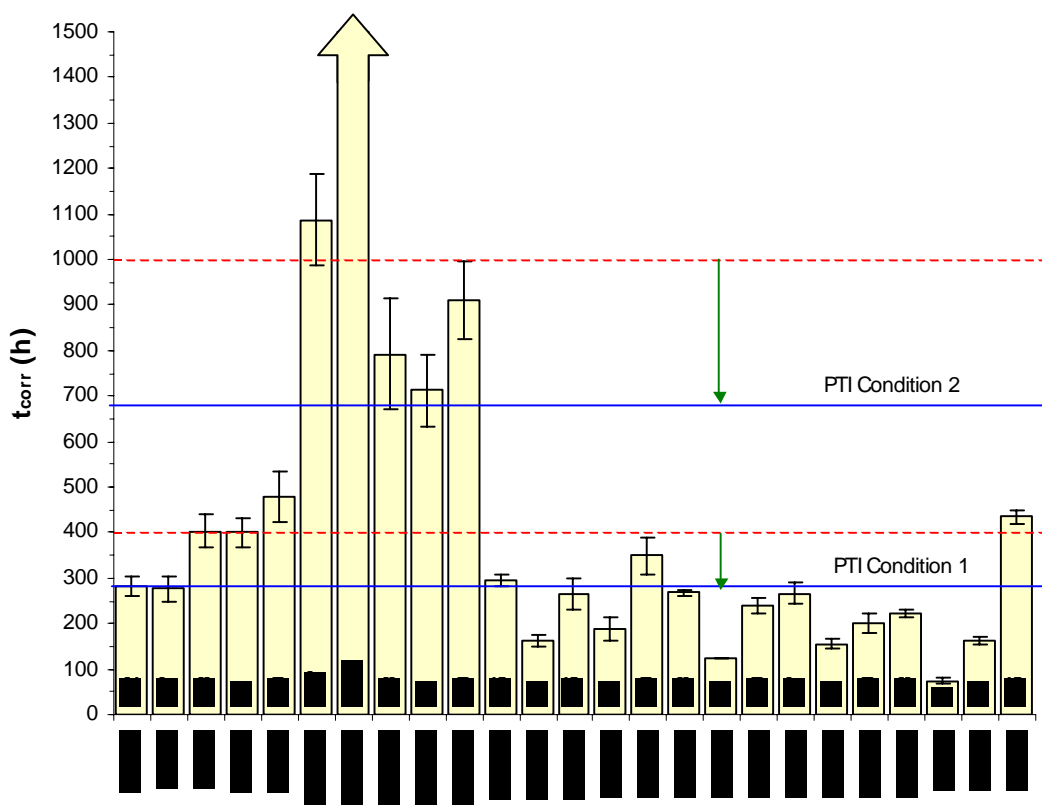
Figure 4.6 – Several grouts pass PTI conditions when effects due to IR drops are significant

Grouts with a high content of silica fume (above 5%) or with fly ash not fully matured fail even the modified Condition 1, indicating the importance of appropriate material proportioning and the necessity for extended curing periods, respectively. These aspects are specifically addressed in the next section.

In summary, corrosion requirements for post-tensioning grouts should explicitly express different limits according to equipment specifications. ACT setups capable of IR compensation should have much lower a limit than the 1,000 hours (Condition 2) currently prescribed by PTI (and the Florida DOT), since this value seems to be suitable only for setups with no IR compensation capability. For the cases presented herein, a value of 700 hours would perhaps be a more suitable condition, since this limit approximately represents the modified Condition 2, highlighted previously in Figure 4.6. Another aspect to be considered, however, is that t_{corr} values could also vary significantly with equipment, user, strand lot, and other variables still not studied and a relative comparison such as that offered by PTI Condition 1 is, probably, a better approach, instead of adopting a fixed value for grout approval. If PTI Condition 1 is deemed too lax, a lower permeability base case grout may be used (such as 0.40 w/c rather than 0.45 w/c).

4.2.2 Performance of different grout groups and IR drops

Four different grout categories were considered for evaluation of the influence of voltage drop compensations, curing periods, and grout constituents on times-to-corrosion.

The values obtained for each of these groups were given previously in Table 4.1 and are presented again in this section, but in graphic format.

As can be noticed in Figure 4.7, the time-to-corrosion, compensated for IR drops or not, is a variable that develops in a varied degree of intensity, depending upon the characteristics of the grout being tested. For instance, when considering the tests run with voltage drop compensation, the plain grout results, PG, increase from 282 hours at 7 days to 401 hours at 28 days (42% increase) and to 479 hours at 56 days (20% increase). For the same age intervals, the fly ash grout's t_{corr}, increases from 74 hours to 162 hours (118%) and finally to 435 hours (169%). This difference in behavior was expected since it is known that fly ash grouts take longer to develop their microstructure when compared to plain mixes.
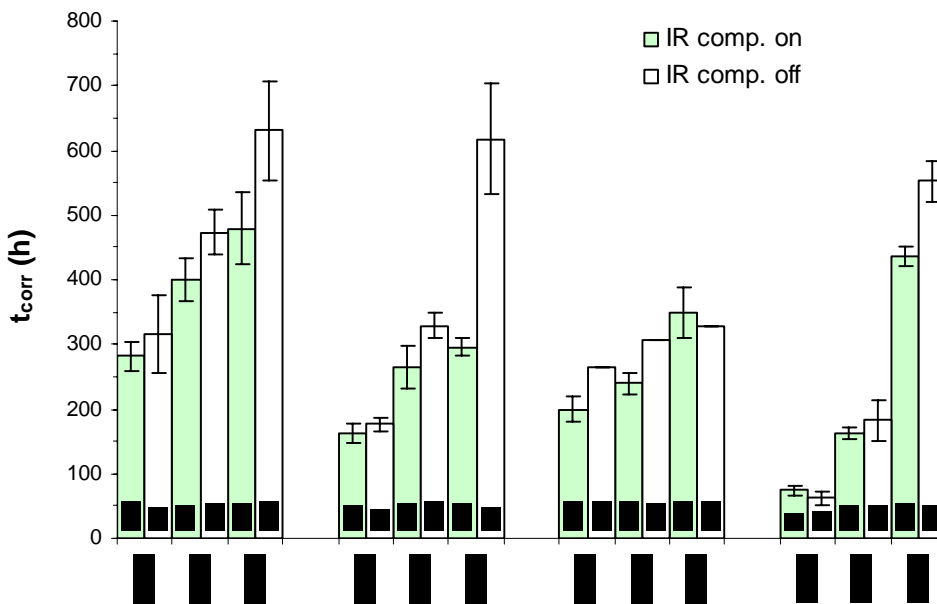
Figure 4.7 – Influence of IR compensation on ACTs for different grout groups

However, when the IR compensation option is not engaged, the value obtained for the fly ash grout at 56 days is only 27% higher than that for the compensated result. This difference should have been more significant since the control mix reaches a 32% discrepancy at the same age, and a more significant resistivity is typically expected from fly ash mixtures. This apparent lack of significance of the IR effect observed in the fly ash grout may be only due to the higher variability verified in the plain grout data or that the delay observed on t_{corr} also reflects on resistivity values, and the 27% would rather correspond to the discrepancy observed on the plain mix at 28 days (18%). Incidentally, it should be noted that the final compensated value obtained for the fly ash grout is only 9% higher than the result obtained for the control grout at 28 days.

The performance along the period of curing for the plain and fly ash grouts can be observed in Figure 4.8. In addition to the aspects mentioned above, the graph shows approximate constant development rates of t_{corr} for the plain mixture, but dramatic increases of the variable after 28 days for the mixture containing fly ash.
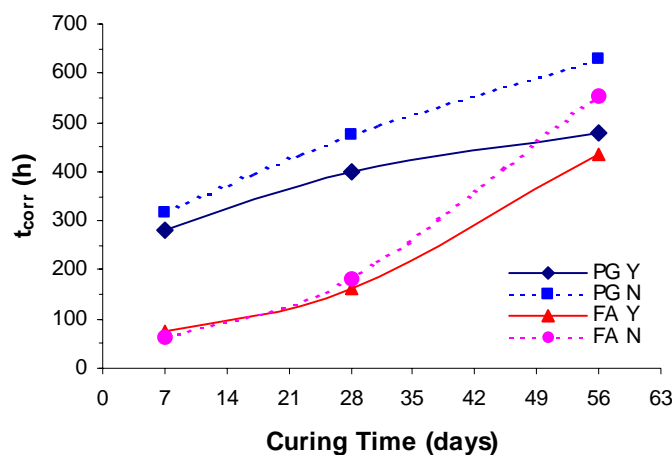
Figure 4.8 - Development of the time-to-corrosion for plain and fly ash grouts with the curing period

Regarding the other two groups, t_{corr} seems to be particularly sensitive to some types of corrosion inhibitor (corrosion inhibitor A is based on calcium nitrite, while the other two are based on organic and/or inorganic formulations), but little difference is observed among silica fume results. This is discussed in the next section.

4.2.2.1 Influence of Grout Constituents

Considering again Figure 4.7, it can be inferred that corrosion inhibitors can produce highly overestimated results when no voltage drop compensation is used. On the other hand, grouts with silica fume in their mixture are influenced by that condition in a much lower degree. When comparing their performances with the control result, however, it is interesting to notice that the two admixtures alone have actually led to lower values of time-to-corrosion. This apparent incongruence corroborates results found in previous tests (Schokker 1999) that show a tendency for grouts with silica fume to produce lower ACT results when compared to plain mixes. Although silica fume additions are known to improve overall characteristics of concretes, the absence of aggregates in grouts is a factor that can in fact undermine silica fume's role on mixes and, instead of improving grouts, being deleterious to them. This would happen because aggregates are the agents directly responsible for the appropriate dispersion of the silica fume particles in concrete, leading to an improved microstructure. In grouts, on the other hand, when no aggregates are present in the mix, a favorable condition for the creation of an interconnected net of undispersed silica fume agglomerates occurs. These

agglomerations of silica fume, characterized in Figure 4.9, may have considerably

facilitated the ingress of chloride ions through the grouts tested. Moreover, the presence

of silica fume agglomerations is also related to alkali-silica reactions (Diamond 1997)

between the concentrated masses of microsilica with the alkaline cementitious products,

generating expansion, internal stresses, cracking and, therefore, access of chlorides.
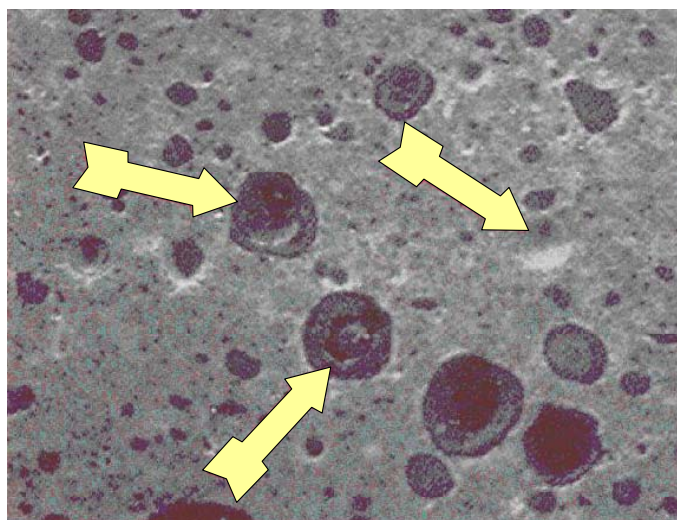
Figure 4.9 – A close view of a grout with silica fume in its mix (w/c = 0.36; silica fume content = 10% by cement replacement; HRWR = 1,242 ml/kg) showing typical agglomerations. The arrow to the right shows an air void. (Photograph by courtesy of Sprinkel, M. M. and Gulyas, R. J.)

The complete series of microsilica grout results is shown in Figure 4.10 and, as

can be seen, there is a tendency for poorer performances as the amount of microsilica

increases, probably due to the phenomena commented in this section, and that involve

this mineral admixture in grouts. Even considering the low result obtained for SF3 56Y,

lesser amounts of silica fume consistently produced better results than higher proportions in all curing ages tested, with only SF5 07Y as an exception.
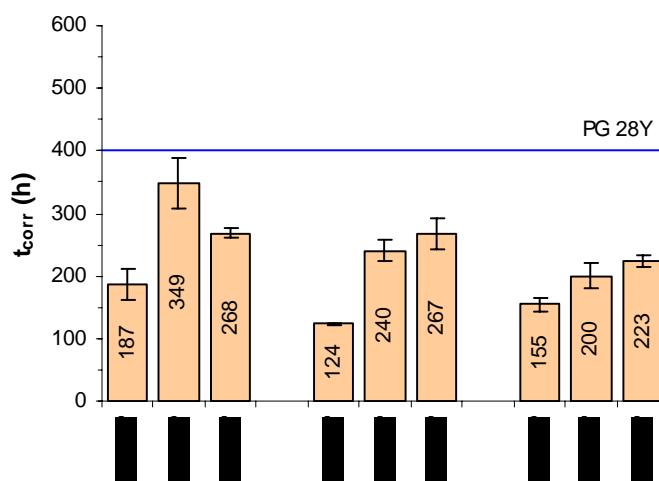
Figure 4.10 – Development of t_{corr} with curing period for three silica fume grouts

Regarding the aspects concerning the grouts tested with corrosion inhibitors in their mix, the only indication that may justify their low results is the fact that their measured resistances (from LPR tests) are probably at a lower level than that necessary to match the t_{corr} found for the plain grout. The three corrosion inhibitor grouts, A, B, and C, reached 193 ± 15, 138 ± 21, and 148 ± 6 kΩcm^2, respectively, while the control result is related to a resistivity that amounts 325 ± 43 kΩcm^2. Therefore, it is possible that the addition of chemical admixtures will reduce the resistivity of grouts with consequent low performances in ACT tests. In addition, the grouts with corrosion inhibitors B and C show higher values of porosity (38 and 39%, respectively), while only the grout with

corrosion inhibitor A showed the same level of permeable voids exhibited by the control mix (35%).

Another aspect to be considered when analyzing the results for the grouts with corrosion inhibitor is the possibility that the quantities used were not appropriate for the voltage used in the ACTs. An indication of this possibility is the result found for the grout with corrosion inhibitor A when no voltage compensation is used and, therefore, a lower potential was applied. The result is 109% higher than the compensated one. In addition, although the dosages used were approved by representatives of the products, the values used are the same ones suggested in the specifications for concrete, not grout.

4.2.2.2 Influence of Grout Age

The results show the influence of minimum curing period for testing depending upon grout characteristics. Regarding plain grouts, Figure 4.11 presents the complete series obtained for different ages. It can be seen that grouts at 21 days can have a performance as satisfactory as that obtained at 28 days. Although no statistical difference can be seen between both results, it is still recommended to run control mixes at 28 days, when the cementitious matrix is closer to be fully mature.

When considering grouts with fly ash in their mixes, however, a curing period of 56 days may be required to fully develop the grout microstructure. This is illustrated in Figure 4.12.
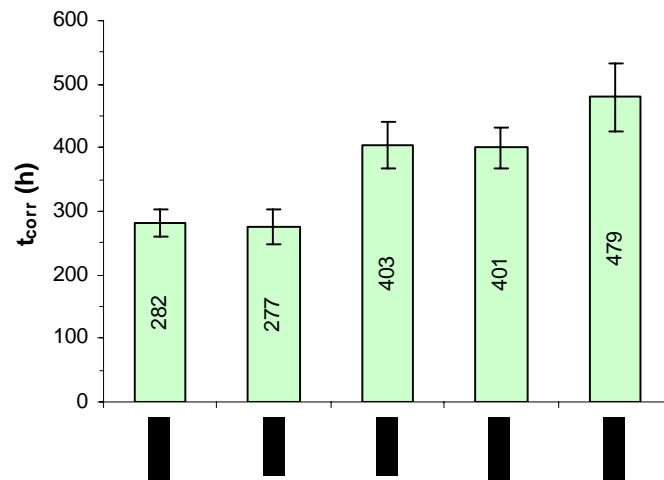
Figure 4.11 - Development of t$_{corr}$ with curing period for a plain grout
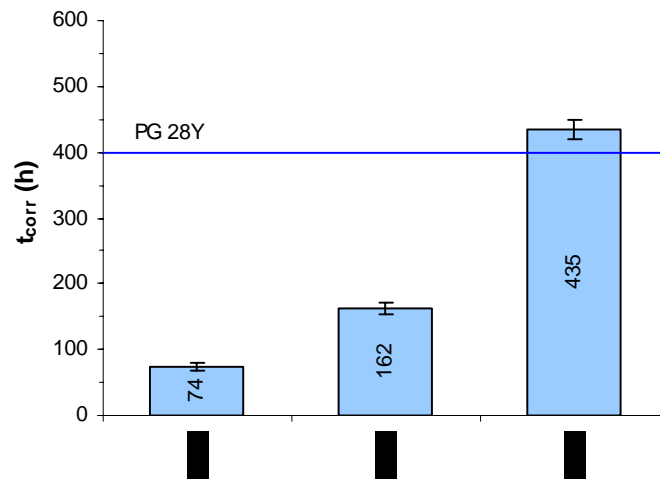
Figure 4.12 - Development of t$_{corr}$ with curing period for a fly ash grout

4.3 VOLUME OF PERMEABLE VOIDS: CORRELATION

The correlation between time-to-corrosion and the measure of porosity obtained (volume of permeable voids) is demonstrated in Figure 3.14 and Figure 4.14.
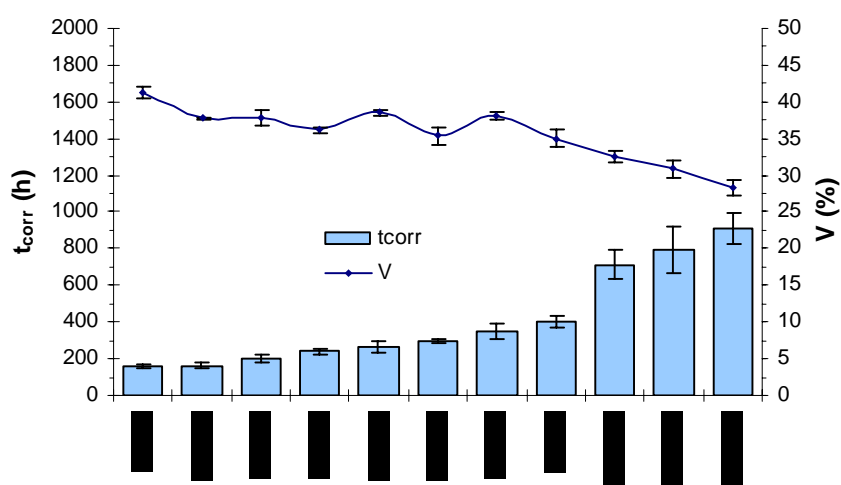
Figure 4.13 - Grout porosity trend with increase of the time-to-corrosion

In Figure 4.13 two distinct groups of grout can be identified: one with times-to-corrosion that are significantly high (above 600 h) and another with values significantly low (below 400 h). In each one of these two groups, the same porosity tendency is observed. However, it seems that other factors besides porosity may be participating in the grouts' ACT performances and dictating a slightly different behavior between the two groups.

The group with denser characteristics (grouts on the right of the graph) seems to have a more direct effect on its t_{corr} values when variations are observed in the porosities.

It is possible that the group with more volume of permeable voids would suffer more influence of permeability and diffusivity, and less influence from variations on porosity. Nevertheless, even considering these aspects, the correlation between the variables V and t_{corr} is evident, as can be seen in Figure 4.14.
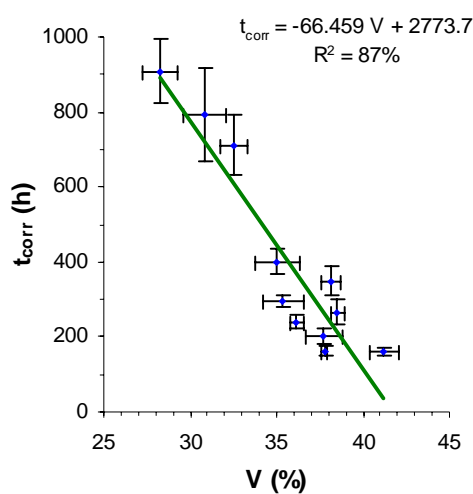
Figure 4.14 – Linear correlation between time-to-corrosion and volume of permeable pores

The expression that linearly correlates the variables V, given in percentage, and t_{corr}, in hours, is rewritten in Equation 4.1:

$$t_{corr} = -66.5V + 2774$$

Equation 4.1

Although the linear fit presents good correlation in the interval considered, it is likely that an exponential fitting would be more appropriate to represent the phenomenological interaction between the variables t_{corr} and V. Hence, V and t_{corr}

limiting values should exist in a manner that an asymptotical behavior should be

observed on their relationship, i.e., a very low V should reflect on an extremely high t_{corr}

as well as a very high V should result on a practically null t_{corr}. In this way, assuming

that the prepackaged grout B, which is characterized by 29% of permeable pores and was

tested for 3,200 h, was near failure and would have allowed corrosion at, say, 3,400

hours, and also assuming that, say, 60% of porosity would lead to an almost

instantaneous corrosion (t_{corr} = 1 h), the correlation in Figure 4.15 is found.
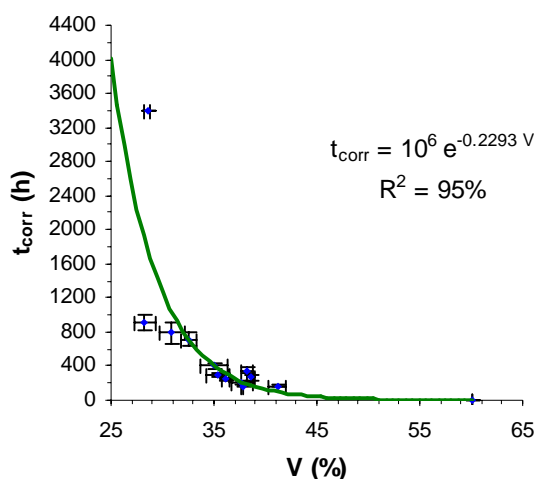
Figure 4.15 - Exponential correlation between time-to-corrosion and volume of permeable pores

The expression that exponentially correlates variable V, given in percentage, and

t_{corr}, in hours, is rewritten in Equation 4.2:

$$t_{corr} = 10^6 e^{-0.23V}$$ **Equation 4.2**

The exponential correlation does not only fit the measured experimental points better, but it also describes in an appropriate phenomenological fashion the relationship between the two variables in consideration. Nevertheless, the two equations found should be valid only in the range of permeable voids investigated (28 – 41%), and extrapolations beyond this range should be considered carefully. In addition, despite the high correlation coefficient found on both cases, few points represent low porosity results and high porosity values do not completely define a well-behaved pattern.

Despite the reservations that one may have when considering the correlations obtained, two important aspects can still be drawn from the data. Firstly, the correlations highlight the strong influence that porosity certainly has on corrosion protection and, secondly, values of porosity as low as 33% correspond to considerably high grout performances, and this could be a useful parameter when estimating ACT results or approving a grout for post-tensioning applications. The linear and exponential expressions give t_{corr} values of 581 and 517 hours, respectively, for that amount of permeable voids.

4.4 ELECTRIC CHARGE: CORRELATION

It was shown before that the amount of electric charge generated during an ACT test could be used to compare performances of different grouts (Section 4.1.2). Mixes of poor performances would allow corrosion and reach high values of current almost instantaneously, generating charges not greater than some hundreds of coulombs, while

grouts of better quality could generate one order of magnitude more. This is depicted to some extent in Figure 4.16.
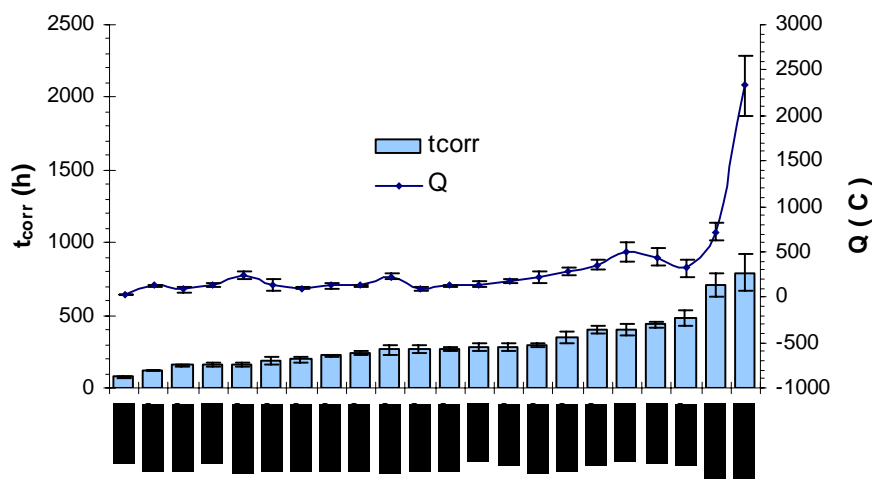
Figure 4.16 - Electric charge trend with increase of time-to-corrosion

It was also noted before that the electric charge, Q, would appropriately characterize grouts because the processes involved in the development of electric currents in an ACT would be intimately related to the properties of absorption, permeability, and diffusivity of the grout tested. Therefore, since these properties would strongly relate to porosity, an exponential relationship between Q and t_{corr} should also be expected, as apparently was the case when considering the correlation between the volume of permeable voids and t_{corr}. Figure 4.17 shows the result of the exponential correlation between Q and t_{corr} as adequate.
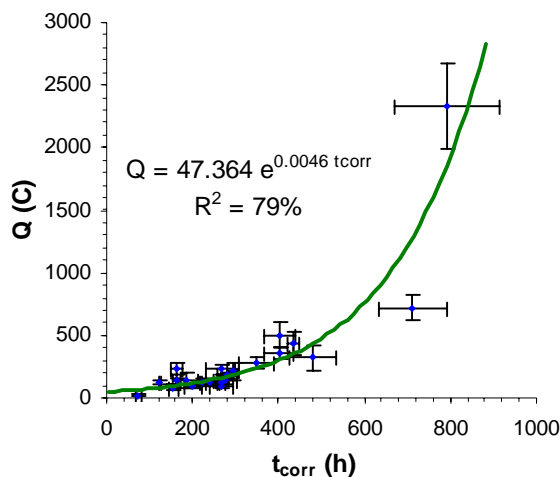
Figure 4.17 - Correlation between time-to-corrosion and electric charge

The expression that correlates Q, given in coulombs, and t_{corr}, in hours, is rewritten in Equation 4.3:

$$Q = 47e^{4.6x10^{-3}t_{corr}}$$

Equation 4.3

This result, however, is of little importance for practical reasons, since one must have the ACT data available in order to determine corrosion protections. Nevertheless, this result corroborates the exponential format assumed for the previous correlation between volumes of permeable voids and times-to-corrosion and indicates that grouts of poor performances (times-to-corrosion below 400 hours), should produce values of charge below 300 C, while grouts of superior performances could reach levels of charge as high as 2,500 C.

4.5 POLARIZATION CORROSION

The polarization corrosion tests that were run before the ACTs were used to determine the open circuit potential, E_{oc}, for each grout type. In previous investigations (Hamilton 1995; Schokker 1999; Hamilton 2000), the correlation between these potentials and their respective times-to-corrosion were investigated and, in spite of the little or no interaction found between these variables, the number of groups tested and lack of sophistication of equipment never allowed a definitive conclusion.

Figure 4.18 exhibits open circuit potentials collected for 26 different grout types, which registered a variety of corrosion protection degrees. It can be noticed that E_{oc} does not change significantly between grouts either if they present little corrosion protection or are examples of excellent performances.
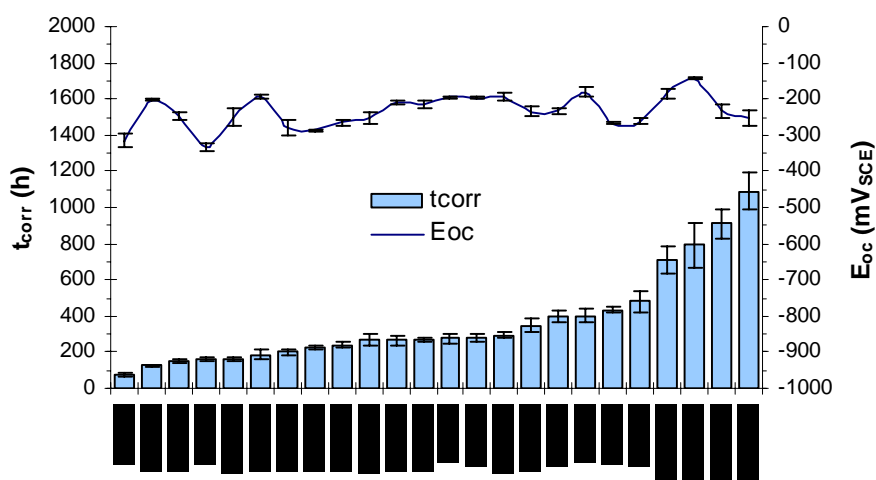
Figure 4.18 - Open circuit potentials obtained for grouts tested afterwards in compensated ACTs

In summary, E_{oc} measurements may be appropriate to indicate whether an element is corroding (such as in half-cell tests), but cannot be used to measure degrees of corrosion protection of post-tensioning grouts. Whether a grout is highly porous, offering negligible corrosion protection, or is constituted by a dense and protective cementitious matrix, the result for open circuit potential is -235 ± 9 mV$_{SCE}$. This value, as expected, is located in the zone qualified in the "Standard Test Method for Half-Cell Potentials of Uncoated Reinforcing Steel in Concrete", ASTM C876–91 (1999), as having probability greater than 90% that no corrosion activity is occurring (half-cell potentials more positive than -461 mV$_{SCE}$).

4.6 POTENTIODYNAMIC POLARIZATION

In potentiodynamic polarization tests, the main idea is to identify linear anodic and cathodic branches that appear when the data obtained is plotted in a semi-log format. These linear responses should develop for, at least, one order of magnitude (or decade), allowing the determination of their respective slopes, or Tafel constants within an acceptable margin of error.

Since activation polarization is not a typical behavior of ACT specimens, as will be demonstrated in this section, the Tafel constants determined in these situations should be regarded merely as tangents to "Tafel-like" slopes. Nevertheless, in this work, the terms Tafel and Tafel-like are used interchangeably, even considering that the former is probably used inappropriately.

4.6.1 Test difficulties

The grout that embeds the steel strand in an ACT specimen is a porous medium that creates a complex situation for electrochemical tests and especially potentiodynamic scans. Not only does the concentration of the different chemical species involved in the processes become a more difficult issue to analyze, but also the mass transport of ions from and towards the interface's double layer is directly affected because of the physical barrier imposed by the grout.

In general, it was found during the experimental program that anodic responses are significantly affected by the type of grout used and, many times, have their Tafel-like behavior hindered, not allowing parameter determinations. The reasons for this problem may be related to some aspects like grout's bulk density, specification of an appropriate range of potentials and the presence of the grout itself. These are discussed in the next sections.

4.6.1.1 Grout barrier action

Figure 4.19 shows potentiodynamic polarization plots obtained for one ungrouted steel strand specimen in a 1% calcium oxide (CaO) solution by mass and for one grouted specimen in a 5% salt (NaCl) solution by mass. The data determined for the ungrouted steel was obtained after tests with strands containing different amount of wires (one to seven) and characterize the corrosion behavior of the steel used in the ACT specimens

(specifications given in the Appendices) when in a high pH environment (above 12.5).
The data determined for the grouted specimen (control grout) was obtained from six
replicates moist cured for 28 days.

Although the bulk electrolytes used in each of the two cases were different, it is
reasonable to consider that, in the second situation, at a certain depth near the steel
surface, a zone free of chlorides does exist. Therefore, the significant differences
observed between both plots are probably a consequence of the barrier imposed by the
grout layer, which affects the ionic mass transport and the speed of the ongoing
electrochemical reactions, modifying in this way the output.
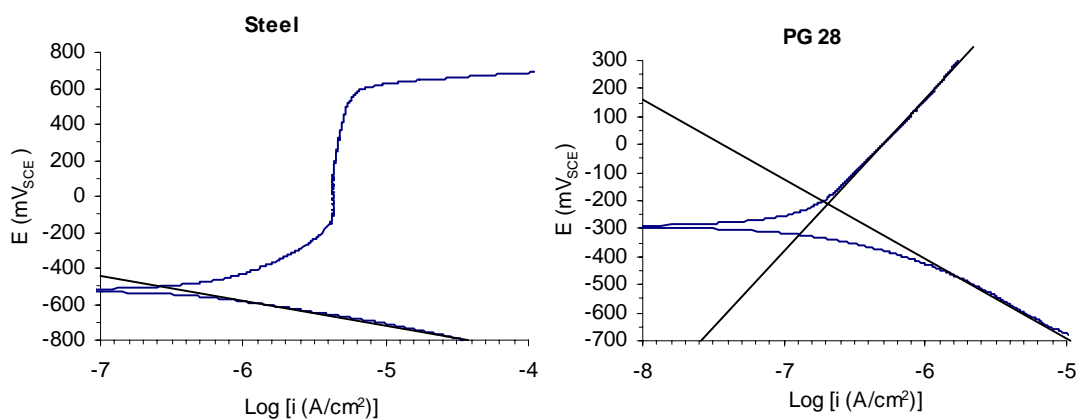
Figure 4.19 - Potentiodynamic plots for the steel used in the ACT specimens in a 1% CaO solution by mass and for a plain grout ACT specimen in a 5% NaCl solution by mass. Data from the tests with ungrouted steel: E_{corr} = -488 ± 10 mV$_{SCE}$; β_c = -127 ± 1 mV; i_{corr} = 0.30 ± 0.03 μA/cm^2. Data from the PG 28 tests: E_{corr} = -284 ± 6 mV$_{SCE}$; β_a = 549 ± 36 mV; β_c = -240 ± 21 mV; i_{corr} = 0.22 ± 0.02 μA/cm^2

When compared to the second plot, the first shows a lower cathodic slope and no anodic constant can be promptly determined. In addition, a passivated state is clearly reached in the first graph, with an evident transpassive response afterwards.

The curve shape obtained in the second graph seems to be better behaved, with anodic and cathodic responses that could indicate a predominant activation polarization response. Nevertheless, further tests pictured in the next plots, reveal that the linearity observed on each curve branch is difficult to be obtained and noise or signal instability is the typical pattern.

4.6.1.2 Range of potentials

Another aspect that may affect potentiodynamic responses on ACT specimens is the range of potentials applied. Typically, for working electrodes in general, a range of 500 mV should be enough to determine the distinct stages of corrosion behavior and the parameters of interest. When ACT specimens are tested, however, this range is not likely to be enough and wider ranges have to be used, generating possible secondary effects on the samples.

The two graphs shown in Figure 4.20 illustrate the response of ACT specimens with the same characteristics and properties that were subjected to different ranges of potentials (600 and 1,400 mV). Two aspects can be highlighted when comparing the two plots. First, the cathodic slopes are considerably higher in the plot on the right and,

second, the two curves on the left seem to agree more with each other, while the curves on the right show more instability on the anodic signal.

As commented earlier, it is widely accepted that activation polarization behavior (which is characterized by a linear signal in a semi-log plot) should develop, at least, for one decade or order of magnitude, allowing the determination of Tafel slopes. Nevertheless, in one of the examples given, a range of potentials as low as 600 mV is barely enough to identify cathodic branches, and insufficient for the anodic ones. An adequate range of potentials, according to the second plot shown, would be from –700 mV_{SCE} to +200 mV_{SCE}, or a 900 mV spread.
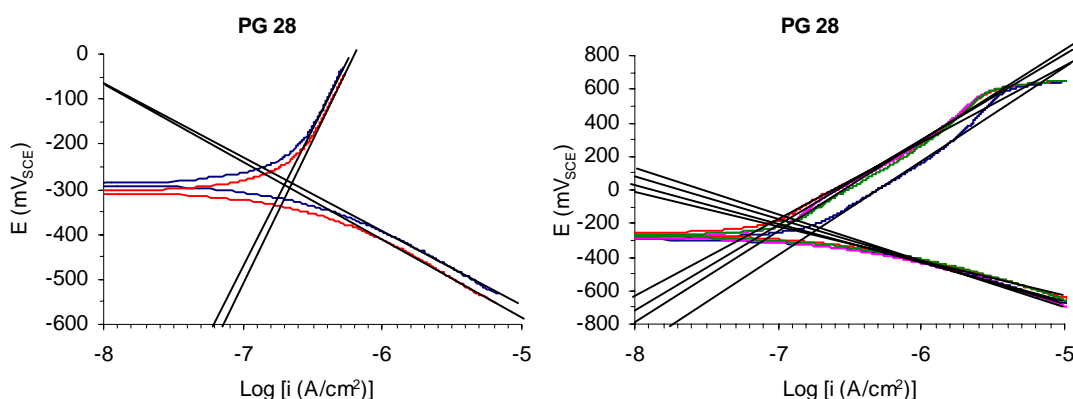
Figure 4.20 - Potentiodynamic plots for plain grout ACT specimens subjected to two different potential ranges. The specimens subjected to the lower range give: E_{corr} = -298 ± 9 mV_{SCE}; β_a = 630 ± 30 mV; β_c = -182 ± 2 mV; i_{corr} = 0.23 $\mu A/cm^2$, while the specimens subjected to the higher range give: E_{corr} = -277 ± 7 mV_{SCE}; β_a = 482 ± 19 mV; β_c = -269 ± 14 mV; i_{corr} = 0.21 ± 0.03 $\mu A/cm^2$

In summary, based on these observations, it is reasonable to claim that a wide range of potentials is necessary to obtain Tafel-like behavior from grouted specimens, and that high potentials may condition the samples and affect results.

4.6.1.3 Grout bulk density

Tafel-like responses were consistently difficult to obtain throughout the tests conducted, particularly when considering the one-decade requirement. In addition to the concerns with the range of potentials and the physical barrier imposed by grouts on ACT specimens, there is also the problem related to the considerable amount of noise observed in some of the results, as can be verified in Figure 4.21. It seems that tests conducted on samples with higher porosity values result in a significant amount of noise. In addition, they seem to have more difficulty in developing an anodic Tafel-like behavior.

Although the data collected seem to indicate more problems when grout porosity is high, a conclusion in this direction is difficult to make because the variable was not completely isolated, and the high potentials applied may be affecting overall responses as well. The first three graphs in Figure 4.21 (FA 07, CI B 28, and SF5 07) have a commonality of high values of permeable voids (39.5, 37.8, and 37.2%) and wide range of potentials. These graphs show intense noise and, in two of the plots, significant disagreement between the curves obtained, with consequent high parameter variability. For instance, the graph for FA 07 gives, for one curve, an E_{corr} equal to –311 mV_{SCE}, while the other gives –781 mV_{SCE}. The curves for SF5 07 give, for E_{corr}, -874 and –603 mV_{SCE} and, for i_{corr}, 6.03 and 0.72 $\mu A/cm^2$. The last two plots with lower values of permeable voids (30.9 and 28.3%) and a narrower range of potentials applied show no noise and much more agreement between the curves obtained. The results for PG 28 seem to confirm the hypothesis of less noise and variability on samples with less porosity, even when the potentials applied are high.
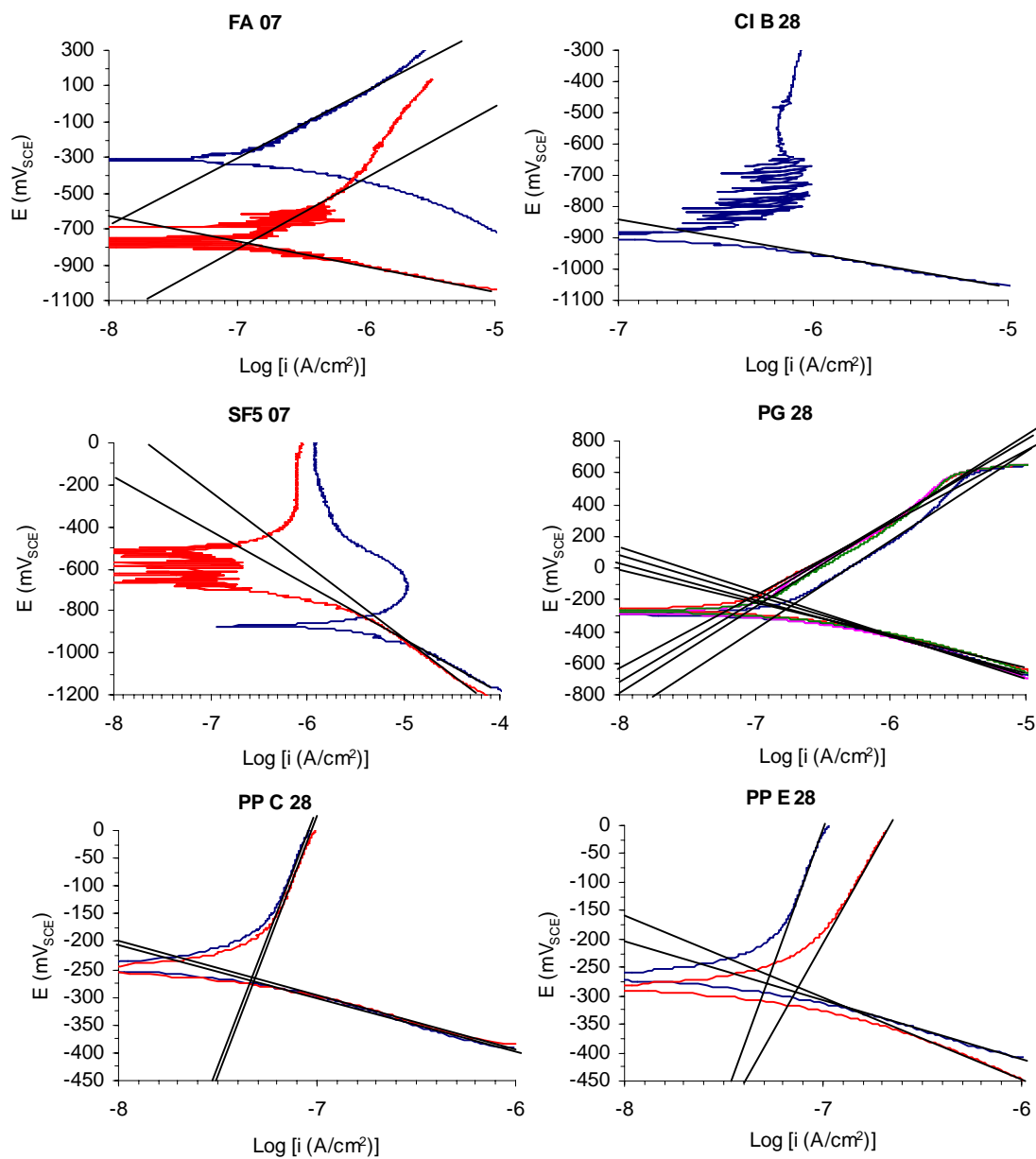
Figure 4.21 - Potentiodynamic plots for different types of grout. The plots are organized in a descendant order of porosity: FA 07 (39.5%); CI B 28 (37.8%); SF5 07 (37.2%); PG 28 (35%); PP C 28 (30.9%); PP E 28 (28.3%). Noise seems to be more intense in the first cases.

4.6.2 Corrosion Potential vs. Time-to-Corrosion

Corrosion potentials, E_{corr}, correspond to a steady-state condition between anodic and cathodic reactions in a similar way that equilibrium potentials, E_o, correspond to a redox balance of a single substance, and similarly to the way that open circuit potentials, E_{oc}, characterize the mixed potential condition reached during a polarization corrosion test.

Although E_{corr} measurements do experience a considerable influence from the type of grout, they show little to no correlation with the corrosion protection degree of grouts. This is illustrated in Figure 4.22, where an overall erratic trend in E_{corr} measurements is observed while the time-to-corrosion significantly increases.
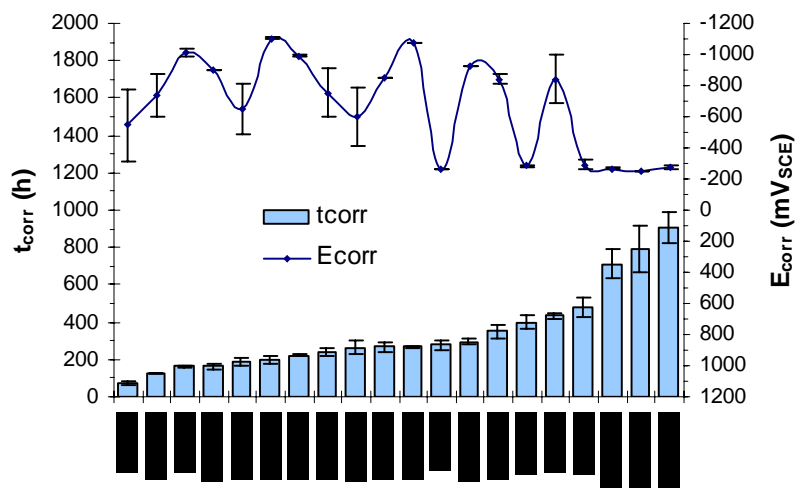
Figure 4.22 - Variation of corrosion potentials, E_{corr}, with times-to-corrosion.

However, it can be also noticed from the figure that E_{corr} measurements tend to be grouped in two distinct potential levels: one near -300 mV$_{SCE}$ and another involving values more likely to be in a range of potentials that goes from -600 to $-1,100$ mV$_{SCE}$.

This can be more readily verified in Figure 4.23, where the two variables, E_{corr} and t_{corr}, are plotted in a Cartesian arrangement. Therefore, it is possible to infer that when E_{corr} is less negative (-271 ± 7 mV$_{SCE}$), nothing can be concluded in respect to the grout's corrosion protection, but when E_{corr} reaches highly negative values (-845 ± 46 mV$_{SCE}$), the grout's performance in an ACT is likely to be insufficient (t_{corr} equals to 232 ± 25 hours).
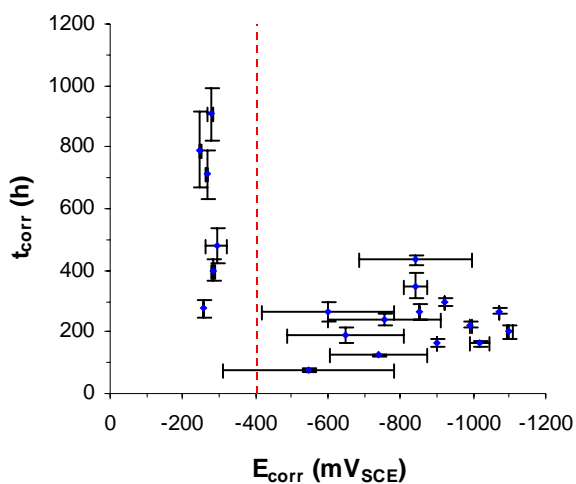
Figure 4.23 - High values of E_{corr} tend to correspond to low corrosion protection of grouts

It should be noticed, however, that the result found for the fly ash grout at 56 days reaches a considerable value of E_{corr} (around -800 mV$_{SCE}$) but the grout performs, on

average, better than the control grout during the ACT tests. Further testing in this area is

needed to investigate these trends to arrive at more firm conclusions.

4.6.3 Current density vs. time-to-corrosion

The graph shown in Figure 4.24 illustrates the results of current density

measurements for each grout tested.
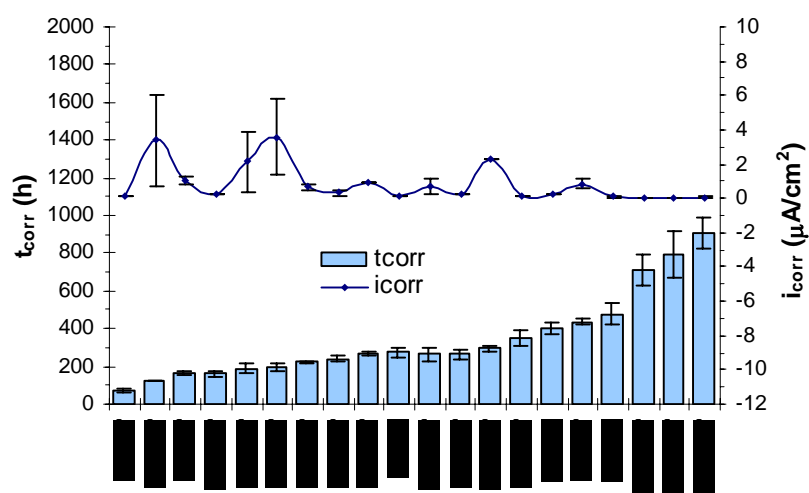
Figure 4.24 - Current density measurements for different types of grout

The current density (corrosion rate) measurements taken during the experimental

program did not reflect any influence from the types of grout used in the tests. All mixes

tested provided the same low level of corrosion rate, varying from 0.03 to 5.2 $\mu A/cm^2$

(0.3 to 60 μm/yr). The averaged corrosion rate, 0.87 μA/cm^2 (10 μm/yr) would lead to

the dissolution of 1 mm of steel by the end of 100 years, indicating a passivated state of

the samples, independently of the grout type. This result was expected since the

alkalinity of any of the mixes tested can be assumed as very high, with supposedly little

variations between them.

Incidentally, from the graph, one can notice that more variability is present on

some silica fume results, which can be also a consequence of the problem regarding

agglomeration occurrences that was discussed earlier in Section 4.2.2.1.

4.6.4 Tafel Constants vs. time-to-corrosion

Twenty different types of grout were tested in potentiodynamic polarization tests

and their plots, in general, allowed easy identification of the cathodic Tafel-like behavior.

Practically all the cathodic curves developed a straight segment for approximately one

decade at a minimum, allowing the calculation of cathodic Tafel constants. On the other

hand, due to differences in quality of the anodic responses, the plots for each grout can be

divided into three different categories that are presented next.

Figure 4.25 shows the first category, which is comprised of the only three cases

that allowed clear identification of anodic linear branches. Grout FA 56, however, was

tested four times and only one curve is satisfactory, but shows a quite different overall

pattern where no cathodic Tafel-like behavior is present.
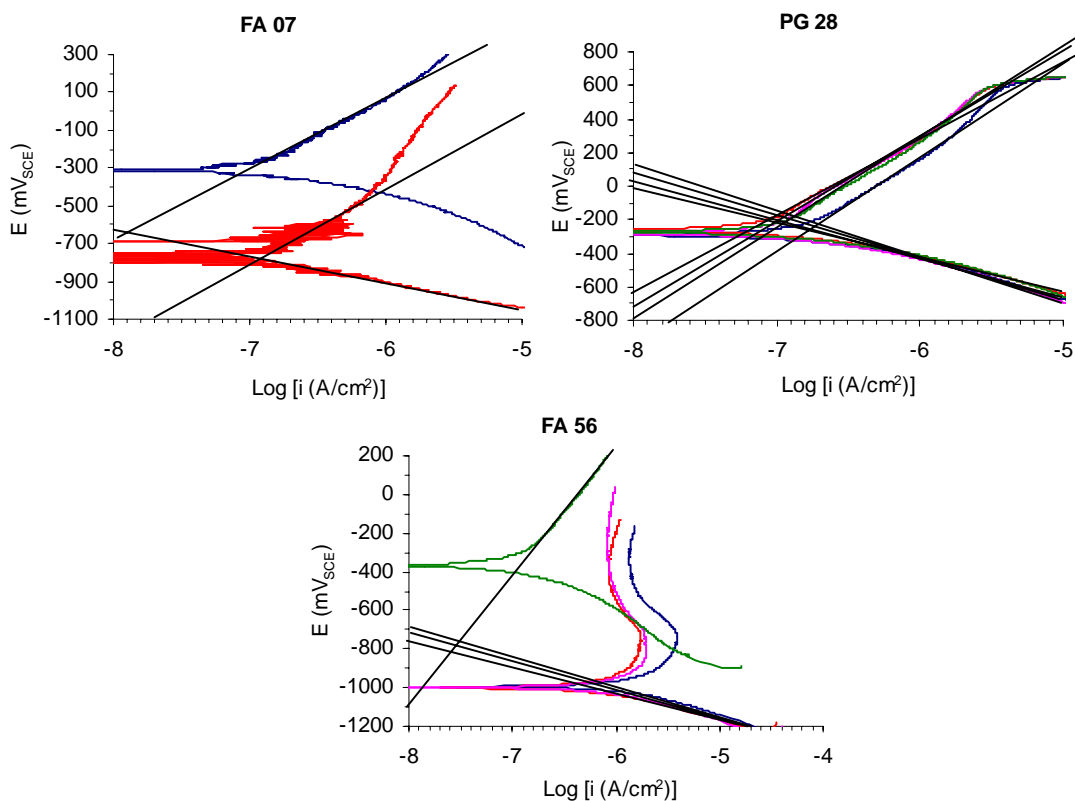
Figure 4.25 - Potentiodynamic plots showing satisfactory anodic and cathodic Tafel-like behaviors

The second category, shown in Figure 4.26, is composed of six cases that allowed limited identification of the anodic Tafel-like responses. Five cases generated limited responses probably because small ranges of potentials were used, while one case probably suffered with the grout's high porosity or with the high values of potentials applied, as speculated previously. The remaining eleven cases generated no anodic Tafel-like behavior and presented a varied pattern of anodic development length from grout to grout. Figure 4.27 and Figure 4.28 present these cases, which can be grouped in a third category of results. It should be noted from these figures that seven of the cases

illustrated are results for silica fume grouts and that the problem regarding agglomeration of silica fume particles could have the same effect in the readings as high porosity would, perhaps confirming this problem.
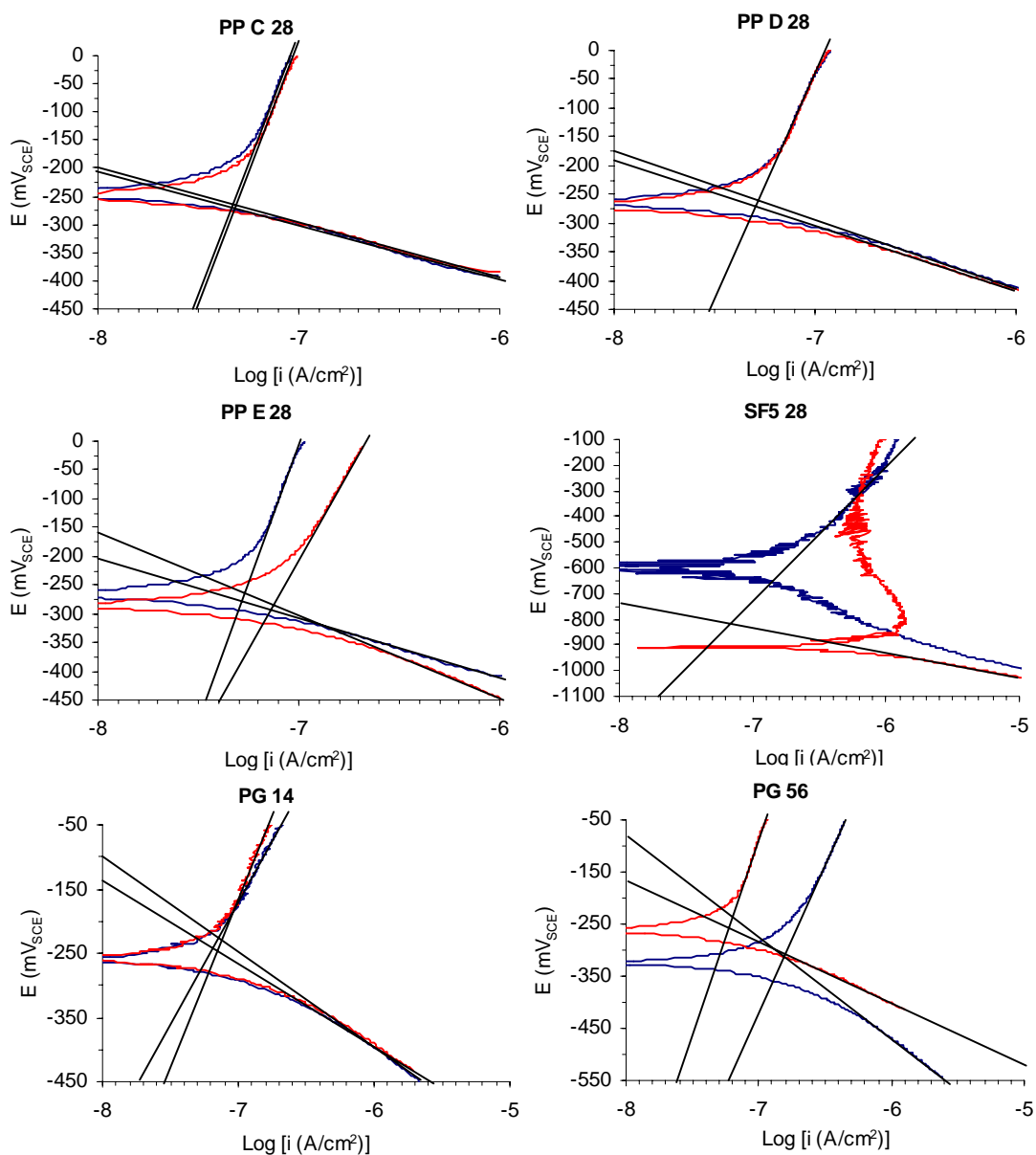
Figure 4.26 - Plots showing satisfactory cathodic and limited anodic Tafel-like behaviors
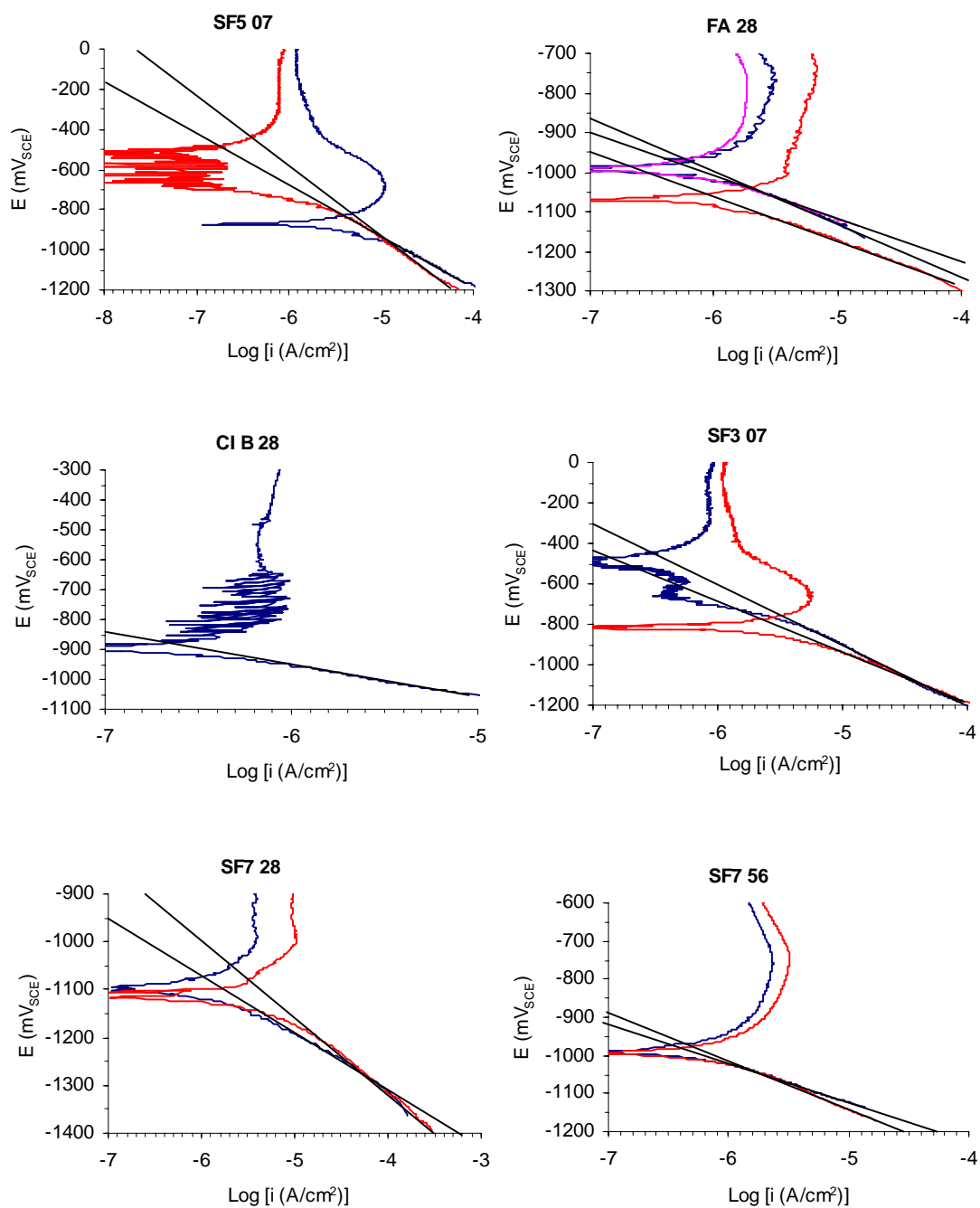
Figure 4.27 - Potentiodynamic plots showing only cathodic Tafel-like behaviors.
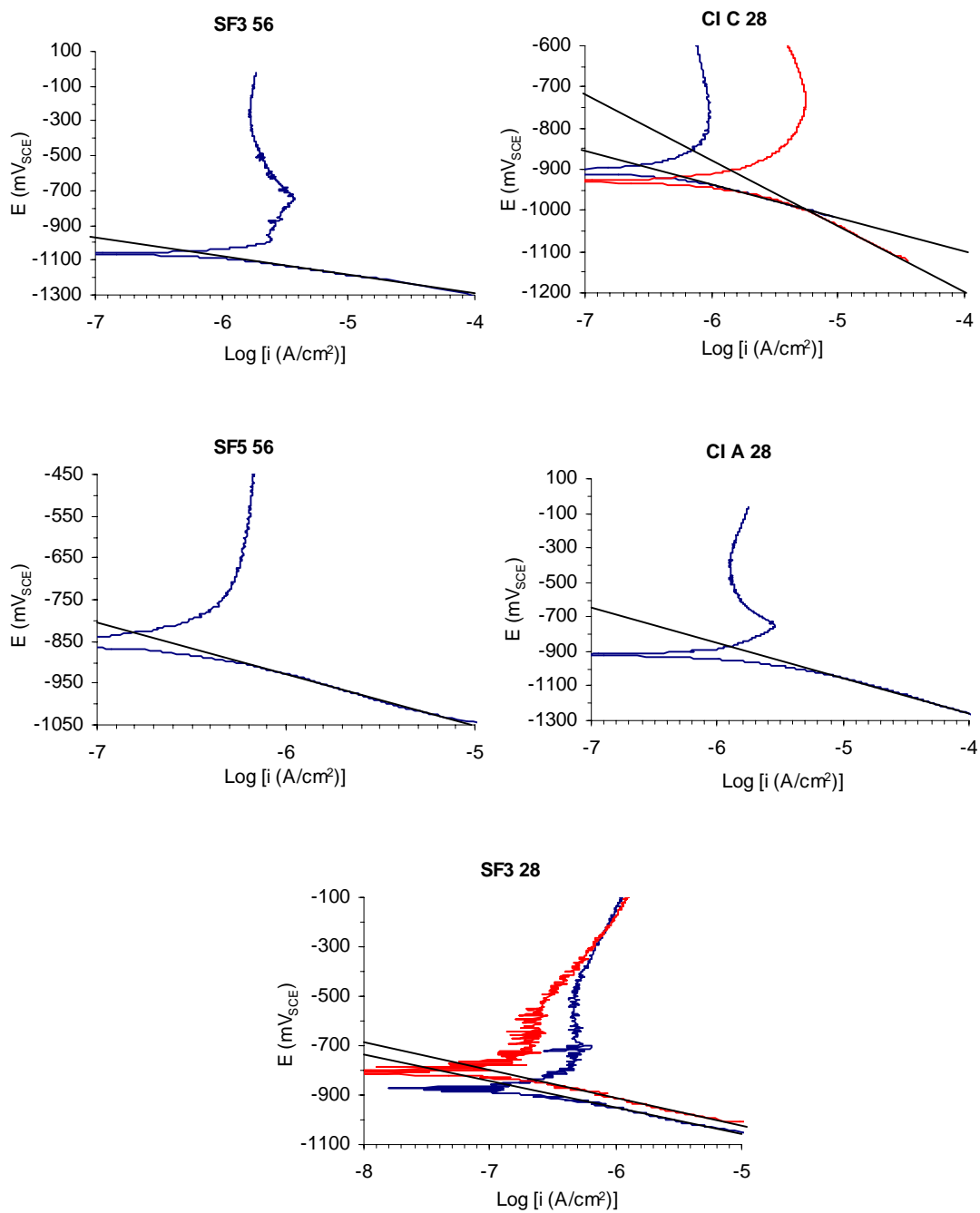
Figure 4.28 – More potentiodynamic scans showing only cathodic Tafel-like behaviors.

As can be seen, even when the anodic branches follow erratic paths, the cathodic Tafel-like curves can still be defined in most of the cases. Each aspect of these curves is analyzed in the next sections.

4.6.4.1 Cathodic Tafel Constant (β_c)

Figure 4.29 shows several different types of grout and their respective times-to-corrosion and cathodic Tafel constants.
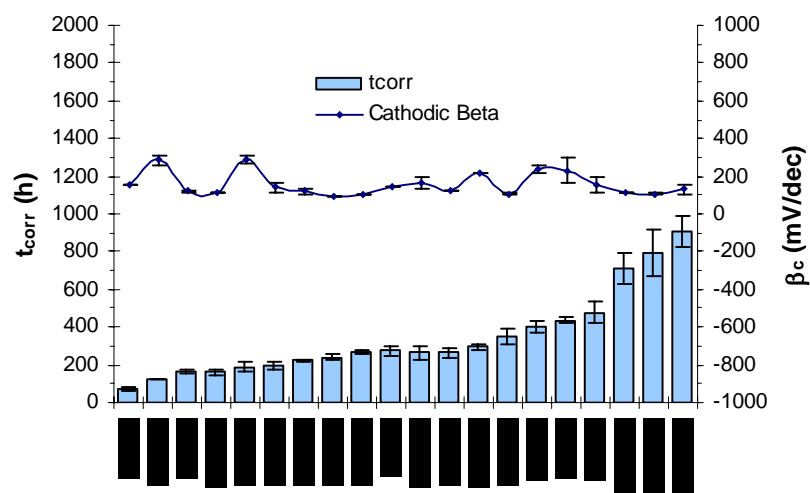
Figure 4.29 - Cathodic Tafel constant found for different types of grout (average: 157 ± 14 mV)

As can be seen, the significant increase in t_{corr} seems not to affect in any way the constant β_c, which can be considered invariable throughout the grouts tested. The β_c

values range from 91 to 287 mV, with an average of 157 ± 14 mV and no interaction is observed with the quality of the grouts tested regarding their corrosion protection. This result was already expected, since the cathodic behavior, in this case, is supposed to reflect the responses for hydrogen or oxygen evolutions, being independent of grout characteristics.

4.6.4.2 Anodic Tafel Constant (β_a)

Figure 4.30 shows the trend obtained for anodic Tafel constants determined for grouts with increasing times-to-corrosion.
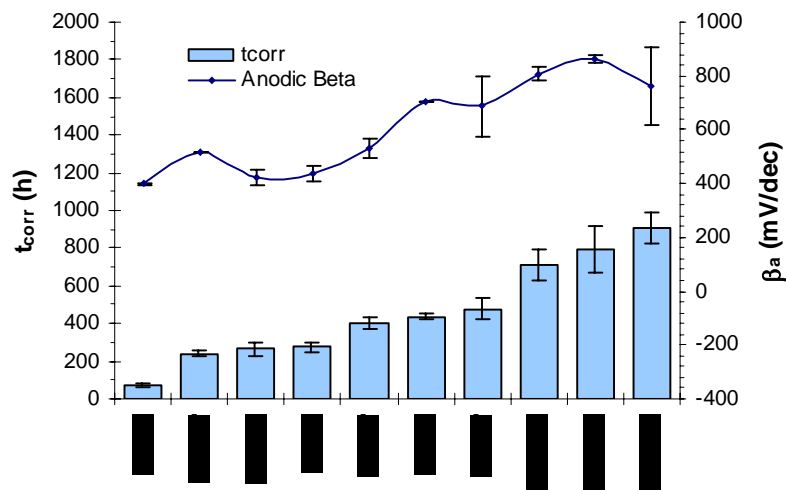
Figure 4.30 - Anodic Tafel constant found for different types of grout.

As can be seen, β_a consistently increases with increasing times-to-corrosion. Upon plotting both variables, β_a and t_{corr}, as in Figure 4.31, their excellent agreement can be verified because of, firstly, the high adherence of the experimental points to the fitted curve and, secondly, because these points are fairly distributed along the interval investigated.
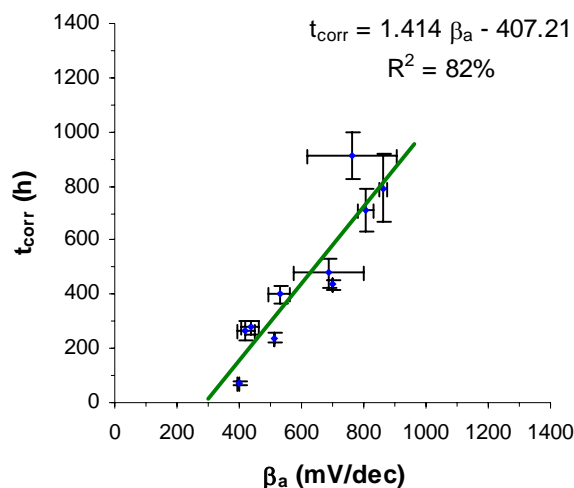
Figure 4.31 - Correlation between anodic Tafel constant and t_{corr}

The correlation equation given in the figure can be written, with no important precision loss, where t_{corr} is given in hours and β_a in mV, as:

$$t_{corr} = 1.4\beta_a - 400$$

Equation 4.4

Although anodic Tafel constants seem to be an excellent option for qualification

of grouts regarding their corrosion protection degree, the use of β_a in this sense should be

still considered with reservations. As commented before, roughly only half of the

potentiodynamic tests conducted provided appropriate corrosion behavior for

determination of anodic slopes. In addition, only three out of twenty grouts produced an

anodic Tafel-like length of at least one decade and one of these three grouts had to have

four replicates tested to allow one satisfactory result. Still, this result was suspicious

because its patterns varied significantly from the other three. Considering all these

points, it is remarkable that such a good correlation still could be found between β_a and

t_{corr}. Additional data are necessary to corroborate the correlation found.

4.6.4.3 Constant B

The results found for anodic Tafel constants, together with their cathodic

counterparts allow the calculation of the constant B for the grouts tested according with

Equation 4.5 (all variables given in mV per decade):

$$B = \frac{\beta_a \beta_c}{2.303(\beta_a + \beta_c)}$$

Equation 4.5

The results are presented in Figure 4.32. As can be seen, B seems neither to be

influenced by the type of grout tested nor by the grout's performance in ACT tests.
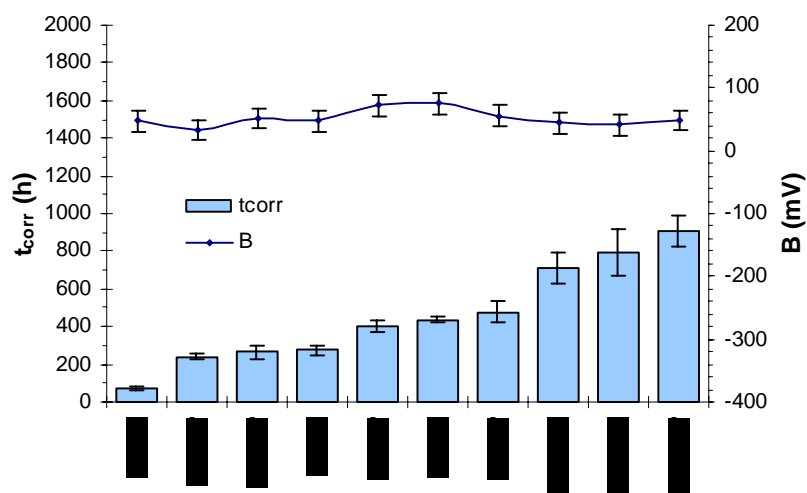
Figure 4.32 - Constant B found for nine types of grout (average: 52 ± 16 mV)

The minimum value observed for B is 34 mV and the maximum is 75 mV. These values are in the same order of magnitude than the values indicated in the literature for structural concrete: from 26 to 52 mV. The average found, 52 ± 16 mV, coincides with the upper limit, which is the value associated to passive conditions of structural concrete.

4.7 POTENTIODYNAMIC LINEAR POLARIZATION RESISTANCE

The difficulties observed in potentiodynamic polarization measurements were not an issue during LPR readings. In fact, each LPR test runs faster and with considerably higher repeatability, when compared to other potentiodynamic scans. This is probably a consequence of the much lower range of potentials necessary to obtain the polarization

resistances. Such range of potentials, which is on the order of 40 mV or, in other words,

10 to 20 times lower than the ranges required for regular potentiodynamic scans, would

not condition the working electrode, preventing corrosion products or oxide layers to

form between the strand surface and the encasing grout. Hence, no interaction of these

products and layers in the grout's pores would occur, reducing any signal noise,

distortion, and instability of the readings.

During the experimental program, however, some of the grouts were not tested in

LPR tests and had to have their polarization resistance calculated from regular

potentiodynamic scans. Figure 4.33 shows the variation of the polarization resistance,

R_p, for each grout tested, showing also their degree of corrosion protection.
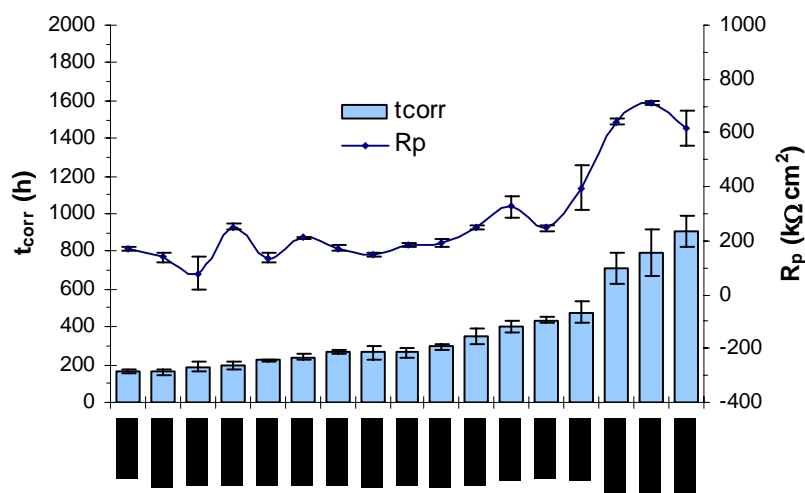
Figure 4.33 - Variation of the polarization resistance, R_p, for different types of grout

As can be noticed, more variability is present on the experimental points for grouts SF3 7Y, PG 28Y, PG 56Y, and PP E 28Y. The polarization resistances for these tests, together with the values found for grouts PP C 28Y and PP D 28Y, were calculated with data collected from regular potentiodynamic scans, not LPR tests *per se*. These grouts are highlighted in Table 4.2, which presents again the list of grouts used in the previous graph and identifies those tests whose R_p values were calculated from regular potentiodynamic data with much higher potential ranges, since this type of tests employ considerably higher values of potentials in order to define Tafel-like regions

Table 4.2 - R_p and t_{corr} values obtained from LPR and regular potentiodynamic scans (highlighted)

Grout	R_p, kΩcm^2	t_{corr}, h	ΔE (mV)
FA 28Y	169 $\pm$ 6	162 $\pm$ 9	40
CI B 28Y	138 $\pm$ 21	163 $\pm$ 14	40
SF3 07Y	79 $\pm$ 62	187 $\pm$ 25	2,100
SF7 28Y	251 $\pm$ 10	200 $\pm$ 20	40
SF7 56Y	136 $\pm$ 20	223 $\pm$ 8	40
SF5 28Y	211 $\pm$ 5	240 $\pm$ 17	40
SF3 56Y	172 $\pm$ 9	268 $\pm$ 8	40
CI C 28Y	148 $\pm$ 6	265 $\pm$ 34	40
SF5 56Y	183 $\pm$ 6	267 $\pm$ 25	40
CI A 28Y	193 $\pm$ 15	295 $\pm$ 13	40
SF3 28Y	249 $\pm$ 8	349 $\pm$ 40	40
PG 28Y	325 $\pm$ 43	401 $\pm$ 33	500, 1600, 1800
FA 56Y	246 $\pm$ 13	435 $\pm$ 15	40
PG 56Y	397 $\pm$ 82	479 $\pm$ 55	500
PP D 28Y	641 $\pm$ 11	712 $\pm$ 78	500
PP C 28Y	711 $\pm$ 9	793 $\pm$ 124	500
PP E 28Y	618 $\pm$ 62	909 $\pm$ 85	500

In these cases, the polarization resistances were obtained through plotting of the potentiodynamic polarization data in a Cartesian or rectangular coordinate system, instead of a semi-log one. This procedure allowed the calculation of the desired polarization resistances, but probably led to the higher values of standard error observed.

Nevertheless, as can be seen from the data presented, R_p is a variable that is intensely affected by the quality of grouts' corrosion protection, reaching resistances that can be as high as 711 kΩcm^2 for extended values of times-to-corrosion or as low as 79 kΩcm^2 when the times-to-corrosion are deficient.

Therefore, in an attempt to find a correlation between t_{corr} and R_p, the plots pictured in Figure 4.34 are presented. The first one, (a), presents only results found in LPR tests, resulting in a weak correlation between the variables. Probably the main problem is the fact that the data is concentrated in a small range of times-to-corrosion, varying from 150 to 450 hours. However, in the second plot, (b), with the worst point removed (SF7 28), R^2 significantly increases from 29 to 62%, showing that the data is, in fact, consistent. Hence, in order to make more evident the correlation between the variables, the data for grouts SF3 56, SF5 28, and SF5 56 are removed in the third plot, (c), because they give, approximately, the same result that CI C 28 gives (times-to-corrosion of 240, 268, 267, and 265 hours, respectively). In addition, FA 28 (t_{corr} of 162 h) is also removed from the plot, since CI B 28 (t_{corr} of 163 h) also gives, approximately, the same result. The correlation is even increased in the fourth plot, (d), where the remaining data obtained from grouts with mineral admixtures is removed (SF7 56 and SF3 28). It was expected that the data from these types of grout would be more difficult

to fit in the correlations, mainly when the range of times-to-corrosion used is narrow, because, among all the types tested, they were the ones that shown more variability.
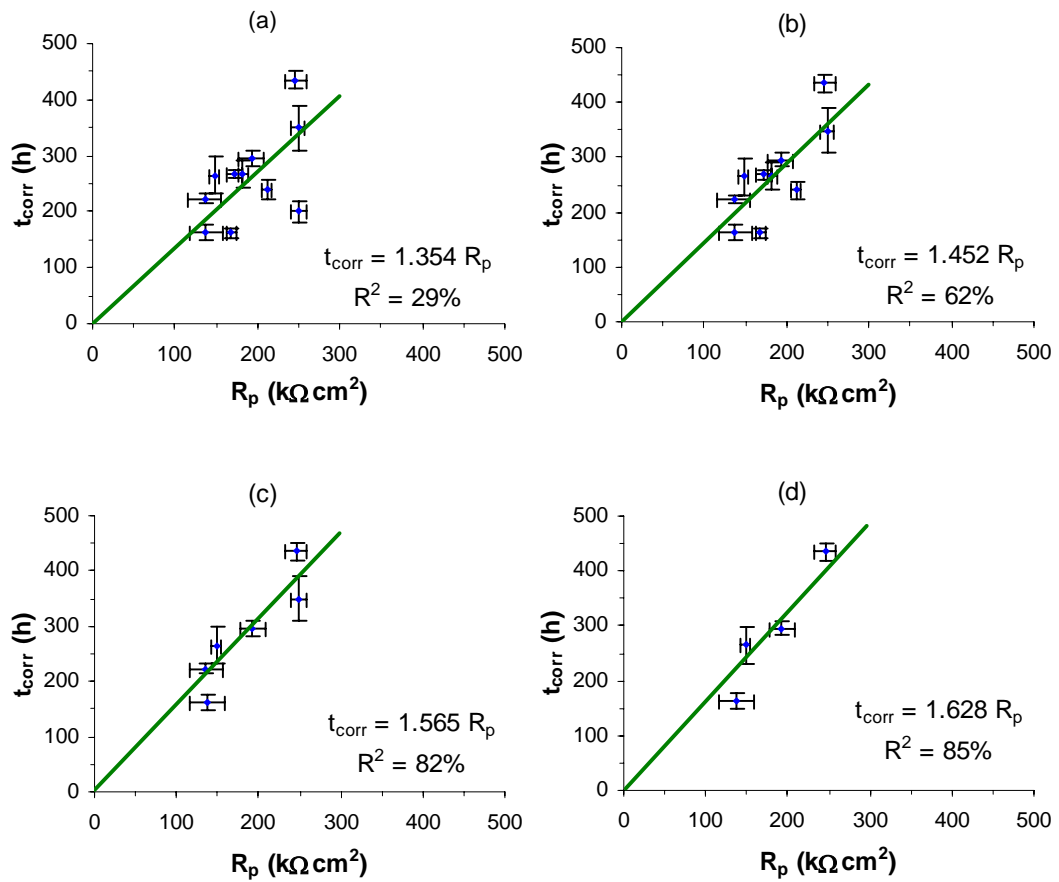
Figure 4.34 - Correlations between t_{corr} and R_p: (a) only data obtained from LPR tests are plotted; (b) the point SF7 28 is removed, significantly increasing R^2; (c) the points SF3 56, SF5 28, and SF5 56 are removed in order to obtain a distribution of fairly equidistant t_{corr} points; (d) only the grouts with no mineral admixtures are plotted

Although considering the problems mentioned, regarding more variability of
some types of grout (on t_{corr}) or even the fact that important data were found with
inappropriate procedures (R_p values related to high values of t_{corr} found from regular
potentiodynamic scans instead of LPR tests), a satisfactory correlation can still be found
when all the information available is used.

Thus, upon plotting all of the values for polarization resistance against their
respective ACT results, the linear correlation pictured in Figure 4.35 is found.

$$t_{corr} = 1.250 \ R_p$$
$$R^2 = 89\%$$
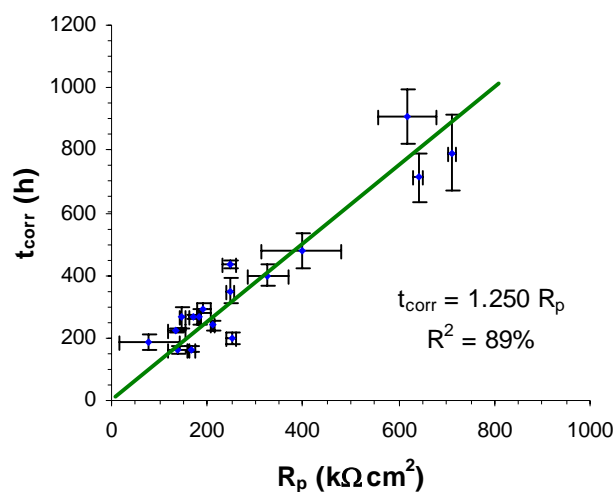
Figure 4.35 - Correlation between R_p and t_{corr}

The correlation between the two variables seems adequate, with values
characterizing grouts of low and average corrosion protection appropriately adhering to
the fit calculated. However, a small gap can be noticed between two apparent groups of

values. In addition, few points representing grouts with high corrosion protection are available and more variability is present on their t_{corr} values.

The equation of correlation is highlighted, in Equation 4.6, where R_p is given in $k\Omega cm^2$ and t_{corr} in hours.

$$t_{corr} = 1.25 R_p \qquad\qquad \textbf{Equation 4.6}$$

Considering the satisfactory correlation between the two variables, the simplicity of LPR measurements, and their high repeatability, the method could be appropriately used to complement or, perhaps, even replace current ACT procedures for estimation of grout's corrosion protection. For instance, a minimum polarization resistance value of 700 $k\Omega cm^2$ may be a reasonable (but restrictive) approval limit, since it is likely to be measured on grouts that would produce a t_{corr} of 875 hours in a compensated ACT test.

Applying the same correction done previously for the t_{corr} condition of 1,000 hours, which gave a compensated value of 700 hours, again the same correction can be adopted. Therefore, for uncompensated systems, the suggested 700 $k\Omega cm^2$ should be modified to 1,000 $k\Omega cm^2$.

5 COMPLEMENTARY RESULTS AND DISCUSSIONS

This chapter complements the results given in the previous chapter. It starts discussing the results obtained for the prepackaged grout that did not allow corrosion. Next, it shows the additional information obtained with the measurements taken from the specimens after their passage from a passive state to a damaged condition. Then, considerations about the electric charge results obtained from the potentiostatic tests are discussed and, finally, it ends with a discussion of possible sources of error in the experimental program.

5.1 PARAMETERS MEASURED FOR PP B 28Y

The prepackaged grout identified as PP B 28Y (moist cured for 28 days and tested in the potentiostatic test with compensation for voltage drops) could not figure in any of the correlation graphs shown in the previous sections because no t_{corr} value could be found for this grout. During its ACT test, as commented before, its specimens never showed any indication of a corrosion process being initiated, even after more than 3,000 hours (more than 4 months) of testing had been elapsed and, for this reason, no time-to-corrosion could be determined.

Nevertheless, since this prepackaged grout was the best grout during the ACT tests, a question rises on how its properties would fit the trends set by the other grouts or whether PP B 28Y would corroborate the results. For instance, its value of porosity

should be below 30% (28% was the lowest value found), its anodic Tafel constant should

be around 2,558 mV (using Equation 4.2), and its polarization resistance should be

around 2,560 kΩcm^2 (using Equation 4.6) or, at least, higher than 711 kΩcm^2 (the highest

value found). These and other parameters are presented in Table 5.1.

Table 5.1 - Measured and expected parameters for grout PP B 28Y

Property	Measured	Expected
V (%)	28.6 ± 0.3	Less than 30
β_a (mV/decade)	2,415 ± 272	2,558
R_p (kΩcm^2)	1,011 ± 226	2,560 or higher than 711
E_{oc} (mV$_{SCE}$)	-162 ± 11	From -334 to -144
E_{corr} (mV$_{SCE}$)	-394 ± 39	Above than -400
i_{corr} (μA/cm^2)	0.17 ± 0.07	From 0.07 to 0.86
β_c (mV/decade)	-462 ± 5	-157 ± 13
B (mV/decade)	168 ± 5	From 34 to 134

Indeed, regarding porosity, the prepackaged grout B presents a value right below

the limit of 30% mentioned, with a volume of permeable voids of 28.6%. This porosity

was reached with a water-cementitious ratio of 0.27, according to the manufacturer's

recommendations.

The grout was not tested in potentiodynamic tests prior to its ACT and, therefore, no anodic Tafel constants corresponding to a passive state can be determined. However, after completion of 3,200 hours of potentiostatic testing without signs of corrosion, potentiodynamic tests were then conducted, allowing the determination of an anodic Tafel constant for the grout of $2,383 \pm 293$ mV. Although this value was measured during an unknown intermediary condition of damage, it considerably agrees with the trend found previously. In fact, the measured value is very close to the quantity determined with the correlation equation obtained when a t_{corr} of 3,200 hours is assumed (2,558 mV).

The value found for R_p of 1011 ± 226 kΩcm^2 is considerably high, but does not correspond to an estimated value using the correlation equation suggested previously, which gives 2,560 kΩcm^2 for 3,200 hours. However, considering the conditions of the test conducted, the value measured can be considered as a reasonable one. Besides, it is higher than the highest value of polarization resistance found for the other grouts ($711 \pm$ 9 kΩcm^2). Another aspect to be considered is the likelihood of the linear correlation found not to be valid for values of polarization resistance much higher than the interval studied and, in fact, an asymptotic behavior could be correct trend. This aspect requires further investigation.

Figure 5.1 presents the curves from which the potentiodynamic parameters were calculated. The same data were used to calculate R_p.
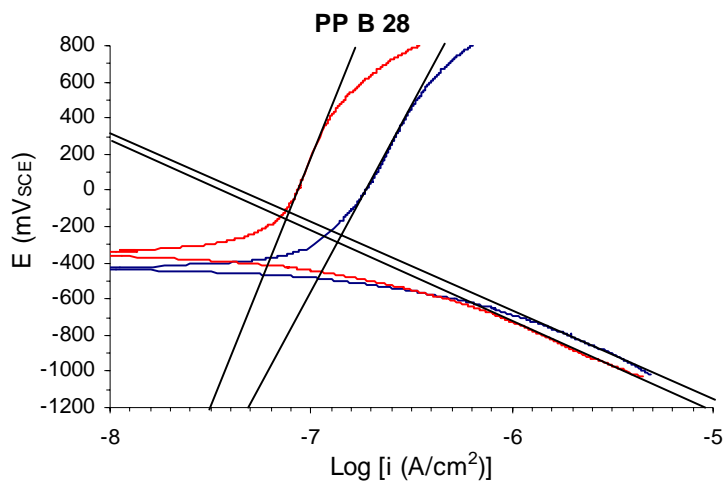
Figure 5.1 - Potentiodynamic curves obtained for prepackaged grout B after 3,200 hours of potentiostatic testing. The parameters calculated are: E_{corr} = -394 ± 39 mV$_{SCE}$; i_{corr} = 0.17 ± 0.07 μA/cm^2; β_a = 2,415 ± 272 mV; and β_c = -462 ± 5 mV

Regarding the result for E_{oc} of -162 ± 11 mV$_{SCE}$ from polarization corrosion tests, the value is in the interval expected, but above the arithmetic mean obtained in those tests, which amounts -235 ± 9 mV$_{SCE}$. Regarding E_{corr}, it was commented before that grouts of high performances are more likely to have their corrosion potentials above the limit of –400 mV$_{SCE}$, having an average result of –271 ± 7 mV$_{SCE}$. Thus, the value measured of –394 ± 39 is reasonable because it is above the mentioned limit and, since the specimens were ACT tested first, it is then higher than the estimated average.

The value determined for i_{corr}, 0.17 ± 0.07 μA/cm^2, is between the estimated minimum and maximum limits for this variable in the tests conducted. The minimum limit is the average found for the four grouts with best performances, which reached

significantly higher t_{corr} values. The maximum limit is the average of the remaining results (see section 4.6.3).

The value determined for β_c = -462 $\pm$ 5 mV is significantly lower than the expected value of -157 $\pm$ 13 mV. This discrepancy consequently affects the result for B, 168 $\pm$ 5 mV, which is outside the expected limits for this parameter (between 34 and 134 mV).

In addition to the fact that the potentiodynamic measurements were taken after many hours of ACT testing, high range of potentials were also used (a range of 1800 mV), which may explain the minor discrepancies observed for this prepackaged grout. Overall, the results corroborate the trends observed.

5.2 BEHAVIOR AFTER THE ONSET OF CORROSION

After the potentiostatic tests were conducted, most of the grouts were tested again in regular potentiodynamic and LPR measurements. The results, which are shown as follows, should set limits for some of the electrochemical parameters, since the condition created when the grouts' protective layer is breached is an extreme one. The undamaged or passive state of the specimens should set the other extreme case.

During the passive state, it was found before that grouts of low corrosion protection would tend to give very negative E_{corr} values, on the order of –845 $\pm$ 46 mV_{SCE}, while nothing could be said about grouts of satisfactory performances.

Therefore, when any of the grouts tested is cracked because of the expansion caused by the corrosion products, their E_{corr} measurements should likely to reach highly negative values as well. This can be seen in Figure 5.2, where E_{corr} equals, on average, to -755 ± 30 mV$_{SCE}$.
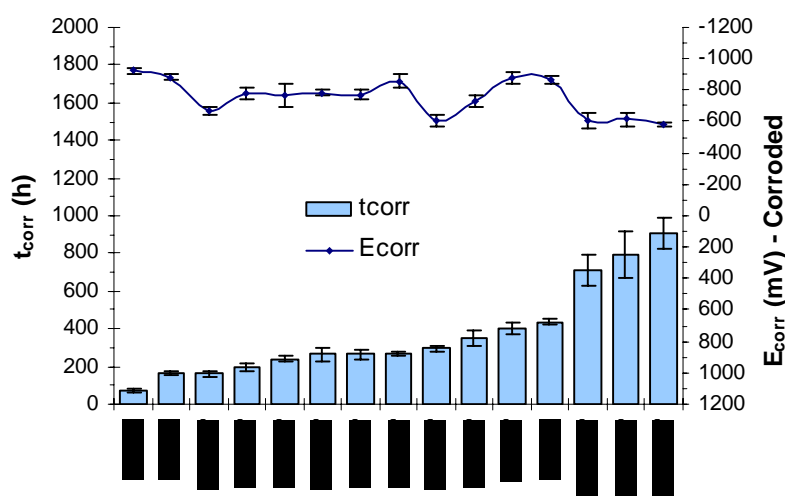
Figure 5.2 - Corrosion potentials measured on grouts previously tested in ACTs

The same tendency for increased values can be observed when corrosion current densities are considered. Figure 5.3 shows the values measured for the corroded state, which average 13 ± 4 μA/cm^2. For comparison, the values measured during the passive state amount to, on average, only 0.86 ± 0.25 μA/cm^2.
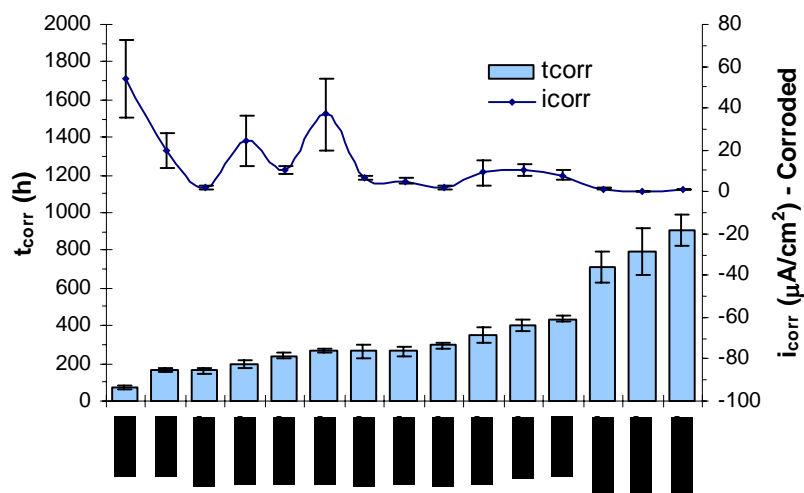
Figure 5.3 - Corrosion current densities measured on grouts previously tested in ACTs

Regarding Tafel constants, it was found before that the cathodic Tafel constant is likely to measure 157 ± 13 mV, with minimum and maximum of 91 and 287 mV, respectively, while the anodic constant is linearly affected by the quality and characteristics of the grout tested. Figure 5.4 shows that the cathodic Tafel constant is still invariant with respect to the grout type, having an average value of 258 ± 17 mV per decade and minimum and maximum of 149 and 374 mV.
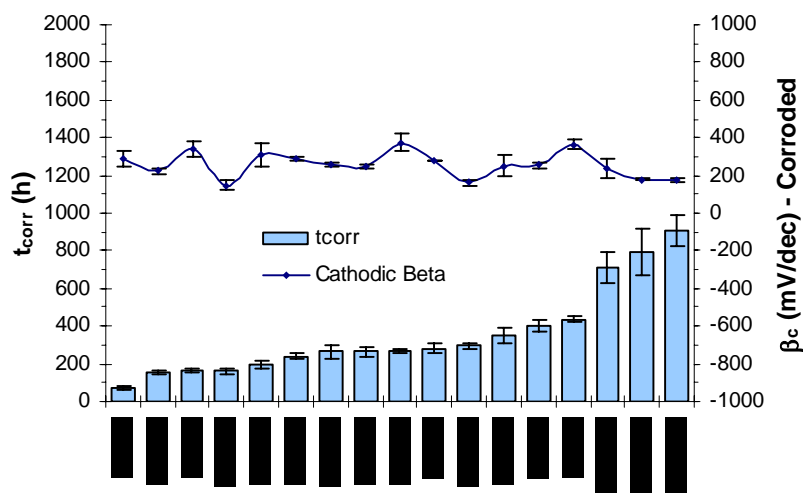
Figure 5.4 - Cathodic Tafel constant measured on grouts previously tested in ACTs

Figure 5.5 shows that the anodic constant looses its dependency on the grout

quality when corrosion is onset, reaching a constant average value of $1,100 \pm 138$ mV per

decade. The fact that this value is considerably higher than the values for β_a measured in

grouts of poor quality, contradicts the correlation found for this variable with respect to

t_{corr}. A corroded specimen should emulate the situation of a grout of unsatisfactory

performance and, according to the correlation found, should give a low value for the

measured anodic Tafel constant.
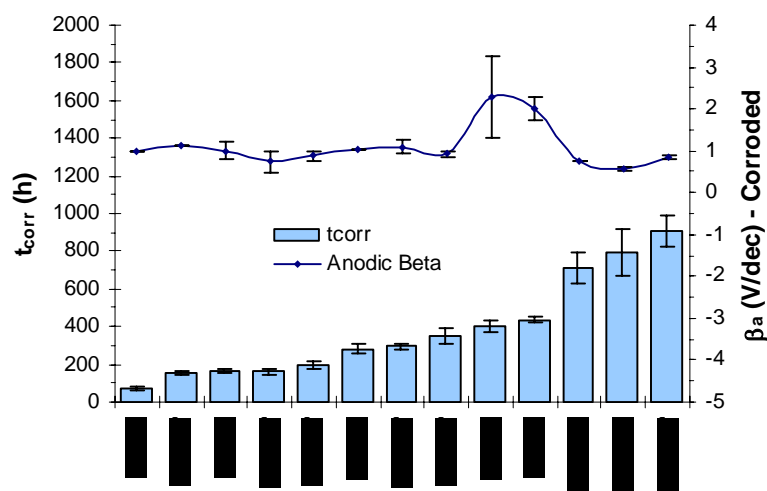
Figure 5.5 - Anodic Tafel constant measured on grouts previously tested in ACTs

The values calculated for the constant B, using the Tafel constants relative to the damaged conditions of grouts, are plotted in Figure 5.6. The average of the values is 86 ± 6 mV, which is higher than the average calculated for the passive condition: 52 ± 16 mV. These two averages can be considered as upper and lower limits to be adopted in electrochemical tests that involve grouts, since they are related to extreme conditions for ACT grout specimens.

Regarding the results for LPR measurements, it can be seen in Figure 5.7 that all tests produce the same very low value of polarization resistance: 33 ± 4 kΩcm^2. This result shows once more that, after cracks are formed in the bulk of grouts, they lose completely their corrosion protection and behave in a similar fashion.
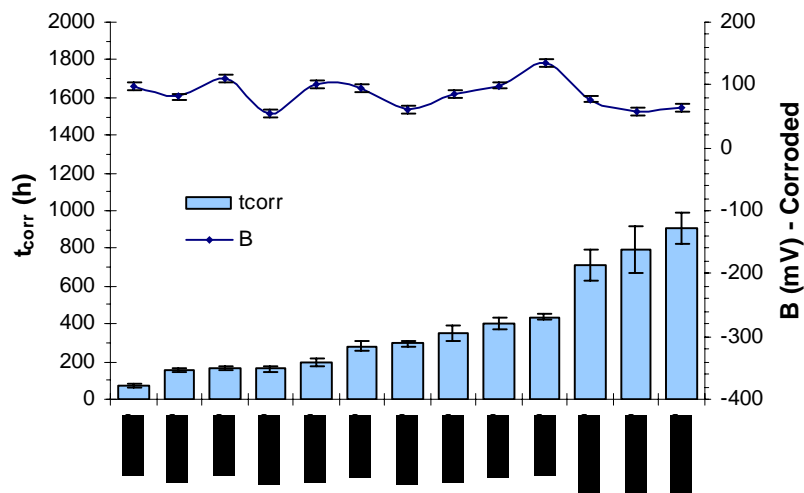
Figure 5.6 - Constant B calculated for grouts previously tested in ACTs
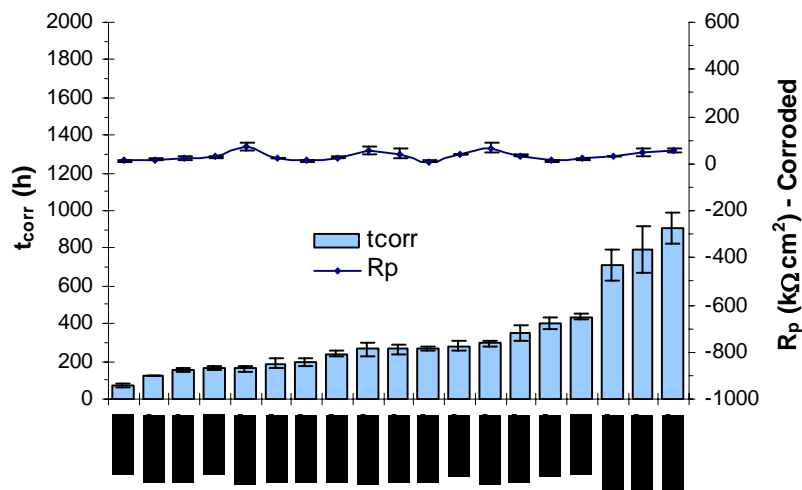
Figure 5.7 – Polarization resistances measured on grouts tested previously in ACTs

5.3 CHARGE LEVEL WITH AND WITHOUT COMPENSATION

Figure 5.8 presents calculated electric charges developed in ACT tests with and without compensation for voltage drops.

As commented previously, all the charge values were calculated considering time values larger or equal to each specimen's individual t_{corr} and currents lower or equal to 10 mA. Hence, in this way, the calculated values can be compared with each other.
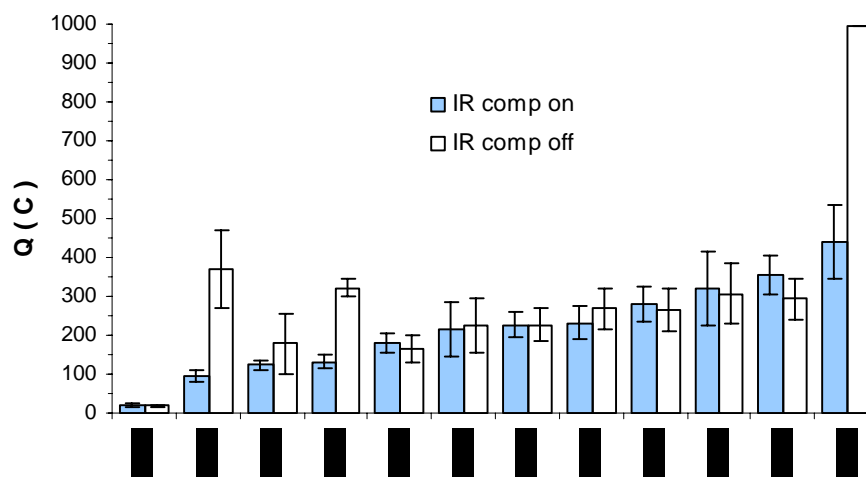
Figure 5.8 - Electric charges in compensated and uncompensated ACTs

As can be seen, the calculated charges tend to reach the same levels either whether the option for compensation of voltage drops is engaged or not. Only three cases shown in the figure are significantly higher during the tests conducted without

compensation. Therefore, confirming the hypothesis outlined earlier regarding the electric charge as a parameter for grout characterization, no significant increase in the level of charge can be expected when the polarization voltage drops. The direct effect of this drop is clearly the increase in the grout's t_{corr}, but, once the corrosion is onset, the physical characteristics of the grout are the factors that will dictate the escalation of the measured current and, consequently, the level of the generated charge.

5.4 ERROR SOURCES

Several factors are likely to have negatively influenced the responses obtained from each of the electrochemical tests. These factors are discussed in this section.

5.4.1 Number of Specimens

The number of specimens used in each of the experiments was determined based upon three aspects: power analyses of the experiments, the number of stations available, and a time limit of two years.

Considering the power analyses, all the experiments were designed based on an Significance Level of 5% and a Power of 80%, i.e., the required number of specimens in each test considered probabilities of 5% (alpha) and 20% (beta) of Type I and Type II errors to occur, respectively. A Type I error occurs when a null hypothesis (e.g.: "there is no difference between two grout test results") is wrongly rejected, while a Type II error

occurs when this null hypothesis is wrongly accepted. Therefore, with a higher probability for a Type II error, it is more likely that no differences may be found between results when these differences actually exist instead of these differences being found when they are actually false. The chances of this happening in this research when, for instance, an Analysis of Variance (ANOVA) is conducted, are even higher because fewer specimens had to be tested due to time and equipment constraints. A high number of specimens, therefore, should reduce both types of error and increase the quality of any statistical analysis conducted.

When the experiments were initiated, only eight stations were available (one setup). Five months later, a new setup was acquired and the number of stations doubled to sixteen. The third setup, however, was only available after the second year of experiments had been initiated, bringing the number of stations to a total of twenty-four. Since thirty-seven different ACTs had to be accomplished, several grouts were run in pairs in the same setup, reducing the number of specimens in these cases from eight to four. This reduction in the number of specimens happened for all grouts with silica fume, fly ash, and with two different corrosion inhibitors (A and B) in their mixes, resulting in 22 tests out of 37 with a reduced number of specimens.

With four specimens to describe the degree of corrosion protection for several grouts, only large discrepancies between t_{corr} results (above 185 h) should have been considered in the previous plots, according to the power analyses. In order to identify differences of 100 hours, for instance, which is more in accordance with the discrepancies found between times-to-corrosion, the number of specimens in a single ACT should have been 14, which is six specimens in excess of one setup's maximum

capacity. The maximum capacity would allow determination of differences between means of 135 hours. This and other requirements are presented in Table 5.2, which presents also the adopted number of specimens per type of test accomplished in this work.

Table 5.2 - Number of specimens required and adopted in each test type

Test	Number of Specimens	
	Required	Adopted
Potentiostatic:		
• All grout types together	14	8 and 4
• Plain grout	8	8
• Prepackaged	8	8
• Corrosion inhibitor	4	4
• Silica fume	7	4
• Fly ash	4	4
Polarization Corrosion	3	8 and 4
Potentiodynamic	2	2
LPR	3	8 and 4
Grout characterization:		
• Volume of permeable pores	2	4 and 2
• Electric charge	3	8 and 4

Due to smaller standard deviations, when the grout types (plain, prepackaged, corrosion inhibitor, silica fume, and fly ash) are considered alone, the number of specimens adopted is adequate, even when only four replicates are considered. The only exception concerns silica fume grouts, whose results are typically low and, therefore, close to each other. The number of specimens adopted for the polarization corrosion, potentiodynamic, LPR, and characterization tests can be also considered adequate.

The higher variability observed in grouts with higher t_{corr} is typically larger than the low results found for grouts with deficient corrosion protection degrees, bringing the necessary number of replicates to higher amounts.

5.4.2 Quality Control of Materials

Perhaps the main problem that occurred during the experimental program was related to the quality of the materials used in the mixes (cement and water), which changed along the period of tests (two years) without any systematic quality control being adopted for detection and compensation of these changes. Regarding the cement used, not only its quality would decrease along the time, because of its hydration with air moisture, but also some variation on its properties should be expected between different batches of the product. Hence, the intent to keep the cement batch constant conflicted with the intent to keep cement fresh. Figure 5.9 illustrates the two aspects of this problem, when tests for the control mix were executed for different batches of cement.

As can be seen, the first batch of cement produces significantly lower results six months later when the test with no compensation for IR drops is conducted, contradicting expectations. Upon testing with the second batch of cement, the expected trend between compensated and uncompensated tests does occur, but a discrepancy can be noted when comparing compensated results between batches. This discrepancy, however, seems to be unimportant, since its magnitude is in the same order of the variability verified in the tests. Therefore, in order to minimize the problem with the cement quality in this

research, smaller amounts of cement were ordered, avoiding long storage periods of the product.
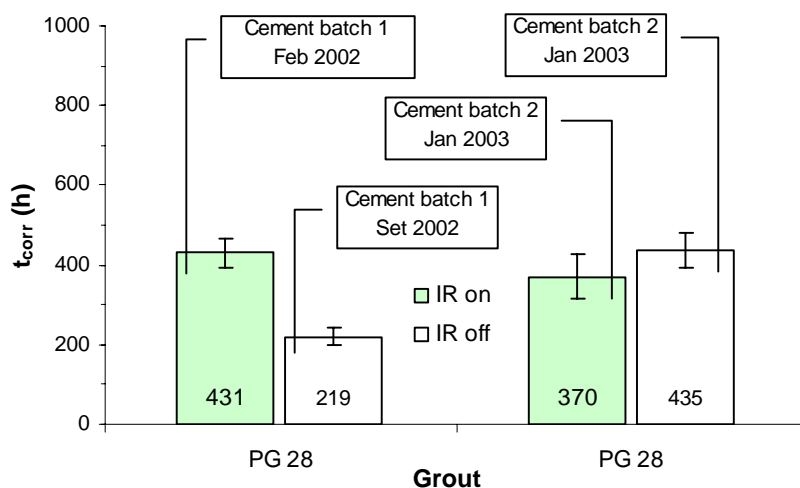
Figure 5.9 - Discrepancies in t_{corr} due to decaying quality and batch variations of cement

Future investigations should take into account the quality of the cement used and try to correct result fluctuations due to this problem. Therefore, besides the good practice of keeping cement in well-sealed containers after the bag is open, it is recommendable to check, for instance, the compression strength of grouts in order to detect any abnormality with the materials used or even mixing and casting mistakes.

Another concern during the experimental program was with the quality of the water used in the mixes. The water collected from a resin-cartridge deionizer was used initially in the mixes. However, the efficiency of this deionizer significantly decreased after some unknown period and many grout batches were cast with considerable amount

of ions in their mixes. Upon resistivity measurements, it was found no detectable

difference between the supposedly deionized water utilized and regular tap water. Thus,

in order to keep consistency among the tests, after 40% of the tests being concluded, it

was decided to continue the experimental program with the use of regular tap water.

The best option to remove ions from the batching water is the use of a still to

obtain distilled water. A still, when cleaned periodically, should not loose significantly

its efficiency along the time and the distilled water, with conductivities on the order of

0.055×10^{-6} siemens per centimeter, should contain considerably less ions than the water

obtained from deionizers (0.1 to 0.20 μS/cm). The actual influence of using distilled

water versus tap water in ACTs is unknown, but distilled water should be used in future

testing due to regional differences in tap water quality.

5.4.3 Corrosion Cell Design

5.4.3.1 Counter electrode

The first four grout tests, namely, PP A 28Y, PP B 28Y, PG 28Y, and PG 07Y,

were conducted with the use of short counter electrodes measuring only 8.5 cm (3.3 in.)

in length. These electrodes were later replaced by electrodes 17 cm (6.7 in.) long, which

were able to completely span the testing region of ACT specimens. This can be verified

in Figure 5.10.
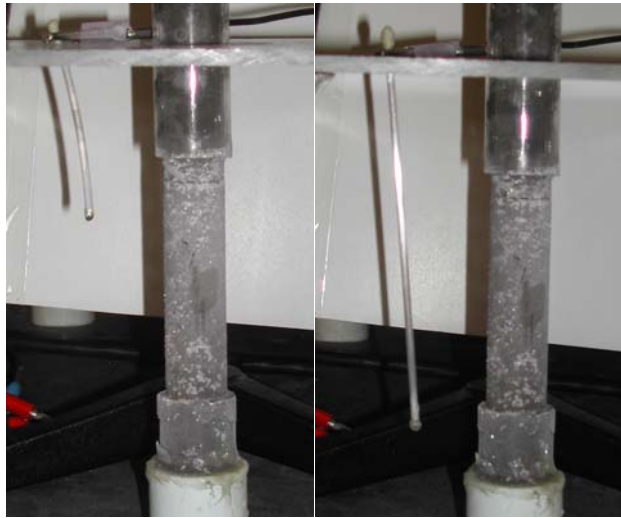
Figure 5.10 - The two counter electrode lengths used

Figure 5.11 shows the incidence of the first spot of corrosion on the specimens when both lengths of counter electrodes were used. Since the tests for prepackaged grouts A and B were not verified for first spot occurrences, only results for 16 grouts were available for the shorter electrode length, while 206 specimens were accounted for the tests with the longer length of electrode.

As can be seen, when the electrode length was too short (result on the right), the distribution of occurrences was uneven, with 43.8% of the cases (18.8% plus 25%) being located on the west side of the specimens, facing therefore the counter electrode, while only 25% of the occurrences faced the other side.
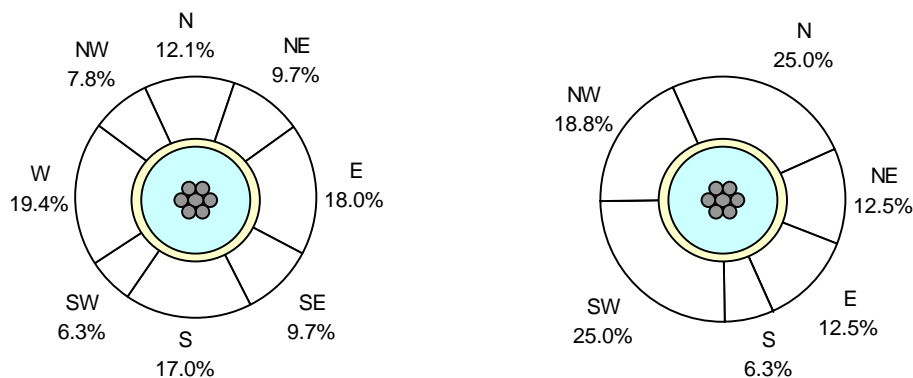
Figure 5.11 – Cross-sections of ACT specimens showing the incidence of occurrences of the first spot of corrosion when the counter electrode is 170 mm long (on the left) and 85 mm long (on the right)

On the other hand, when the counter electrode was long enough (result on left), the incidence of occurrences was fairly well distributed, with 33.5% of the first visible corrosion products facing the counter electrode, while 37.4% occurred on the other side. In addition, 29.6% of the occurrences faced the north side of the specimens, while 33% occurred on the opposite face. These numbers show that, upon using an appropriate length, there is neither necessity for additional counter electrodes in the corrosion cells nor need for counter electrodes with complicated shapes in order to distribute better the cells' electric current flow.

Figure 5.12 corroborates the previous result, showing that a too short of a counter electrode may indeed induce a concentration of the electric flow at a certain location of the ACT specimen. Even considering the low number of specimens tested in this

condition, the tendency for this concentration at the top of the testing region is evident in the graph.
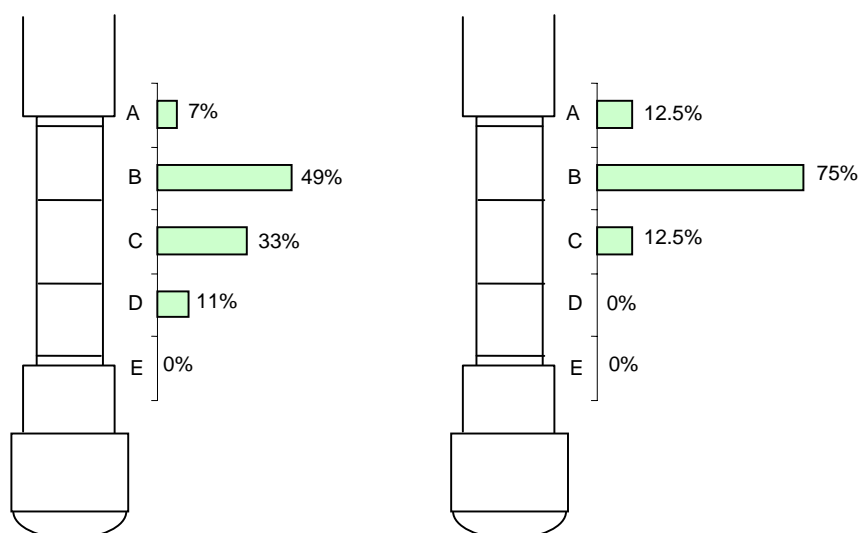
Figure 5.12 - Occurrence distribution of the first sign of corrosion when the counter electrode spans the testing region (on the left) and when it is too short (on the right)

The result found for the longer electrode (graph on the left), however, show that the tendency, although in a lower degree, still exists. Perhaps an even longer counter electrode would reduce this problem to an insignificant degree.

Another way that the counter electrodes used in this research could have influenced the ACT readings is through their own corrosion during the tests. Their core, which is made of copper, can corrode if no preventive measures are taken. If their extremities are not appropriately covered with a sealant, the copper core will be attacked by the salt solution. This phenomenon was observed in some of the tests conducted

because only a layer of adhesive, which turned out later to be too porous, was used to
caulk the counter electrode's extremities, and green corrosion products could be noticed
after some time.

5.4.3.2 Working Electrode

The first design of an ACT specimen (by Lankard et al. 1993) had the prestressing
strand in the testing region delimited by a coating layer of coal tar epoxy. All designs
that followed, including the one used in this work, neglected this step in order to simplify
the manufacture procedure. The second design (by Hamilton 1995) had the grout layer
increased and introduced the use of clear tubing. The author also tried, without adopting
it, the use of split sections of tubing for easy exposition of the testing region. This
procedure is then adopted in this work, as an attempt to reduce cracking and data spread.
The next designs had some dimensions augmented in order to expose more grout to the
electrolyte since the applied potential in the ACTs was significantly lowered (from +600
mV$_{SCE}$ to +200 mV$_{SCE}$). This brief history is illustrated in Figure 5.13.

In addition to complicating the manufacture of specimens, the epoxy coating of
the prestressing strand is not a foolproof measure because, due to its shape, with coiled
wires, it is very difficult to completely cover the strand's external surface area, especially
the portions between wires. Another aspect in the later designs is that consistency was
the primary factor considered, and the idea was to make possible qualitative and not

quantitative analyses on the specimens and grouts tested. Thus, because of these factors, the epoxy coating step in the manufacture of ACT specimens was then ignored.

Figure content:

The prestressing strand is coated with coal tar epoxy, except for the testing region.
ACT Polarization: +600 mV$_{SCE}$

19 mm (0.75 in.) Int. diam. opaque tubing

Not coated
ACT E: +600 mV$_{SCE}$

25.4 mm (1 in.) Int. diam. clear tubing

Exposed with the use of a lathe

Not coated
ACT E: +200 mV$_{SCE}$

Segmented 25.4 mm (1 in.) Int. diam. clear tubing

(Lankard et al. 1993)

(Hamilton 1995)

(Koester 1995); (Schokker 1999)

(Pacheco 2003)

Figure 5.13 - Different ACT specimen designs adopted in different investigations (scale: 1:5)

However, the absence of a delimited prestressing strand surface area may turn the current design of ACT specimens not suitable for potentiodynamic tests because it does not allow a fixed amount of anodic area to form. Figure 5.14 illustrates this problem with a sequence of events that represents an electrolyte front reaching the center of a specimen and, eventually, expanding beyond its testing region.
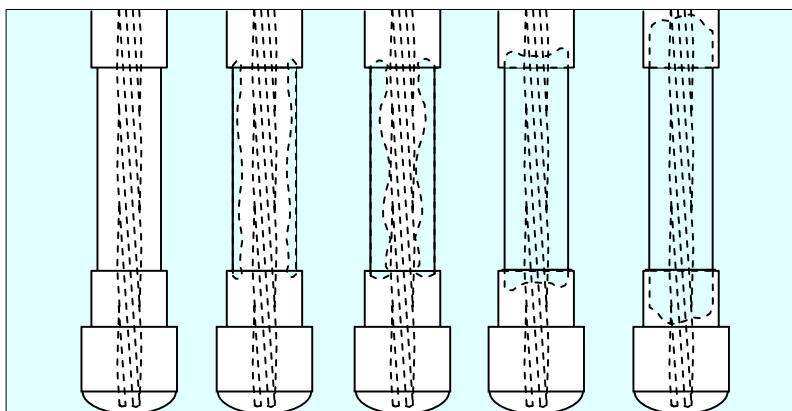
Figure 5.14 - Sequence showing an electrolyte front moving beyond a testing region

Hence, without a delimitation of the amount of steel surface area to be exposed to the testing conditions, significant differences in potentiodynamic and even potentiostatic tests between samples may occur. In a potentiostatic test, the chlorides could find an easier way to reach the prestressing strand when going through the grout outside the testing region. In a potentiodynamic test the situation is more serious because, with unknown and inconsistent areas being exposed to electrolyte from specimen to specimen, comparative results are likely to be distorted.

5.4.4 Differences in equipment

Another small source of error that may have contributed in part with the variability found in the experiments is perhaps due to differences between the setups

used. Older reference electrodes, for instance, have shown discrepancies in potential of

± 11 mV when compared to new ones. This is a difference of $\pm 5.5\%$ in the potential

applied during ACTs, for instance, whose variability was typically in the order of 20 to

30%.

As commented before when discussing the range of potentials applied during

potentiodynamic tests, it is also important to make sure that different setups have the

same settings. Some data obtained during the LPR tests could not be used because scan

rates or sample periods were different from other tests, generating poor results.

5.4.5 Problems that Occurred

5.4.5.1 Casting and Curing

During the sequence of experiments, two tests had to be repeated due to problems

that occurred, for one of them, in the assemblage of the plastic casings and, for the other

one, in the curing process. The former case resulted from an unsuccessful attempt to

simplify the casings' assembling procedure, which allowed too much grout leakage

during the casting step. These leakages had probably created preferential paths inside the

grout layer that, later on, facilitated the ingress of chlorides during the electrochemical

tests.

The problem related to curing occurred because the batch of plain mix that was

supposed to be tested at 56 days was mistakenly taken out of the environmental chamber

and put to test after only 7 days after casting. Realized the mistake immediately after initiating their ACT, the specimens were returned to the environmental chamber, where they stayed for 49 days immersed in water for testing on the right date. Figure 5.15 shows the ACT results for each one of the problematic tests, where the t_{corr} values found can be compared with values considered satisfactory in this work.

As can be verified in the graph, the discrepancy existent between the number obtained with the specimens cast with defective casings and the number considered in this work as a control result has almost the same magnitude of the variability observed in the first case. Perhaps the increase of test variability, in addition to a lower result, is the main consequence observed in ACTs when the casings used are not suitable for the casting procedure. It must also be mentioned that, during the potentiostatic test, two of the specimens that were cast with defective casings instantly corroded as soon as the test begun, and were therefore rejected. For estimation of the t_{corr} value considered as control result (401 h), sixteen specimens were tested and none of them were rejected.

Considering now the result associated with the problematic curing, it can be seen that a significant lost in time-to-corrosion occurs. Although the specimens were taken back to the environmental chamber for appropriate curing, the short period of exposure to the elements, including to chlorides, clearly affected the test outcome. This example only illustrates the importance of appropriate curing of ACT specimens. Moreover, it also highlights the importance of preventing any cracking during the period between the intermediary plastic casing removal to expose the testing region and the placement of specimens in their testing station.
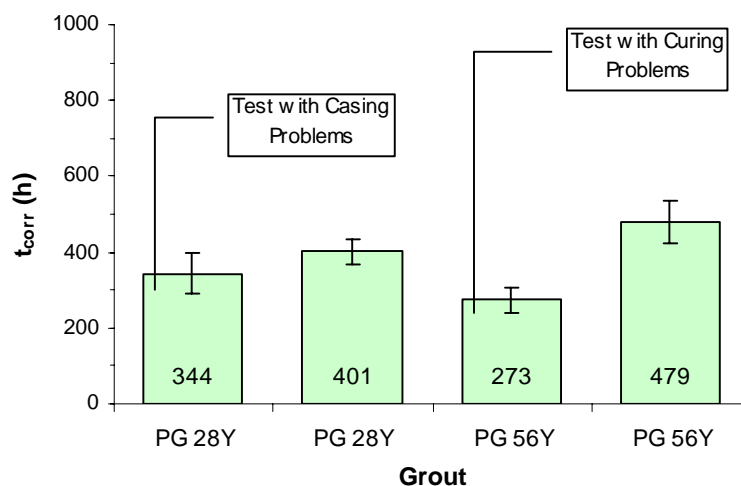
Figure 5.15 - Results for tests with known problems, which were disregarded, and for tests considered satisfactory

In preliminary tests, after removing the intermediary casings from all specimens to be tested, wet rags were used to prevent any cracking. If this procedure is not done carefully or the specimens stay out of their station for too long, cracking is still likely to occur. In order to prevent this, it is recommended to place the specimens as soon as possible in their respective stations, right after each one of the intermediary casings are removed.

5.4.5.2 Plastic Spacers

During the casting step of the ACT specimens, spacers cut from bigger reinforced concrete plastic spacers were used to keep the prestressing strands concentric to their casings. In some occasions, the spacers fitted loosely inside the casings and did not completely prevent eccentricity of the strands. The eccentricities tended to be severe in some instances because of the shape of the spacers.

Figure 5.16 shows an example of this problem, where almost no cover is left at the top of the specimen. An adequately centralized strand is also illustrated for comparison.
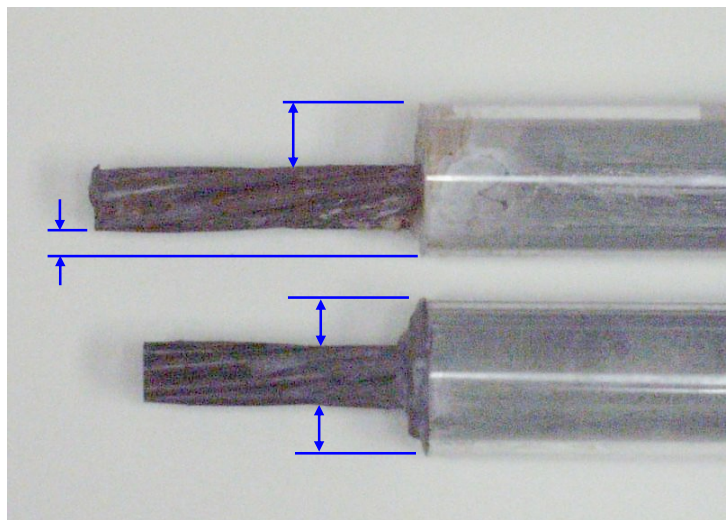
Figure 5.16 – Defective spacers may result in significant strand eccentricities in ACT specimens

During the tests, the problem seemed to be not significant because the lack of cover due to eccentricities on the top of specimens tends to be minimal at the position of the testing zones. The effect of these eccentricities could have become significant if the problem were intensified by additional failure of the spacer located at the bottom of the specimens as well. This problem seemed not to have occurred, since no connection was found between higher eccentricities and lower t_{corr} values. This can be seen in Figure 5.17.
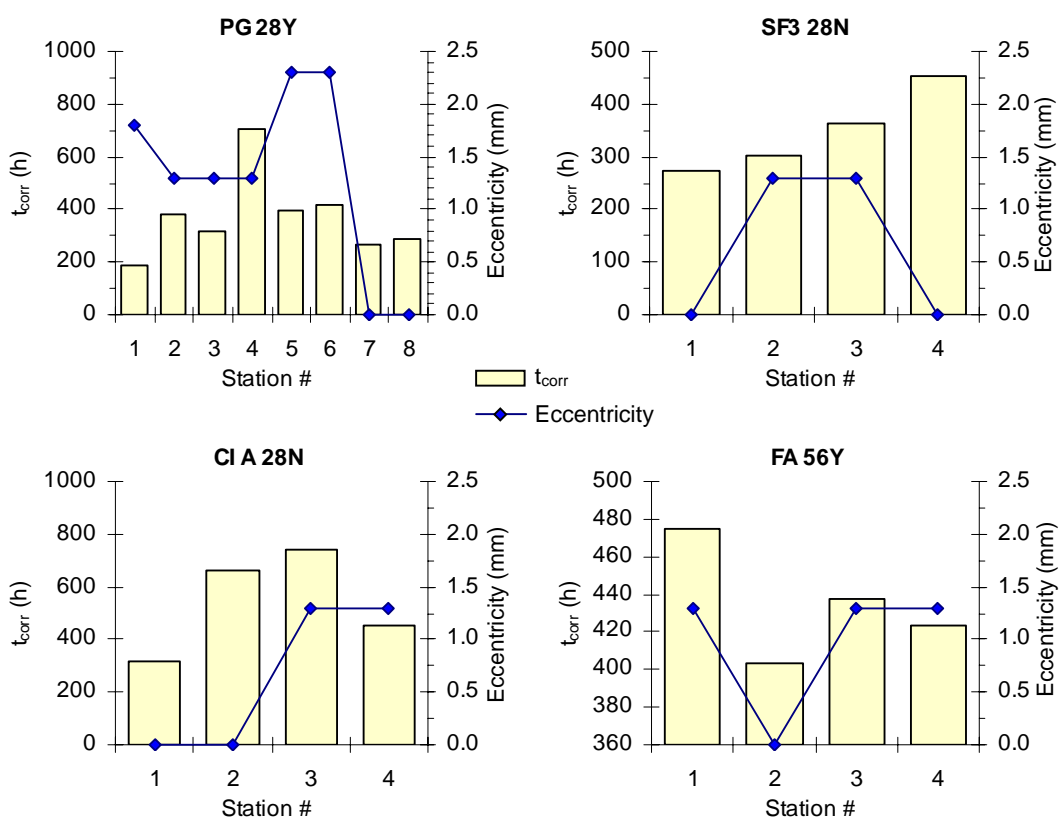
Figure 5.17 - Eccentricities and times-to-corrosion of some tests

6 CONCLUSIONS AND RECOMMENDATIONS

In this chapter, the main findings of the work are summarized and discussed. Recommendations targeting the solution of the problems that occurred during the development of the experimental program are also given, in order to minimize their occurrence or intensity for future investigations. Most importantly, the conclusions and recommendations drawn in this chapter are used as the main elements of a document intended as a standard method and new PTI recommendation for approval of post-tensioning grouts with respect to corrosion protection. This document is presented in the Appendices and is a major contribution of this investigation. Finally, topics for new investigations based on the aspects that remained uncertain or that still need further assessment are suggested.

6.1 CONCLUSIONS OF THE WORK

6.1.1 Characterization tests

Results gathered from two tests allowed qualitative comparisons between the different post-tensioning grouts considered in this work. One test determined the volume of permeable voids in percentage (a measure of permeability) for each grout. The other determined the electric charge passed through the grout layers by means of electrochemical potentiostatic measurements.

The two characterization tests showed that the prepackaged grouts were superior in quality when compared to the other mixes, presenting lower porosity levels at the curing period of 28 days (28 to 31%) and higher charges when a limit of 10 mA was considered (more than 700 C). Inferior in quality, according to the porosity tests, were the mixes containing silica fume, fly ash at early ages (7 and 28 days), and corrosion inhibitors B and C, with values between 36 and 41%. The results for charge indicated that, between those mixes, the silica fume grouts were the ones of poorer quality (less than 150 C). In addition, the calculated charges showed that the fly ash grout had its quality significantly increased after 56 days and that grouts with the three corrosion inhibitors were of marginal quality (between 200 and 300 C).

The data from the porosity tests and from the calculated electric charges corroborate the times-to-corrosion obtained from the ACT tests. Furthermore, it was found that porosities and electric charges could actually be correlated to grout's corrosion protection. The expressions found were given in Equation 4.2 and Equation 4.3.

$$t_{corr} = 10^6 e^{-0.23V}$$

Equation 4.2

$$Q = 47 e^{4.6 x 10^{-3} t_{corr}}$$

Equation 4.3

These equations, where t_{corr} is in hours, V in percentage and Q is in coulombs, indicate that porosities (or, more correctly, volumes of permeable voids) higher than 33% should lead to (compensated) times-to-corrosion above 500 hours and electric charges as high as 2,500 C.

6.1.2 Polarization corrosion tests

The values of open circuit potential obtained from the polarization corrosion tests, which were conducted before the potentiostatic measurements, showed no signs of relationship with grout's level of corrosion protection. The measurements only indicated that no corrosion activity was likely to be occurring (90% of certainty) in each of the grout samples before their ACTs were set to begin. The average value of open circuit potential found (-235 ± 9 mV$_{SCE}$) was considerably far from the threshold limit indicated in the literature of the range of potentials where an uncertain state of corrosion activity would be present (from -461 to -611 mV$_{SCE}$).

6.1.3 Potentiostatic (ACT) tests

6.1.3.1 Comparison between compensated and uncompensated tests

Tests with four different types of grout (plain, with corrosion inhibitor, with silica fume, and with fly ash) at three different ages (7, 28, and 56 days) were conducted with and without correction for voltage drops with the following conclusions:

a) On average, discrepancies due to voltage drops are on the order of 11 to 46%, but can reach values as high as 149%. These numbers indicate that low performance grouts may meet current ACT specifications, being erroneously approved for

post-tensioning applications due to equipment limitations, i.e., higher perceived ACT times in equipments incapable of IR drop compensations;

b) Grouts with different formulations may develop corrosion protection properties along curing periods at different rates. The indication for this was given by the control and fly ash mixes. The former had its time-to-corrosion development along the curing period at apparent constant rates during compensated and uncompensated tests. The later had considerably higher rates after the 28th day of curing. Hence, if a grout fails its ACT, and there are reasons to believe that more curing time may be needed for a positive result (such as presence of fly ash in the mixture), new specimens can be tested again for the same product at a later age (56 days).

c) Grouts with corrosion inhibitors in their formulation showed poor performances when compared with the control mix. However, a dramatic difference was observed between the compensated and uncompensated results found for the grout with corrosion inhibitor A (calcium nitrite), amounting to 109%. This significant difference is a reason to believe that the tests containing corrosion inhibitors may have had inappropriate dosages used, which are in fact suitable for concretes. This possibility should be further investigated in a future work.

d) Grouts with silica fume in their formulation showed poor performances when compared with the control mix. Their problem, however, was the strong possibility that the absence of aggregates in their mixes hindered the proper dispersion of the silica fume particles, creating numerous pockets of the product

inside the grouts that were likely to facilitate the ingress of the aggressive agents. This facilitation would occur because of interconnection of these pockets, creating a path for the electrolyte to easily reach the prestressing strand and because of internal cracking due to alkali-silica reactions.

6.1.3.2 Adjusting and expanding PTI guidelines

The Post-Tensioning Institute currently recommends in its "Specification for Grouting of Post-Tensioned Structures" (2003) that a grout should be approved if its degree of corrosion protection, measured in an ACT test, is higher than the protection given by a 0.45 water-cementitious ratio neat grout. Furthermore, in the comments section, the document mentions a target time-to-corrosion above 1,000 hours.

The results found in this work indicate that the 1,000 hours should be an appropriate value only for uncompensated ACTs, if not too stringent even in these cases. After all, only two out of five industrialized grouts tested that are currently available in the market met this requirement during this test program. In addition, the result found in this work for the neat grout ($t_{corr} = 401$ h), which is higher than several other results, is considerably lower than that limit. This discrepancy between the two guidelines creates an awkward situation, in which a grout may meet one apparently appropriate condition, but would not be even close to the other one.

Laying aside the suspicion that the 1,000 hours may or may not be appropriate even for uncompensated tests (clearly an issue needing further investigation), this value, together with the average maximum discrepancy found when the IR drop effect was not corrected (46%), was useful for the determination of an equivalent limit of 700 hours for compensated ACTs. In this way, considering that corrosion requirements for post-tensioning grouts should explicitly express different limits according to equipment specifications, ACT setups capable of IR compensation should have a value of 700 hours, while the 1,000 hours would continue as the value to be considered for uncompensated systems.

ACT results may also vary between laboratories. This is evident since several of the grouts tested in this program are approved for use by the Florida DOT, which requires a 1,000-hour minimum ACT. Hence, the comparison with a control 0.45 neat grout is more interesting in a sense that ACTs may still be influenced by other factors such as equipment, user, strand lot, and a relative comparison would consider these factors in a qualitative way. In addition, if this comparison is deemed too lax, a lower permeability base case grout, such as 0.40 w/c, may be used instead.

These aspects are considered in the proposal presented in the Appendices for a new standard procedure for evaluation of post-tensioning grouts with respect to their level of corrosion protection. In this proposed standard, the rigorous fixed values are excluding conditions, exempting outstanding grouts of further testing. Should a grout not meet its fixed required value (1,000 h for uncompensated and 700 h for compensated tests), a comparison with a control mix is then required for the grout's approval. For rigorous field conditions (structures subjected to marine, heavy urbanized, or freezing

environments), the control mix should be a 0.40 water-cementitious ratio neat grout, while a 0.45 may be used otherwise.

6.1.4 Potentiodynamic tests

Several of the curves obtained from this test were not appropriate for calculation of the variables of interest (E_{corr}, i_{corr}, β_a, and β_c). It was observed that the main reason for this problem was the inappropriate range of potentials used during the measurements. When too small, the potential range would not allow the development of the anodic branches for long enough. When too high, the potentials applied would cause distortion on the signals. An appropriate range of potentials seems to be from –700 to +200 mV in relation to the grout's open circuit potential. Another aspect noticed is that the grout itself and its porosity may also increase signal noise and instability of the curves.

In addition to inappropriate potential ranges and the grout physical presence, it is also believed that the ACT specimens' current design is not suitable for potentiodynamic tests because it does not allow a fixed amount of anodic area to form.

Although the difficulties to obtain relevant and sufficient information from the potentiodynamic tests, the following conclusions could be drawn:

a) The values of corrosion potential, E_{corr}, showed some signs of connection to the degree of corrosion protection of grouts. A correlation equation was not found, but the results for E_{corr} indicated that an approach similar to the one adopted today

for half-cell measurements (that indicate the possibility of corrosion activity) may be also adopted in this case for determination of grouts' corrosion protection. The results showed that grouts of poorer performances in ACTs ($t_{corr} = 232 \pm 25$ h) had significantly higher E_{corr} measurements (from –600 to –1,100 mV_{SCE}), while nothing could be affirmed when low E_{corr} values (271 ± 7 mV) were found.

b) The current densities (corrosion rates) determined reflected no influence from the types of grout used in the tests. All mixes tested provided the same low level of corrosion rate that, on average, would lead to the dissolution of 1 mm of steel in 100 years, indicating a passivated state of all samples.

c) No significant effect was also noted for β_c, which measured invariably 157 ± 14 mV per decade, when grouts of different corrosion protection were tested.

d) The values measured for β_a, however, consistently increased for increasing ACT times-to-corrosion, allowing a well-defined correlation equation between the two variables to be found. Nonetheless, due to the problems mentioned previously, it is recommended that further experiments be conducted in order to validate the expression found. This expression, where t_{corr} is given in hours and the constant β_a is in mV/decade, as was presented in Equation 4.4.

$$t_{corr} = 1.4\beta_a - 400$$

Equation 4.4

e) Although the anodic constant is apparently influenced by t_{corr}, this did not affect constant B. The minimum and maximum values observed for B were 34 mV and

75 mV, respectively. These values are in the same order of magnitude as the

values indicated in the literature for structural concrete: from 26 to 52 mV and,

the average found (52 ± 16 mV) coincides with the upper limit, which is

commonly associated to passive conditions of structural concrete. When corroded

(damaged), the specimens were tested again and the constant B was, on average,

86 ± 6 mV. This increase observed on the value is likely to be a result of the

significant volume of corrosion products accumulated around the strands.

6.1.5 LPR tests

Although part of the data was not obtained with appropriate experimental

procedures, where much higher than necessary potentials were used, a strong correlation

could be found between the variables t_{corr} and R_p. The expression that correlates the two

variables is highlighted, in Equation 4.6 where R_p is given in $k\Omega cm^2$ and t_{corr} in hours.

$$t_{corr} = 1.25 R_p$$
<div align="right">**Equation 4.6**</div>

Considering the satisfactory correlation between the two variables, the simplicity of

LPR measurements, and their high repeatability, the method is considered in the standard

proposed in the Appendices, to complement or even replace potentiostatic procedures for

estimation of a grout's corrosion protection. For this intent, a restrictive polarization

resistance value of 700 $k\Omega cm^2$ is suggested. Since this value was determined from a

correlation between variables from tests with compensation for voltage drops, a similar reasoning made for t_{corr} gave the value of 1,000 $k\Omega cm^2$ for uncompensated conditions.

6.2 CONCLUSIONS APPLIED: A NEW STANDARD METHOD

As mentioned before, a standard method for evaluation of the degree of corrosion protection of post-tensioning grouts is presented in the Appendices of this work. This standard method uses the main conclusions drawn from this research, listed above, in a way that post-tensioning grouts are evaluated in a more appropriate and faster way when compared with other methodologies currently being adopted. The proposed standard also considers equipment availability and the existence of fly ash in the grout mixture, which should be given the chance to be tested at older ages, in addition to the usual 28 days. These aspects are represented schematically in Figure 6.1 where, for simplicity, casting and curing periods each have a length of one month.

The standard proposed in this work is intended to replace the associated section in the current PTI specifications for evaluation of corrosion protection of post-tensioning grouts. The main development achieved with this substitution would be clearly the possibility of knowing about the protective character of a grout immediately after completion of its curing period. In a laboratory with only one set of the necessary equipment to use, grout's corrosion performance would be evaluated at least 3 times faster than evaluations that follow current methodology.
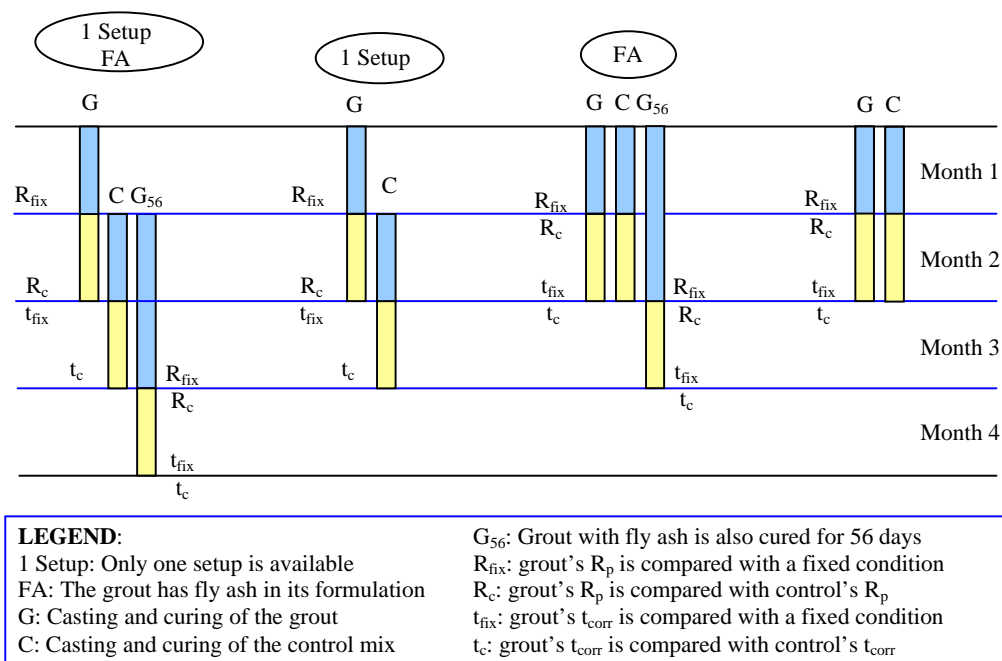
Figure 6.1 – Testing possibilities and variables considered in the standard proposed

Additional important contributions of the proposed document are adjustments to limiting conditions, according to setup capabilities (for IR compensation) and appropriate consideration of grouts with fly ash in their mixture.

6.3 RECOMMENDATIONS FOR NEW INVESTIGATIONS

New investigations should avoid or minimize the occurrence of the problems discussed in the previous chapter. Among those problems, it is critical that new studies focus in two specific aspects:

a) The number of specimens in all tests should be increased whenever possible. This will increase the significance level of the results and prevent experimental points to have low significance when outlier outcomes occur and need to be disregarded. Specifically, the number of specimens to be run in potentiodynamic tests should be three, at a minimum, and not two as it was in this work;

b) The amount of variability should be further diminished by refining ACT specimen design. A suggestion is to consider only the central wire of prestressing strands when manufacturing the specimens. With appropriate delimitation with an epoxy coating of the wire segment cast in the testing region, the variability is likely to be contained. Naturally, this action would demand further investigations to analyze whether specimen's dimensions and potential applied would have to be altered.

6.4 SUGGESTIONS OF NEW RESEARCH TOPICS

As discussed previously, some points in this work have still to be confirmed or need additional data that would indicate more appropriate values for certain parameters. These points are listed as follows:

a) Confirm that anodic constants are influenced by grouts' corrosion protection by verifying the validity of the correlation equation found between the two variables.

b) To confirm that IR drops' magnitude build with increasing ratios in fly ash grouts by testing them for several curing periods (such as 7, 14, 21, 28, 35, 42 49, and 56 days). This would also confirm the relevance of having standards that consider IR drop compensations in their specifications.

c) To confirm the problem observed in silica fume grouts regarding formation of agglomerations that reduce the effective thickness of the grout cover in ACT specimens. This problem may be eliminated with the use of slurried silica fume.

d) To confirm that E_{corr} measurements are able to identify the likelihood of degrees of corrosion protection in a similar fashion that half-cell potentials do in relation to corrosion activity.

e) To investigate the high value found for the constant B (86 mV/decade) when potentiodynamic readings were made on damaged ACT specimens.

f) To investigate whether the current ACT control mixture (plain 0.45 water-cementitious ratio neat grout) and the proposed one for severe field conditions (plain 0.40 water-cementitious ratio neat grout) are appropriate.

g) To investigate whether the current ACT limit of 1,000 hours or the proposed one of 700 hours are appropriate. Similarly, the values of 1,000 kΩcm^2 for uncompensated and 700 kΩcm^2 for compensated systems should be also verified. As a suggestion, the uncompensated values can be assumed as baseline conditions, and an expression that would consider pertinent variables (such as w/c and admixture content) would give the values for uncompensated conditions.

Instead of running potentiostatic test to find IR drop amounts, LPR measurements

with and without compensation could provide the amount of drop in each case.

h) Investigate the appropriate amounts of the different corrosion inhibitors to be used

in grout mixes.

Investigations using current ACT specimens' design could still be used if

moderate potential ranges are used (from –700 to +200 mV$_{SCE}$). Eventually, however, a

new specimen design would need to be adopted for minimum data spread. This new

specimen design should demand an additional investigation itself.

Another aspect that should be confirmed in a future study is the possibility that

specimens were conditioned by the LPR measurements conducted prior to the

potentiostatic tests. In this work, it was assumed that the voltages applied would be

insignificant and there would be no need to have separated specimens for those tests.

APPENDICES

APPENDIX A: Proposed New ACT Standard

Standard Test Method for
Evaluation of the Corrosion Protection Capability of Post-Tensioning Grouts (The Accelerated Corrosion Test for Grouts)

1. Scope

1.1. This test method covers the evaluation of grouts intended to post-tensioning applications with respect to their level of corrosion protection.

1.2. *This standard does not address safety issues. It is the responsibility of the user to establish appropriate safety and health practices.*

2. Referenced Documents

2.1. *ASTM* Standards:

A 416 Standard Specification for Steel Strand, Uncoated Seven-Wire for Prestressed Concrete

C 938 Standard Practice for Proportioning Grout Mixtures for Preplaced-Aggregate Concrete

C 939 Standard Test Method for Flow of Grout for Pre Placed Aggregate Concrete

G 3 Practice for Conventions Applicable to Electrochemical Measurements in Corrosion Testing

G 5 Standard Reference Test Method for Making Potentiostatic and Potentiodynamic Anodic Polarization Measurements

G 59 Standard Test Method for Conducting Potentiodynamic Polarization Resistance Measurements

3. Significance and Use

3.1. This test method is suitable for quality control and for use in research and development work.

3.2. The results obtained by the use of this test method shall not be considered as a means for estimating the structural properties of prestressing steels.

3.3. Due to specific testing conditions, the results obtained by the use of this test method shall not be related directly to actual service life of grouts.

4. Apparatus

4.1. The casing assembling apparatus consists of the following:

4.1.1. Auxiliary *tubing support*, to facilitate the assemblage of the casings (FIG. 1).

4.2. The casting apparatus consists of the following:

4.2.1. *Balance*, sensitive to at least 1 g (0.035 oz).

4.2.2. *Container*, measuring 30 cm (11.8 in.) in diameter and 40 cm (15.7 in.) in height or large enough to hold the amount of grout to be mixed.

4.2.3. *High-shear mixer blade*, capable of varying rotation speeds.

4.2.4. *Support*, to hold the specimens in an upright position during casting and curing (FIG. 2).

4.3. The testing apparatus consists of the following:

4.3.1. *Multiplexer*, to electrically connect each sample to a potentiostat.

4.3.2. *Potentiostat*, to control the voltage difference between the samples and the reference electrode.

4.3.3. *Reference electrode*, which shall be part of each corrosion cell to provide a voltage baseline for the measurements. A saturated calomel electrode is specified for use (Note 2).

4.3.4. *Bulk solution*, which shall be composed of distilled or deionized water and a content of 5% of the solution weight of sodium chloride.

4.3.5. *Counter electrode*, made of an inert metal such as platinum or graphite shall measure 17 cm (6.7 in.) in length, which is enough to pass the exposed grout region of specimens.

4.3.6. *Corrosion cell container* with support for electrodes (see FIG. 6).

Note 1 - During the casting procedure, the user may choose also to run quality control tests, such as the fluidity test given in Test Method C939. In this case, the user shall refer to the proper standard methods for additional equipment requirements.

Note 2 - This test method specifies only one type of reference electrode, but others may also be used, such as copper-copper sulfate electrodes. In this case, the potentials measured should be converted to saturated calomel equivalent potentials. The appropriate technique can be found in Practice G3.

Note 3 - *Working electrodes*, i.e., the samples to be tested, shall compete the corrosion cells.

5. Test Specimens

5.1. *Preparing for casting*:

5.1.1. Casing segments shall be cut from PVC tubing, following the dimensions given in FIG. 3. Clear PVC shall be used in order to facilitate casting steps and to allow identification of major casting flaws. Additionally, end caps shall also be available for casing assemblage.

5.1.2. Using the auxiliary tubing support, the casings are assembled as illustrated in FIG. 1 and the junctions are caulked with silicone and held in place with duct tape. After this, the end caps may be cemented to the extremity corresponding to the short plastic segment.
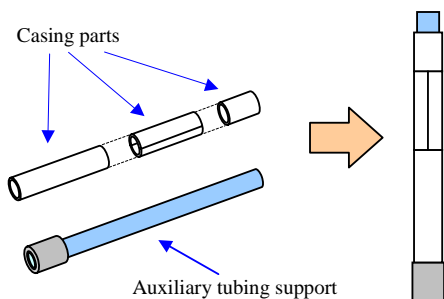
FIG. 1 Auxiliary tubing support is used to keep the casing parts together, allowing caulking and taping of their junctions

5.1.3. Strand segments to be used in the experiments shall be cut from the same reels of Grade 270 prestressing steel (Specification A416). The requirements given in FIG. 3 shall be followed. Previously to casting, they shall be beveled at the ends and thoroughly cleaned with acetone, removing accumulated impurities.

5.1.4. Additional elements that shall be available prior to the casting step are the plastic spacers, which may be cut from larger spacers used in structural concrete construction. These elements are also illustrated in FIG. 3. The spacers should provide a snug fit inside the casing.

5.1.5. After allowing a minimum of one hour for the silicone applied to the casing junctions to vulcanize, the specimens shall be tested for leakages, fixing any apparent defects.

5.1.6. With the casings ready, a spacer should be attached to a strand extremity, and this end inserted inside a casing. The casings then can be put in an upright position with the help of an appropriate support and the casting procedure may start. An example on how to hold a set of specimens in an upright position is shown in FIG. 2.
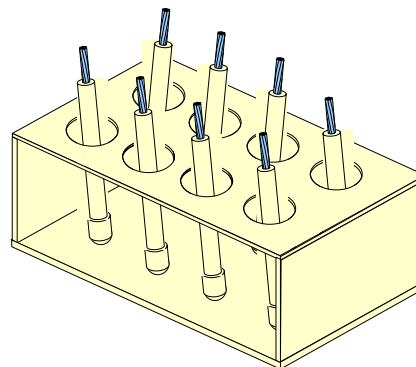
FIG. 2 Set of specimens in a rack

5.2. *Casting*:

5.2.1. A minimum of twelve specimens per grout to be tested shall be cast during this step. Eight specimens shall be used in the potentiostatic test, while four shall be used in LPR measurements (Note 4).

5.2.2. Weigh grout materials. Distilled (or deionized) water shall be used in each mix.

Note 4 - It is recommended, however, that a minimum of three additional specimens be fabricated to assure that twelve visually flawless specimens are available for each grout.

5.2.3. The mixing of grout shall follow Practice C938 with the use of a high shear mixer blade in an appropriate container.

5.2.4. The casings, without removal of their strands, shall be filled with grout in three lifts. Each lift consists of filling with approximately 1/3 of their volume with grout, slowly moving the strand, and, tapping the casing, vibrating them. This procedure should minimize the occurrence of air bubbles and voids in the specimen.
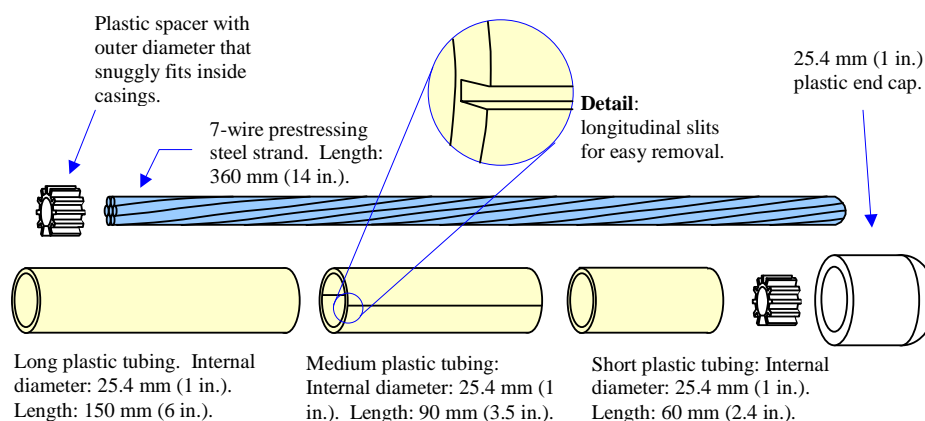
FIG. 3 Casing parts, spacers, and prestressing strand

5.2.5. Then, the second spacer is attached to the top of each specimen and the samples are taken to an environmental chamber for the curing period (28 days or, in the case of mixtures containing fly ash, also at 56 days) (Note 5). Specimens shall remain in a vertical position throughout casting and curing. A schematic of a specimen after casting is shown in FIG. 4.
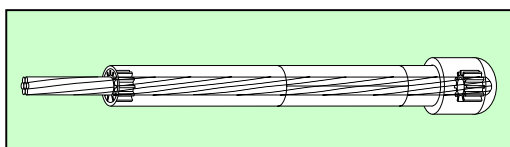
FIG. 4 Schematic of an assembled specimen

Note 5 - It is recommended that a protection be placed on the protruding prestressing strands in order to avoid heavy surface corrosion that may occur on them because of the high humidity level of environmental chambers.

6. Instrumentation

6.1. *Corrosion Cell*:

6.1.1. Upon finishing the curing period for each grout to be tested, the middle plastic section is easily removed due to the existence of the longitudinal slits diametrically localized in that part of the casings, exposing the testing region of the samples.

6.1.2. Each specimen shall be immediately placed in its respective corrosion cell in order to hinder cracking occurrence.

6.1.3. Once inside their corrosion cells, defects are easily checked with the rotation of the specimens and careful visual evaluation. A typical defect is shown in FIG. 5. Specimens with obvious defects should be discarded.
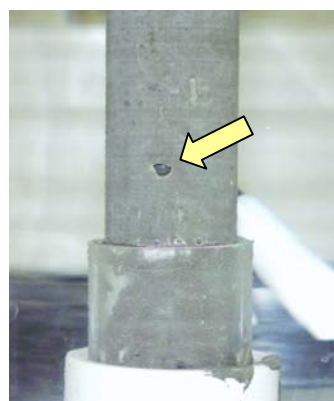
FIG. 5 Typical specimen defect

6.1.4. With the specimens to be tested in place, the connections are made and the corrosion cell shall be placed in the configuration in the schematic presented in FIG. 6.

6.2. *Test settings*:

6.2.1. The settings to be used in the potentiodynamic linear polarization resistance test and in the potentiostatic test shall be the ones given in TABLE 3 (Note 6).
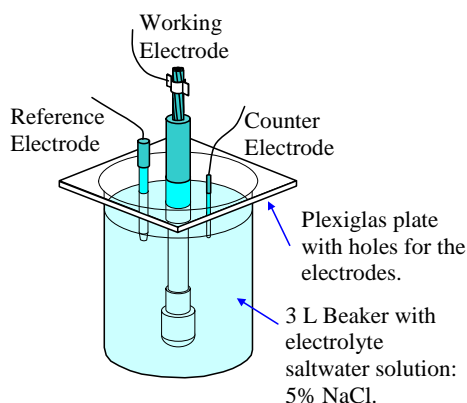
FIG. 6 Corrosion cell

TABLE 3 - Test settings

Test	Value
LPR:	
Analysis region (mV)	5
Initial E (mV) vs. E_{oc}	–20
Final E (mV) vs. E_{oc}	+20
Potentiostatic:	
Sample period (min)	30
Initial E (mV_{SCE})	+200

Note 6 - The analysis region of 5 mV corresponds to the range of potentials about the open circuit voltage of the specimens being measured that is considered approximately linear for determination of R_p. Details for both electrochemical tests are available in Test Methods G59 and G5. Other details regarding electrochemical measurements are found in Practice G3.

7. Experimental Procedure

7.1. *Grout approval*:

7.1.1. With this standard method, a grout with fly ash in its formulation (Note 7) can be approved for post-tensioning applications with respect to its corrosion protection degree in eight circumstances shown in FIG. 7. A grout not containing fly ash can be approved anytime during a four step testing process. The multi-layered approval system allows a grout with evident corrosion protection properties to forgo more extensive (and time consuming) testing.

7.1.2. *The first* is immediately after the curing period of 28 days of the grout is satisfied and its R_p is found. The value shall not be lower than 1,000 $k\Omega cm^2$ (setups without IR drop compensation capability) or 700 $k\Omega cm^2$ (tests compensating for IR drops).

7.1.3. *The second* chance is immediately after the curing period of 28 days of the control grout is satisfied and its R_p is found. The R_p of the grout being tested shall not be lower than the R_p of the control grout.

7.1.4. *The third* circumstance occurs immediately after the grout being tested has its t_{corr} calculated. The grout t_{corr} shall not be lower than 1,000 hours (without compensation for IR drops) or 700 hours (with compensation).

7.1.5. *The fourth* and last chance for a grout without fly ash in its formulation to be approved for post-tensioning applications is also a verification of its potentiostatic result. The grout t_{corr} shall not be lower than the t_{corr} found for the control grout.

7.1.6. *The remaining* circumstances are a repetition of the same previous assessments, but shall consider the results for the tests conducted with the extra specimens cast when the grout to be tested has fly ash in its mixture. These extra specimens shall be moist cured for 56 days in order to allow the grout to develop its full protective characteristics against corrosion.

Note 7 - A grout with fly ash in its formulation may demand 56 days to develop its degree of corrosion protection, instead of the typical 28 days. Prepackaged grouts, whose formulation is unknown by other than the manufacturers, may therefore be considered as grouts with fly ash and be also given the chance to be tested at 56 days.

7.2. *Flow chart*:

7.2.1. All combinations for grout approval and the conditions for rejection are illustrated in the flowchart presented in FIG. 7. The possibilities of one or two setups available for the tests are also considered in the planning. Three or more setups do change significantly the sequence of experiments and assessments.

8. Precision and Bias

8.1. The maximum difference between two LPR readings taken on the same grout for the same conditions should be 70 $k\Omega cm^2$.

8.2. The maximum difference between determinations of two t_{corr} values in respect to the same grout and taken under the same conditions should be 60 hours.

9. Keywords

9.1. Post-tensioning grout; corrosion activity; electrochemical tests; degree of corrosion protection of post-tensioning grouts; degree of corrosion protection; accelerated corrosion test.

FIG. 7 Experimental procedure to test the corrosion protection degree of post-tensioning grouts
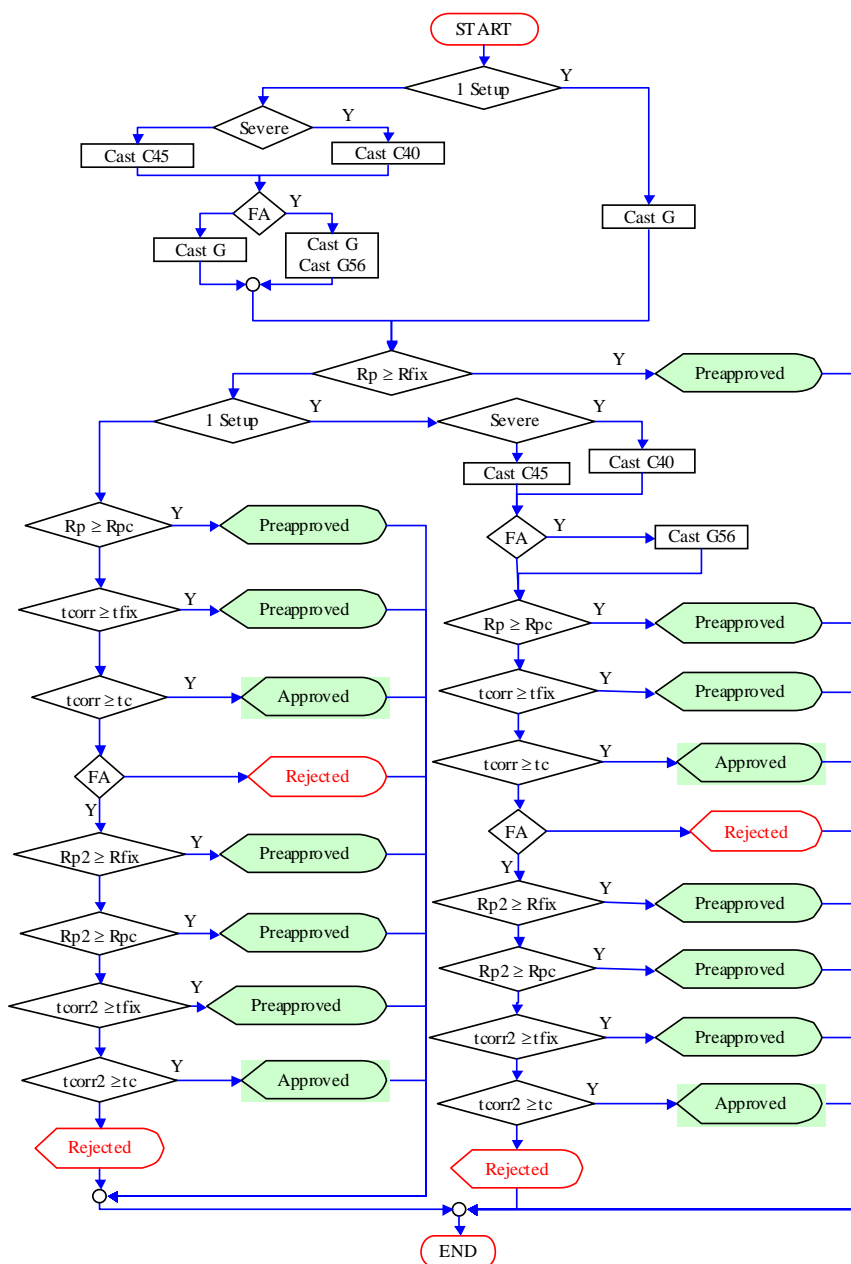
LEGEND:

1 Setup: only one setup is available
Severe: severe field conditions are specified
FA: The grout contains fly ash
Rp: LPR result for the grout at 28 days
tcorr: Potentiostatic result for the grout at 28 days
Rp2: LPR result for the grout at 56 days
tcorr2: Potentiostatic result for the grout at 56 days

C40: Control grout (w/c = 0.40)
C45: Control grout (w/c = 0.45)
Rfix: 1000 or 700 kΩcm^2 (IR comp)
Rpc: LPR result for the control grout
tfix: 1000 h or 700 h (IR comp)
tc: Potentiostatic result for the control

Accelerated Corrosion Testing Method (ACTM)
Background and Procedure

The Accelerated Corrosion Testing Method was based on the method developed by Thompson, Lankard, and Sprinkel[1] in a FHWA sponsored study and refined at the University of Texas at Austin[2,3]. The corrosion test uses anodic polarization to accelerate corrosion by providing a potential gradient, driving negatively charged chloride ions through the grout to the steel. The ACTM is intended to provide a relative comparison of a grout's corrosion resistance. The time to corrosion cannot be directly related to field performance, but can be compared with grouts with known acceptable performance. The ACTM is particularly useful in determining combinations of admixtures that may adversely affect a grout's corrosion performance. A grout which shows a longer average time to corrosion in the ACTM than a neat grout with 0.45 water-cement ratio is considered satisfactory for use in bonded post-tensioning applications covered by this specification.

SPECIMEN PREPARATION

The test specimens consist of a short length of prestressing strand in a grouted clear PVC mold casing as shown in Figure 1. A minimum of 6 specimens should be used to test a given grout. It may be useful to fabricate additional specimens to ensure that 6 uncracked and undamaged specimens will be available for testing.

1 mm = 0.394 in
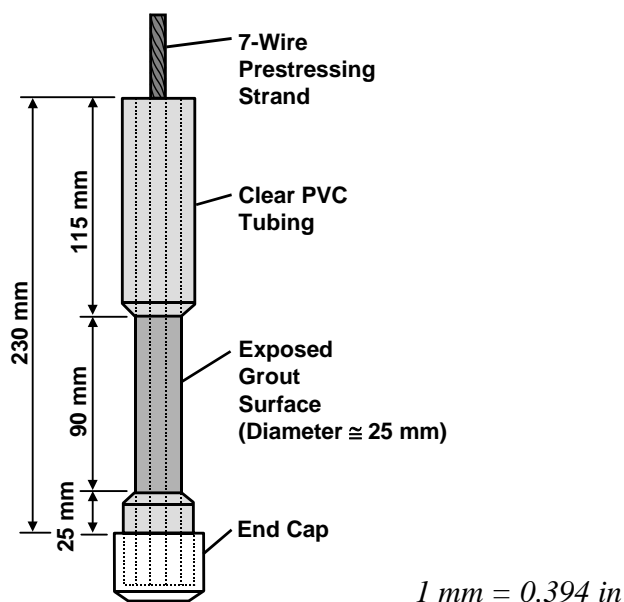
Figure 1: Specimen Dimensions

A plastic spacer is fitted in the bottom of the PVC cap to keep the strand spaced concentrically within the PVC casing. The end cap is then cemented to the PVC casing. The 12.7 mm (0.5 in) diameter strand is beveled at one end for ease of insertion into the spacer, and the strand is cleaned with acetone to remove surface buildup. The grout mix is prepared using distilled water and is placed into the casing in 3 stages. Before the strand is inserted, the PVC casing is filled to approximately 1/3 with grout. The strand is then inserted into the assembly. The casing is filled in 2 more equal lifts, and the strand is slowly rotated between lifts to allow air bubbles to escape. A spacer is inserted at the top of the casing to hold the strand in place. The specimens are placed in racks and allowed to cure for 7 days in a moist curing room.

After 7 days of curing, a portion of the PVC casing is removed with a rotary wire brush, taking care not to damage the grout. Two radial cuts are made first followed by two longitudinal cuts. The length of casing may be removed using other methods as long as care is taken to avoid damage to the grout. After removal of the casing, the specimen is immediately wrapped in a wet towel to prevent cracking prior to immersion in the NaCl solution.

The specimens are connected to the electrodes and allowed to soak in the NaCl solution for approximately 15 minutes during which time the free corrosion potential is recorded. Testing begins by applying a potential of +200 mV (approximately 400 mV above the free corrosion potential) to each station. The applied potential of +200 mV$_{SCE}$ is within the passive region of the polarization curve for the strand.

INSTRUMENTATION

During testing, the specimens are immersed in a 5% NaCl solution in a 3000 ml beaker. The beaker is covered with a Plexiglas cap with holes for the electrodes. A gel-filled saturated calomel electrode is used as a reference electrode. A potentiostat is used to apply the +200 mV$_{SCE}$ through the counter electrode in each station. A multiplexer sends data back to a PC one station at a time. Corrosion potential (E$_{corr}$) is measured from the reference electrode relative to the working electrode, and the corrosion current (i$_{corr}$) is found by measuring the voltage across the 100 Ω resistor in-line with the lead on the counter electrode. A diagram and picture of one of the experimental stations is shown in Figure 2.

Chemical and mineral admixtures will change the omhic resistance (or IR drop) of the grout. Grouts with different omhic resistances will have different polarized potentials at the steel/grout interface. The polarization read by the potentiostat cannot be read directly at the steel/grout interface, so differences in the omhic resistance of the grout will affect the actual polarization potential. For this reason, a potentiostat that includes IR compensation is preferable.
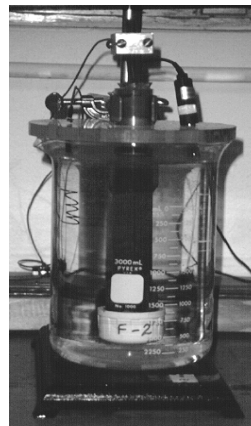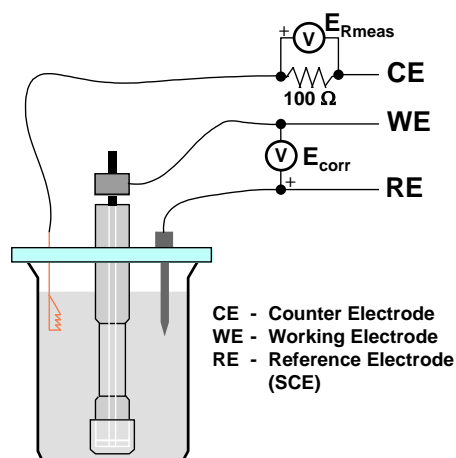
Figure 2: (a) schematic of experimental station (b) test setup

BEHAVIOR

Typical initial behavior after potential is applied is shown in Figure 3. This initial high corrosion current followed by a rapid reduction is helpful in isolating and correcting a faulty station early in testing. Once a specimen corrodes, the corrosion current typically increases by orders of magnitude very rapidly as shown in Figure 4. The spike in corrosion current is immediate in many specimens, but in some cases the rise begins gradually. The time to corrosion is estimated as the time where the sharp rise in corrosion current begins on the plot.

CORROSION RESISTANCE

The Accelerated Corrosion Testing Method provides relative comparison of the corrosion protection provided by different grouts. For each grout tested, the average time to corrosion should be found from the average of a minimum of 6 specimens. If 8 or more specimens are tested, the high and low values may be removed before computing the average. For the grout under investigation, a comparison test should be run with a 0.44 water-cement ratio neat grout. This comparison grout should be tested by the same technician using the same equipment and the same number of specimens should be tested. The samples should be fabricated using cement and strand from the same batch. Strand condition should be as close as possible to the strand used in the test grout (strand that is noticeably more corroded should be discarded). The grout is considered satisfactory for bonded post-tensioned applications as outlined in this specification if the average time to corrosion from the test grout is longer than the average time to corrosion of the 0.45 water-cement ratio comparison grout.
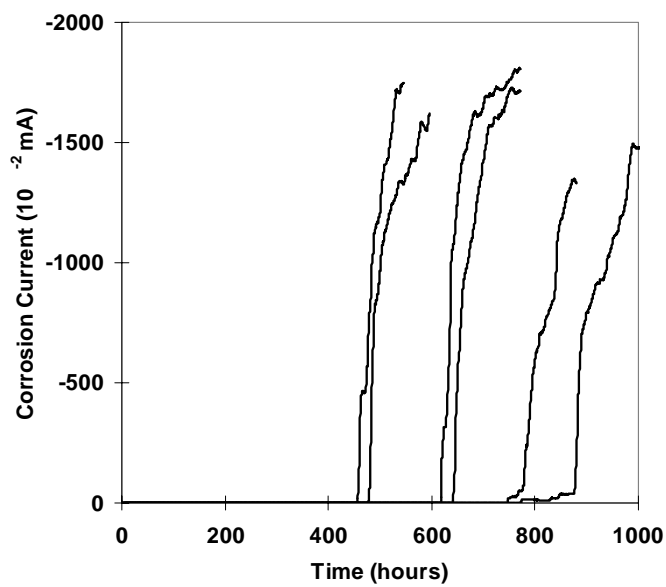
Figure 3: Initial Behavior of Corrosion Current with Time[3]
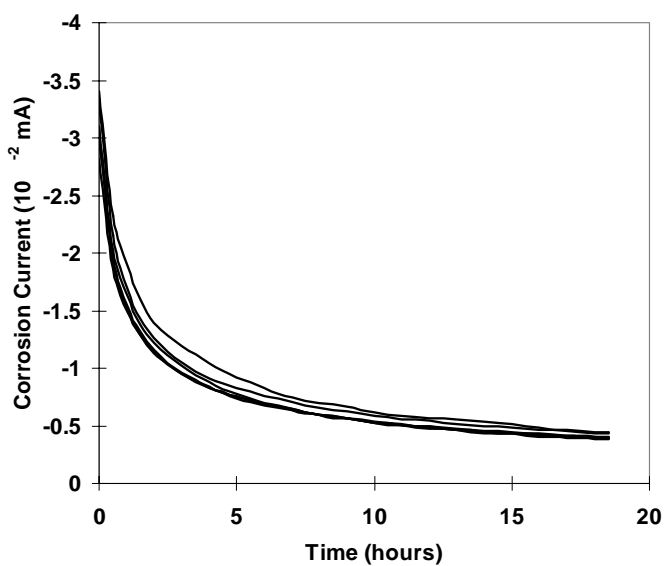
Figure 4: Behavior of Corrosion Current with Time[3]

REFERENCES

1. **Thompson, N.G., Lankard, D., and Sprinkel, M.,** "Improved Grouts for Bonded Tendons in Post-Tensioned Bridge Structures," *FHWA-RD-91-092*, Cortest Columbus Technologies, January 1992.
2. **Hamilton, H.R., III,** "Investigation of Corrosion Protection Systems for Bridge Stay Cables," *Ph.D. Dissertation*, The University of Texas at Austin, September 1995.
3. **Schokker, A.J., Koester, B.D., Breen, J.E., and Kreger, M.E.,** "Development of High Performance Grouts for Bonded Post-Tensioned Structures," Research Report 1405-2, Center for Transportation Research, Bureau of Engineering Research, The University of Texas at Austin, December 1999.

APPENDIX C: Prestressing Strand Report

Instee Industries Inc.
Carbon Steel Wire Rod Specification

Parameter	Quality Characteristics	
1. Steel Description	¼, 16, 3/8, & 5/16 1080	
2. Quality	For C Strand application, ASTM A416 requirements Acid Cleaning Quality	
3. Preferred Refining Route	No Aluminum Additions Coarse Grain Practice Mandatory	
4. Chemical Composition (% by weight)	**Range**	**Target**
a. Carbon	0.78 – 0.82	0.80
b. Manganese	0.60 – 0.80	0.70
c. Phosphorus	0.015 Max	0
d. Sulfur	0.015 Max	0
e. Silicon	0.15 - 0.30	0.2
f. Copper	0.15 Max	0
g. Nickel	0.08 Max	0
h. Chromium	0.12 Max	0
i. Molybdenum	0.03 Max	0
j. Tin	0.010 Max	0
k. Aluminum	trace	0
l. Nitrogen	0.006 Max	0
		0
5. Rod Diameter	+ .016" or - .016"	
6. Ovality	0.012" Max	0
7. Surface Quality		
a. Decarburization	0.003" Max (Partial) / 0 (Carbon Free)	
b. Laps / Seams	0.004"Max.(Ind)0.008"Max.(Cum.)	
c. Fins, Rolled-in Defects, Roll Marks	Restricted (No Surf. Damage Breaks up to 90% Red.)	
d. Abrasions, Snags, Burrs, Cut Ends	Restricted (No Surf. Damage Breaks up to 90% Red.)	
e. Rust	Light Rust Acceptable, No Pitting Allowed	
8. Non-Metallic Inclusions / Center Segregation	Restricted (No Center Bursting up to 95% Reduction)	
9. Metallurgical Structure		
a. % Proeutectoid Ferrite	Minimum Allowed	
b. % Proeutectoid Cementite	Not Allowed	
c. % Martensite	Not Allowed	
10. Physical and Mechanical Properties	**Range**	**Target**
a. Recommended Scale Oxide Weight	0.7% Max	0.4%
b. UTS (Individual)	165 – 175 ksi	168 ksi
c. UTS (Heat Average)	165 – 172 ksi	168 ksi
d. UTS Range Within Heat		4 ksi Max
e. Reduction of Area		40%
11. Coil Packaging		
a. Rod Coil Weight	4000 lb Min, 6000 lb Max	
b. Tag Identification	P.O.#, Size, Grade, Heat #, Coil #, Weight	
c. Tag Location	Bands only—One (1) on Coil ID, One (1) on Coil OD,	
12. Certification	Each heat certified for chemistry, Min, Max, Ave., and number tested UTS, ROA, diameter and ovality. The certification should be sent or faxed prior to shipment, and accompany the shipment. Deviations must be approved prior to shipment by the Insteel Technical Manager.	

APPENDIX D: Cement Mill Test Report

LAFARGE CORPORATION

CEMENT MILL TEST REPORT
Whitehall Plant
Silo: B-1 Type: II

Date: October 2001

Chemical Analysis (%)					Physical Tests			
Total Alkalies	0.81				Fineness: blaine, m^2/kg			391
Loss on ignition	1.1				% Passing (325 mesh)			97.9
Insoluble residue	0.24							
					Soundness:			
					% Autoclave Expansion			0.00
Silicon dioxide (SiO_2)	20.8							
Aluminum oxide (Al_2O_3)	4.6				Setting Time: Gillmore			
Ferric oxide (Fe_2O_3)	3.9				Initial (minutes)			220
Calcium oxide (CaO)	62.5				Final (minutes)			330
Magnesium oxide (MgO)	2.2				Vicat: Initial (minutes)			180
Sulfur trioxide (SO_3)	2.8							
					% Air Content			7.8

	ASTM	AASHTO				
Mineralogical Composition:	C-150-97	M-85	Compressive Strength:	Mpa	psi
Tricalcium silicate (C_3S)	52	49	3 day	26.5	3850
Dicalcium silicate (C_2S)	21	23	7 day	31.6	4580
Tricalcium aluminate (C_3A)	6	6			
Tetracalcium aluminoferrite (C_4AF)	12	12			

The test results given above were made on a cement composite from a Denver/Vezin sampler grinding into the silo listed above. The Bogue Compounds are calculated using the ASTM and AASHTO formulas. This cement complies with the specifications listed below.

Specifications: ASTM C-150-97
AASHTO M-85

This report is in compliance with your request.

Approved by

Lorraine E. Faccenda
Lorraine E. Faccenda
Supervisory Chemist

CEMENT GROUP/WHITEHALL PLANT
5160 Main Street, Whitehall, PA 18052
Office: (610) 262-7831 Fax: (610) 261-9020 (800) 523-9211

APPENDIX E: Experimental Data Summary

Grout	Undamaged Condition										Damaged Condition					
	V (%)	$-E_c$(mV)	i_c(A/cm2)	β_a(mV)	$-\beta_c$(mV)	R_p (Ωcm2)	B (mV)	E_{oc}(mV)	t_{corr}(h)	Q(C)	$-E_c$(mV)	i_c(A/cm^2)	β_a(mV)	$-\beta_c$(mV)	R_p(Ωcm2)	B(mV)
PG 07Y	33							198	282	179	658	1.5E-06	1020	280	40000	95
PG 07N	33							198	315	166	658	1.5E-06	1020	280	40000	95
PG 14Y	32	258	1.1E-07	435	146	436690	47	196	277	136						
PG 21Y	28							180	403	504						
PG 28Y	35	284	2.2E-07	531	240	325370	72	232	401	355	884	1.0E-05	2296	254	12566	99
PG 28N	35	284	2.2E-07	531	240	325370	72	232	474	294	884	1.0E-05	2296	254	12566	99
PG 56Y	37	293	1.1E-07	689	157	396825	55	261	479	319						
PG 56N	37	293	1.1E-07	689	157	396825	55	261	630	307						
PP A 28Y								253	1087							
PP B 28Y	29							162	1500		394	1.1E-07	2415	462	1010714	168
PP C 28Y	31	248	4.0E-08	862	106	710877	41	144	793	2327	616	5.3E-07	566	177	50300	58
PP D 28Y	33	267	5.0E-08	807	116	641403	44	184	712	717	607	1.4E-06	757	234	31480	78
PP E 28Y	28	276	6.5E-08	763	130	617584	48	232	909		581	9.0E-07	861	174	58580	63
CI A 28Y	35	921	2.3E-06		213	192697		194	295	215	601	2.3E-06	1098	163	66942	62
CI A 28N	35	921	2.3E-06		213	192697		194	617	225	601	2.3E-06	1098	163	66942	62
CI B 28Y	38	900	3.0E-07		114	137670		250	163	232	671	2.0E-06	736	149	72117	54
CI B 28N	38	900	3.0E-07		114	137670		250	177	268	671	2.0E-06	736	149	72117	54
CI C 28Y	39	601	7.0E-07	421	165	148233	51	253	265	226	783	6.4E-06	928	257	54670	87
CI C 28N	39	601	7.0E-07	421	165	148233	51	253	329	227	783	6.4E-06	928	257	54670	87
SF3 07Y	38	651	2.1E-06		287	78756		195	187	137					20278	
SF3 28Y	38	839	1.2E-07	750	106	248967	40	234	349	282	730	9.0E-06	931	250	33693	85
SF3 28N	38	839	1.2E-07	750	106	248967	40	234	329	267	730	9.0E-06	931	250	33693	85
SF3 56Y	37	1070	8.9E-07		104	172290		216	268	125	859	3.7E-05		374	9877	
SF5 07Y	37	739	3.4E-06	1055	284		97	203	124	125					17458	
SF5 28Y	36	755	3.6E-07	513	91	211337	34	264	240	124	768	1.0E-05		289	25707	
SF5 28N	36	755	3.6E-07	513	91	211337	34	264	307	180	768	1.0E-05		289	25707	
SF5 56Y	37	854	2.4E-07		127	182757		212	267	98	770	5.2E-05		249	42911	
SF7 07Y	38							247	155	84	799	9.4E-06	1140	223	24620	81
SF7 28Y	38	1101	3.6E-06		140	250583		280	200	96	781	2.4E-05	885	313	13090	100
SF7 28N	38	1101	3.6E-06		140	250583		280	266	368	781	2.4E-05	885	313	13090	100
SF7 56Y	38	992	6.6E-07		120	136178		286	223	125	849	2.5E-05		294	6905	
FA 07Y	39	546	1.3E-07	399	150	163292	47	316	74	21	923	5.4E-05	1000	292	11406	98
FA 07N	39	546	1.3E-07	399	150	163292	47	316	62	18	923	5.4E-05	1000	292	11406	98
FA 28Y	41	1016	1.1E-06		120	168599		334	162	132	883	2.0E-05	998	345	26895	111
FA 28N	41	1016	1.1E-06		120	168599		334	183	323	883	2.0E-05	998	345	26895	111
FA 56Y	41	841	8.3E-07	703	230	246086	75	268	435	441	865	7.9E-06	2011	365	20336	134
FA 56N	41	841	8.3E-07	703	230	246086	75	268	552	994	865	7.9E-06	2011	365	20336	134

REFERENCES

Ahmad, S. (2003). Reinforcement Corrosion in Concrete Structures, Its Monitoring and Service Life Prediction – A Review. *Cement and Concrete Composites, 25(4-5),* 459-471.

Al-Amoudi, O. S. B., Rasheeduzzafar, Maslehuddin, M., & Al-Mana A. I. (1993). Prediction of Long-Term Corrosion Resistance of Plain and Blended Cement Concretes. *ACI Materials Journal, 90(6),* 564-569.

Al-Tayyib A. J. & Khan, M. S. (1988). Corrosion Rate Measurements of Reinforcing Steel in Concrete by Electrochemical Techniques. *ACI Materials Journal, 85,* 172-177.

Andrade, C., Macias, A., Feliu, S., Escudero, M. L., & Gonzalez, J. A. (1990). *Quantitative Measurement of the Corrosion Rate Using a Small Counter Electrode in the Boundary of Passive and Corroded Zones of a Long Concrete Beam.* Corrosion Rates of Steel in Concrete, ASTM STP 1065, N. S. Berke, V. Chaker, and D. Whiting, Eds., American Society for Testing and Materials, Philadelphia, pp. 134-142.

Andrade, J., Dal Molin, D., & Ribeiro, J. L. D. (2003). A Critical Analysis of Chloride Penetration Models in Reinforced Concrete Structures. *SP 207-14 HPC, and Performance and Quality of Concrete Structures,* 217-228.

ASTM C 642 (1997). Standard Test Method for Density, Absorption, and Voids in Hardened Concrete. *American Society of Testing and Materials*, West Conshohocken, PA.

ASTM C 876 (1999). Standard Test Method for Half-Cell Potentials of Uncoated Reinforcing Steel in Concrete. *American Society of Testing and Materials*, West Conshohocken, PA.

ASTM C 939 (2002) – *Standard Test Method for Flow of Grout for Pre Placed Aggregate Concrete (Flow Cone Method). American Society of Testing and Materials*, West Conshohocken, PA.

ASTM G 1 (1999). Standard Practice for Preparing, Cleaning, and Evaluating Corrosion Test Specimens. *American Society of Testing and Materials*, West Conshohocken, PA.

ASTM G 102 (1999). Standard Practice for Calculation of Corrosion Rates and Related Information from Electrochemical Measurements. *American Society of Testing and Materials*, West Conshohocken, PA.

ASTM G 15 (2003). Standard Terminology Relating to Corrosion and Corrosion Testing. *American Society of Testing and Materials*, West Conshohocken, PA.

ASTM G 16 (1999). Standard Guide for Applying Statistics to Analysis of Corrosion Data. *American Society of Testing and Materials*, West Conshohocken, PA.

ASTM G 3 (1999). Standard Practice for Conventions Applicable to Electrochemical Measurements in Corrosion Testing. *American Society of Testing and Materials*, West Conshohocken, PA.

ASTM G 5 (1999). Standard Reference Test Method for Making Potentiostatic and Potentiodynamic Anodic Polarization Measurements. *American Society of Testing and Materials*, West Conshohocken, PA.

ASTM G 59 (2003). Standard Test Method for Conducting Potentiodynamic Polarization Resistance Measurements. *American Society of Testing and Materials*, West Conshohocken, PA.

Baweja, D., Roper, H., & Sirivivatnanon, V. (1996). *Corrosion of Steel in Marine Concrete: Long-Term Half-Cell Potential and Resistivity Data.* Performance of Concrete in Marine Environment, Third CANMET/ACI International Conference, Proceedings, St. Andrews by-the-Sea, Canada, SP-163, V. M. Malhotra, Ed., 89-110.

Baweja, D., Roper, H., & Sirivivatnanon, V. (1999). Chloride-Induced Steel Corrosion in Concrete: Part 2 – Gravimetric and Electrochemical Comparisons. *ACI Materials Journal, 96(3),* 306-312.

Berke, N. S. (1991). *Corrosion Inhibitors in Concrete. Concrete International, 13,* 24-27.

Berke, N. S., Shen, D. F., & Sundberg, K. M. (1990). *Comparison of Current Interruption and Electrochemical Impedance Techniques in the Determination of Corrosion Rates of Steel in Concrete. The Measurement and Correction of Electrolyte Resistance in Electrochemical Tests,* ASTM STP 1056, L. L. Scribner and S. R. Taylor, Eds., American Society for Testing and Materials, Philadelphia, 191-201.

Breysse, D. & Gérard, B. (1997). Modelling of Permeability in Cement-Based Materials: Part 1 – Uncracked Medium. *Cement and Concrete Research, 27(5),* 761-775.

Cohen, J. (1988). *Statistical Power Analysis for the Behavioral Sciences.* Lawrence Erlbaum Associates, Publishers (Second Edition).

Diamond, S. (1997). Alkali Silica Reactions – Some Paradoxes. *Cement and Concrete Composites, 19,* 391-401.

Dickson, T. J., Tabatabai, H., & Whiting, D. A. (1993). *Corrosion Assessment of a 34-Year-Old Precast Post Tensioned Concrete Girder. PCI Journal, 38(6),* 44-51.

Diederichs, U., & Schutt, K. (1989). *Silica Fume Modified Grouts for Corrosion Protection of Post Tensioning Tendons.* SP 114-57, Trondheim Conference, 1173-1195.

El Maaddawy, T. A. & Soudki, K. A. (2003). Effectiveness of Impressed Current Technique to Simulate Corrosion of Steel Reinforcement in Concrete. *Journal of Materials in Civil Engineering, 15(1),* 41-47.

Escalante, E. (1990). *Elimination of IR Error in Measurements of Corrosion in Concrete.* The Measurement and Correction of Electrolyte Resistance in Electrochemical Tests, ASTM STP 1056. L. L. Scribner and S. R. Taylor, Eds., American Society for Testing and Materials, Philadelphia, 180-190.

Gu, P.; Elliot, S.; Hristova, R.; Beaudoin, J. J.; Brousseau, R.; & Baldock, B. (1997). A *Study of Corrosion Inhibitor Performance in Chloride Contaminated Concrete by Electrochemical Impedance Spectroscopy. ACI Materials Journal, 94(5),* 385-395.

Hamilton, H. R. (1995). *Investigation of Corrosion Protection Systems for Bridge Stay Cables.* PhD Dissertation, The University of Texas at Austin.

Hamilton, H. R., Breen, J. E., & Frank, K. H. (1998). Bridge Stay Cable Corrosion Protection. I: Grout Injection and Load Testing. *Journal of Bridge Engineering, 3(2),* 64-71.

Hamilton, H. R., Wheat, H. G., Breen, J. E., & Frank, K. H. (2000). Corrosion Testing of Grout for Posttensioning Ducts and Stay Cables. *Journal of Structural Engineering, 126(2),* 163-170.

Hornain, H., Marchand, J., Buhot, V., & Moranville-Regourd, M. (1995). Diffusion of Chloride Ions in Limestone Filler Blended Cement Pastes and Mortars. *Cement and Concrete Research, 25(8),* 1667-1678.

Hussain, S. E., & Rasheeduzzafar (1994). *Corrosion Resistance Performance of Fly Ash Blended Cement Concrete. ACI Materials Journal, 91(3),* 264-272.

Idriss, A. F., Negi, S. C., Jofriet, J. C., & Hayward, G. L. (2001). *Corrosion of Steel Reinforcement in Mortar Specimens Exposed to Hydrogen Sulphide, Part 1: Impressed Voltage and Electrochemical Potential Tests. Journal of Agricultural Engineering Research, 79(2),* 223-230.

Jones, D. A. (1996). *Principles and Prevention of Corrosion.* Prentice Hall (Second Edition)

Kirkpatrick, T. J., Weyers, R. E., Anderson-Cook, C. M., & Sprinkel, M. M. (2002). Probabilistic Model for the Chloride-Induced Corrosion Service Life of Bridge Decks. *Cement and Concrete Research, 32,* 1943-1960.

Koester, B. D. (1995). *Evaluation of Cement Grouts for Strand Protection using Accelerated Corrosion Tests.* MSc. Thesis, The University of Texas at Austin.

Kraemer, H. C. & Thiemann, S. (1987). *How Many Subjects? Statistical Power Analysis in Research.* Sage Publications.

Lankard, D. R., Thompson, N., Sprinkel, M. M., & Virmani, Y. P. (1993). *Grouts for Bonded Post Tensioned Concrete Construction: Protecting Prestressing Steel from Corrosion. ACI Materials Journal, 90(5),* 406-414.

Li, C. Q. (2001). *Initiation of Chloride-Induced Reinforced Corrosion in Concrete Structural Members – Experimentation. ACI Structural Journal, 98(4),* 502-510.

Liu, W., Hunsperger, R. G., Chajes, M. J., Folliard, K. J., & Kunz, E. (2002). Corrosion Detection of Steel Cables using Time Domain Reflectometry. *Journal of Materials in Civil Engineering, 14(3),* 217-223.

Loretz, T., & French, C. (1995). *Corrosion of Reinforcing Steel in Concrete: Effects of Materials, Mix Composition, and Cracking. ACI Materials Journal, 92(2),* 181-190.

Millard S. G., Law, D., Bungey, J. H., & Cairns J. (2001). Environmental Influences on Linear Polarization Corrosion Rate Measurement in Reinforced Concrete. *NDT&E International, 34,* 409-417.

Montemor, M. F., Simões, A. M. P., & Ferreira, M. G. S. (2003). Chloride-Induced Corrosion on Reinforcing Steel: from the Fundamentals to the Monitoring Techniques. *Cement & Concrete Composites, 25(4-5),* 491-502.

Montemor, M. F., Simões, A. M. P., & Salta, M. M. (2000). Effect of Fly Ash on Concrete Reinforcement Corrosion Studied by EIS. *Cement & Concrete Composites, 22,* 175-185.

Peng, J., Li, Z., & Ma, B. (2002). Neural Network Analysis of Chloride Diffusion in Concrete. *Journal of Materials in Civil Engineering, 14(4),* 327-333.

Post-Tensioning Institute (2003). *Guide Specification for Grouting of Post Tensioned Structures (1st Ed.).* PTI Committee on Grouting Specifications, Post-Tensioning Institute.

Rasheeduzzafar, Dakhil, F. H., Al-Gahtani, A. S., Al-Saadoun, S. S., & Bader, M. A. (1990). *Influence of Cement Composition on the Corrosion of Reinforcement and Sulfate Resistance of Concrete. ACI Materials Journal, 87(2),* 114-122.

Rha, C. Y., Kim, W. S., Kim, J. W., & Park, H. H. (2001). Relationship between Microstructure and Electrochemical Characteristics in Steel Corrosion. *Applied Surface Science, 169-170,* 587-592.

Schiessl, P. & Raupach, M. (1992). Monitoring System for the Corrosion Risk of Steel in Concrete Structures. *Concrete International, 14(7),* 52-55.

Schokker, A. J. (1999). *Improving Corrosion Resistance of Post Tensioned Substructures Emphasizing High Performance Grouts.* PhD Dissertation, The University of Texas at Austin.

Schokker, A. J., Breen, J. E., & Kreger, M. E. (2002). Simulated Field Testing of High Performance Grouts for Post-Tensioning. *Journal of Bridge Engineering, 7(2),* 127-133.

Schupack, M. (1971). Grouting Tests on Large Post-Tensioning Secondary Nuclear Containment Structures. *PCI Journal, 16(2),* 84-97.

Schupack, M. (1974). Admixture for Controlling Bleed in Cement Grout Used in Post-Tensioning. *PCI Journal, 19(6),* 28-39.

Schupack, M. (1994). Studies of the Bissell Bridge: *Post Tensioning Tendons after 35 years. Concrete International, 16(3),* 50-54.

Stansbury, E. E. & Buchanan, R. A. (2000). *Fundamentals of Electrochemical Corrosion.* ASM International. The Materials Information Society.

Zivica, V. (2001). Possibility of Improvement of Potentiodynamic Method for Monitoring Corrosion Rate of Steel Reinforcement in Concrete. *Bulletin of Material Science, 24(5),* 555-558.

VITA

ALEXANDRE RODRIGUES PACHECO

Permanent Address:
Rua Riachuelo, 400/513 Porto Alegre, RS, Brazil 90010-272

E-mails: arp170@psu.edu; apacheco@ppgec.ufrgs.br

EDUCATION

2000-2001   Cornell University
Three semesters of Ph.D. coursework.
Supervisor: Prof. Sarah L. Billington

1993-1996   Federal University of Brazil at Rio Grande do Sul – UFRGS
M.Sc., Structural Engineering
Thesis: *"Viscoelastic Analysis through Finite Element Method and Numerical Inversion of the Laplace Transform"*
Adviser: Dr. Guillermo Juan Creus

1987-1992   Federal University of Brazil at Rio Grande do Sul - UFRGS
B.Sc., Civil Engineering

PROFESSIONAL EXPERIENCE

July 1997 - present   **Assistant Professor**, at UFRGS, Porto Alegre, RS, Brazil
June 96 - May 97   **Researcher**, at LEME/UFRGS, Porto Alegre, RS, Brazil
July - Dec. 1996   **Visiting Lecturer**, at URI, Santo Ângelo, RS, Brazil
May - Sept. 1995   **Resident Engineer**, ESBEL, Porto Alegre, RS, Brazil

TEACHING EXPERIENCE

1. **Mechanics**, undergraduate course at UFRGS
2. **Structural Mechanics I**, undergraduate course at UFRGS
3. **Pathology of Constructions**, undergraduate course at URI
4. **Materials of Construction**, undergraduate course at URI

SELECTED PUBLICATIONS

Pacheco, A.R., Campos Filho, A., Campagnolo, J.L., & Gastal, F.P.S.L (1997). Simulating Processes of Rehabilitation of RC Structures via the Finite Element Method. *Proceedings for the 18th CILAMCE*, Brasília, Brazil, Oct. (in Portuguese).

Pacheco, A.R. & Creus, G.J. (1997). Viscoelastic Analysis of Laminated Structures through Numerical Inversion of the Laplace Transform. *Revista Internacional de Métodos Numéricos para Cálculo y Diseño en Ingenieria, 13,* Universitat Politècnica de Catalunya, Spain (in Portuguese).